



Search for electroweak production of supersymmetric particles in final states with two τ -leptons in $\sqrt{s} = 13$ TeV pp collisions with the ATLAS detector

The ATLAS Collaboration

Three searches for the direct production of τ -sleptons or charginos and neutralinos in final states with at least two hadronically decaying τ -leptons are presented. For chargino and neutralino production, decays via intermediate τ -sleptons or W and h bosons are considered. The analysis uses a dataset of pp collisions corresponding to an integrated luminosity of 139 fb^{-1} , recorded with the ATLAS detector at the Large Hadron Collider at a centre-of-mass energy of 13 TeV. No significant deviation from the expected Standard Model background is observed and supersymmetric particle mass limits at 95% confidence level are obtained in simplified models. For direct production of $\tilde{\chi}_1^+ \tilde{\chi}_1^-$, chargino masses are excluded up to 970 GeV, while $\tilde{\chi}_1^\pm$ and $\tilde{\chi}_2^0$ masses up to 1160 GeV (330 GeV) are excluded for $\tilde{\chi}_1^\pm \tilde{\chi}_2^0 / \tilde{\chi}_1^+ \tilde{\chi}_1^-$ production with subsequent decays via τ -sleptons (W and h bosons). Masses of τ -sleptons up to 500 GeV are excluded for mass degenerate $\tilde{\tau}_{L,R}$ scenarios and up to 425 GeV for $\tilde{\tau}_L$ -only scenarios. Sensitivity to $\tilde{\tau}_R$ -only scenarios from the ATLAS experiment is presented here for the first time, with $\tilde{\tau}_R$ masses excluded up to 350 GeV.

1 Introduction

Supersymmetry (SUSY) [1–7] postulates the existence of a bosonic (fermionic) partner for each fermionic (bosonic) particle of the Standard Model (SM), whose spin differs by one half unit from each corresponding SM particle. In models that conserve R -parity [8], the lightest supersymmetric particle (LSP) is stable and can be an excellent dark-matter candidate [9, 10].

In the simplified SUSY models considered in this article, the sector of SUSY particles with only electroweak interactions contains charginos ($\tilde{\chi}_i^\pm$, $i = 1, 2$, in order of increasing masses), neutralinos ($\tilde{\chi}_j^0$, $j = 1, 2, 3, 4$, in order of increasing masses), charged sleptons ($\tilde{\ell}$), and sneutrinos ($\tilde{\nu}$). Charginos and neutralinos are the mass eigenstates formed from linear superpositions of the superpartners of the Higgs bosons and electroweak gauge bosons. The charged sleptons are the superpartners of the charged leptons and are denoted by subscripts reflecting the chirality of the SM partner fields, referred to as $\tilde{\ell}_L$ or $\tilde{\ell}_R$, respectively. The slepton mass eigenstates are a mixture of $\tilde{\ell}_L$ and $\tilde{\ell}_R$, and are labeled as $\tilde{\ell}_k$ ($k = 1, 2$ in order of increasing mass). In this work, the scalar superpartners of the left-handed τ -lepton ($\tilde{\tau}_L$) and right-handed τ -lepton ($\tilde{\tau}_R$) are assumed to be mass degenerate unless explicitly stated, and are referred to as “staus.” All SUSY scenarios considered in this publication conserve R -parity and the LSP is the $\tilde{\chi}_1^0$.

Although they are experimentally challenging, final states with τ -leptons are of particular interest in SUSY searches. Light sleptons could play a role in the co-annihilation of neutralinos in the early universe, and models with light stau decays into light neutralinos can shed light on the nature of dark matter [11]. Furthermore, should SUSY or any other physics beyond the Standard Model (BSM) involving leptons be discovered, independent studies of all three lepton flavors are necessary to investigate the coupling structure of the new physics, especially concerning lepton universality.

The first SUSY scenario considered is the direct production of stau pairs, either with mass degenerate or non-degenerate $\tilde{\tau}_{L,R}$, which decay directly into a τ -lepton and the LSP 100% of the time. The second scenario, referred to as the “Intermediate stau” channel, includes the production of mass-degenerate neutralinos and charginos, $\tilde{\chi}_1^\pm \tilde{\chi}_2^0$ and $\tilde{\chi}_1^+ \tilde{\chi}_1^-$, which decay into the lightest neutralino only through intermediate staus or τ -sneutrinos with equal branching fraction. The stau and sneutrino masses are assumed to be halfway between the $\tilde{\chi}_2^0/\tilde{\chi}_1^\pm$ and $\tilde{\chi}_1^0$ masses. The search for $\tilde{\chi}_1^\pm \tilde{\chi}_2^0$ production is separated into final states with two same-sign (SS) or opposite-sign (OS) τ -lepton pairs. The third SUSY scenario, referred to as the “Intermediate Wh ” channel, is the direct production of mass-degenerate neutralinos and charginos, $\tilde{\chi}_1^\pm \tilde{\chi}_2^0$, which decay via the lightest neutral Higgs boson (h), consistent with the SM Higgs boson with a mass of 125 GeV, a W boson and two neutralinos. In this case, the final state under consideration contains two hadronically decaying τ -leptons from the Higgs boson decay and one charged light lepton (e, μ) from the W boson decay. The light lepton may be the result of a $W \rightarrow \tau \nu$ decay where the τ -lepton decays leptonically. For all three searches presented in this publication, the final state includes two hadronically decaying τ -leptons, low jet activity and large missing transverse momentum, $\mathbf{p}_T^{\text{miss}}$, from the neutralinos and neutrinos. Representative diagrams of the targeted signal processes can be found in Figure 1.

Previous results from the ATLAS experiment have set exclusion limits at 95% confidence level on these SUSY models with the Run 1 and partial Run 2 data samples [12–15]. The CMS experiment also sets comparable exclusion limits [16–18]. This search extends the current ATLAS reach to higher chargino masses and smaller mass differences between $\tilde{\chi}_2^0/\tilde{\chi}_1^\pm/\tilde{\tau}$ and $\tilde{\chi}_1^0$ using the increased statistics of the full Run 2 data sample. It also achieves sensitivity to $\tilde{\tau}_R$ pair production scenarios for the first time from ATLAS, by introducing the use of machine learning algorithms.

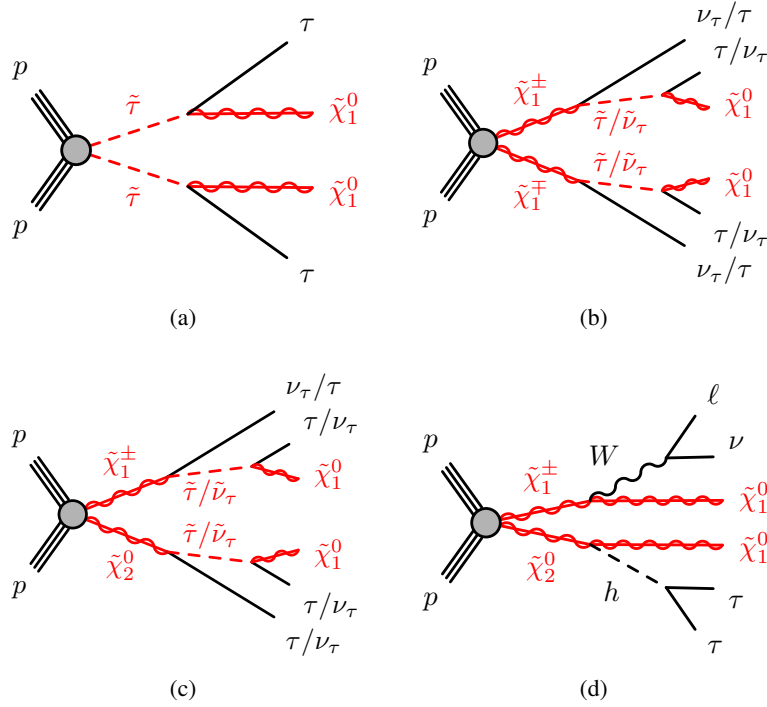


Figure 1: Representative diagrams of SUSY scenarios, which are being searched for in this publication. Direct stau production is shown in (a), while (b) and (c) show the processes considered for the Intermediate stau channel. The process for the Intermediate Wh channel is shown in (d). In all cases, the subsequent decays contain a final state with at least two τ -leptons. In the case of $\tilde{\chi}_1^\pm \tilde{\chi}_2^0$ production (c), the final state can contain more than two τ -leptons.

The publication is structured as follows: the ATLAS detector is briefly introduced in Section 2 followed by a description of the data and simulated samples used in Section 3 and the reconstruction of events in Section 4; the general analysis strategy is outlined in Section 5, followed by the details of the Direct stau, Intermediate stau, and Intermediate Wh searches in Sections 6, 7, and 8, respectively; the systematic uncertainties are discussed in Section 9 and the results are presented in Section 10, before conclusions are drawn in Section 11.

2 ATLAS detector

The ATLAS experiment [19] at the Large Hadron Collider (LHC) is a multipurpose particle detector with a forward–backward symmetric cylindrical geometry and a near 4π coverage in solid angle.¹ It consists of an inner tracking detector (ID) surrounded by a thin superconducting solenoid providing a 2 T axial magnetic field, electromagnetic and hadron calorimeters, and a muon spectrometer. The ID covers the pseudorapidity range $|\eta| < 2.5$. It consists of silicon pixel, silicon microstrip, and transition

¹ ATLAS uses a right-handed coordinate system with its origin at the nominal interaction point (IP) in the center of the detector and the z -axis along the beam pipe. The x -axis points from the IP to the center of the LHC ring, and the y -axis points upwards. Cylindrical coordinates (r, ϕ) are used in the transverse plane, ϕ being the azimuthal angle around the z -axis. The pseudorapidity is defined in terms of the polar angle θ as $\eta = -\ln \tan(\theta/2)$. Angular distance is measured in units of $\Delta R \equiv \sqrt{(\Delta\eta)^2 + (\Delta\phi)^2}$.

radiation tracking detectors. Lead/liquid-argon (LAr) sampling calorimeters provide electromagnetic (EM) energy measurements with high granularity. A steel/scintillator-tile hadron calorimeter covers the central pseudorapidity range ($|\eta| < 1.7$). The endcap and forward regions are instrumented with LAr calorimeters for both the EM and hadronic energy measurements up to $|\eta| = 4.9$. The muon spectrometer (MS) surrounds the calorimeters and is based on three large superconducting air-core toroidal magnets with eight coils each. The field integral provided by the toroids ranges between 2.0 and 6.0 T m across most of the detector. The muon spectrometer includes a system of precision tracking chambers and fast detectors for triggering. A two-level trigger system is used to select events [20]. The first-level trigger is implemented in hardware and uses a subset of the detector information to accept events at a rate below 100 kHz. This is followed by a software-based trigger that reduces the accepted event rate to 1 kHz on average depending on the data-taking conditions. An extensive software suite [21] is used in the reconstruction and analysis of real and simulated data, in detector operations, and in the trigger and data acquisition systems of the experiment.

3 Data and simulated event samples

The data sample considered in this publication corresponds to 139 fb^{-1} of proton–proton (pp) LHC collision data collected between 2015 and 2018 with the ATLAS detector, at a center-of-mass energy of 13 TeV. Data quality requirements are imposed to ensure that only events in which the entire ATLAS detector was functioning well are used [22].

Simulated events produced with several Monte Carlo (MC) event generators are used to predict yields for background contributions from SM processes and for possible SUSY signals. To account for pileup, all simulated events are overlaid with multiple pp collisions simulated with the soft QCD processes of PYTHIA 8.186 [23] using the A3 set of tuned parameters [24] and the NNPDF2.3_{LO} leading-order (LO) parton distribution functions (PDFs) [25]. For all samples showered with PYTHIA 8, EVTGEN 1.2.0 [26] is used to simulate the decays of bottom and charmed hadrons. The simulated events are weighted such that the pileup conditions match those of the data and are required to satisfy the trigger selections. The response of the detector to particles is modeled with an ATLAS detector simulation [27] based on GEANT4 [28] for almost all SM background simulation. A few minor electroweak Z +jet processes with very small yields for these searches use a fast simulation based on a parameterisation of the performance of the ATLAS EM and hadronic calorimeters [29] and on GEANT4 elsewhere.

Final states with at least two hadronically decaying τ -leptons, low jet activity and a large $\mathbf{p}_T^{\text{miss}}$ are included in this analysis. As a result, SM background processes containing both real and misidentified τ -lepton final state contributions are considered. These backgrounds are summarised in the following paragraphs.

The production of top-quark pairs ($t\bar{t}$) and single top quarks in the Wt and s -channels is performed with POWHEG BOX v2 [30–33], with the NNPDF2.3_{LO} PDF set at next-to-leading-order (NLO) in the Matrix element (ME) calculations and the ATLAS underlying-event tune A14 [34]. Electroweak t -channel single-top-quark events are simulated using the POWHEG BOX v2 event generator. The parton shower (PS), fragmentation, and the underlying event are simulated using PYTHIA 8.186 with the NNPDF2.3_{LO} PDF set and a corresponding set of A14 tuned parameters. The top-quark mass is set to 172.5 GeV. The $t\bar{t}$ sample is normalized to the cross-section prediction at next-to-next-to-leading-order (NNLO) in QCD including the resummation of next-to-next-to-leading-logarithmic (NNLL) soft-gluon terms calculated using TOP++ 2.0 [35–41]. The cross-section for single-top-quark is computed for the Wt -channel at NLO in QCD with NNLL soft gluon corrections [42, 43], and to NLO in QCD for the t - and s -channels. Top-quark

pair production with an additional W or Z boson is calculated using `AMC@NLO 2.2.2` [44] at NLO in the ME calculations, while fragmentation and hadronization are simulated with `PYTHIA 8.186`. The underlying-event tune A14 is used with the `NNPDF2.3LO` PDF set, and the cross-sections are normalized using NLO predictions [45, 46].

Events with $Z/\gamma^* \rightarrow \ell\ell$ ($\ell = e, \mu, \tau$) and $W \rightarrow \ell\nu$ produced in association with jets (including jets initiated by heavy flavor quarks) are simulated with `SHERPA 2.2.1` [47, 48]. MEs are calculated for up to two additional partons at NLO and four additional partons at LO, using the `Comix` [49] and `OPENLOOPS` [50, 51] generators and merged with the `SHERPA PS` [52] using the `MENLOPS` prescription. The `NNPDF3.0NNLO` [53] PDF set is used in conjunction with a dedicated PS tuning developed by the `SHERPA` authors. The W/Z +jets events are normalized using their NNLO cross-sections [54].

Fully leptonic and semileptonic decaying diboson and triboson samples (VV and VVV , where $V = W, Z$) are simulated with the `SHERPA 2.2.1` and `SHERPA 2.2.2` generator at NLO. In this setup, multiple matrix elements are matched and merged with the `SHERPA` parton shower based on Catani–Seymour dipole factorisation using the `MENLOPS` prescription [55, 56]. The virtual QCD corrections for matrix elements at NLO accuracy are provided by the `OPENLOOPS` library. Samples are simulated using the `NNPDF3.0NNLO` set, along with the dedicated set of tuned parton-shower parameters developed by the `SHERPA` authors.

Contributions from Higgs boson events produced by gluon–gluon fusion and vector-boson fusion are modeled using `POWHEG BOX v2` with the `NNPDF3.0NNLO` PDF and showered using `PYTHIA 8.186`. Associated production of a Higgs boson with a vector boson and a Higgs boson in association with two top quarks are simulated using `PYTHIA 8.186` and `AMC@NLO`, respectively. All Higgs boson samples are normalized to the cross-sections from Ref. [57].

SUSY signal model samples are simulated to allow the interpretation of the search results in terms of SUSY parameters and use the ATLAS fast detector simulation. Signal samples are simulated using `AMC@NLO 2.2.3` interfaced to `PYTHIA 8.186` with the A14 tune for the PS modeling, hadronization, and underlying event. The ME calculation is performed at tree level and includes the emission of up to two additional partons. The PDF set used for the generation is `NNPDF2.3LO`. The ME–PS merging uses the `CKKW-L` [58] prescription, with a matching scale set to one quarter of the mass of the pair of produced particles. Signal cross-sections are calculated with `RESUMMINO v2.0.1` to NLO in the strong coupling constant, adding the resummation of soft gluon emission at next-to-leading-logarithm accuracy (NLO+NLL) [59, 60]. The nominal cross-section and the uncertainty are taken from an envelope of cross-section predictions using different PDF sets and factorisation and renormalization scales, as described in Ref. [61].

4 Event reconstruction

After data quality requirements are applied, events with at least one reconstructed primary vertex [62] are selected. A primary vertex is defined to have at least two associated charged-particle tracks with transverse momentum $p_T > 500$ MeV and be consistent with the beam spot envelope. If there are multiple primary vertices in an event, the one with the largest $\sum p_T^2$ of the associated tracks is chosen.

Jets are reconstructed from particle-flow objects calibrated at the EM scale [63] using the anti- k_t algorithm [64, 65] with a radius parameter of 0.4. Jet energies are corrected for detector inhomogeneities, the non-compensating response of the calorimeter, and pileup effects [66, 67]. The impact due to pileup is accounted for using a technique based on jet areas that provides an event-by-event and jet-by-jet

correction [68]. Jets that are likely to have originated from pileup are not considered in the analysis [69]. Jets are required to have $p_T > 20$ GeV and $|\eta| < 2.8$, and events containing jets that are likely to have arisen from detector noise or cosmic rays are removed [70].

Jets containing b -hadrons (b -jets) are identified using the *DL1r* algorithm [71, 72], a multivariate discriminant making use of track impact parameters and reconstructed secondary vertices. Candidate b -jets are required to have $|\eta| < 2.5$. A working point is used that has a p_T -independent b -tagging efficiency of 77% and light-jet (c -jet) rejection factor of 140 (4), based on studies using simulated $t\bar{t}$ events.

Electron candidates are reconstructed by matching clusters in the EM calorimeter with charged-particle tracks in the ID. Electrons are required to have $p_T > 25$ GeV, $|\eta| < 2.47$, and to satisfy the “loose” working point according to a likelihood-based identification algorithm detailed in Ref. [73]. Muon candidates are reconstructed from MS tracks matching ID tracks; they are required to have $p_T > 25$ GeV and $|\eta| < 2.7$ and satisfy the “medium” quality criteria described in Ref. [74]. Events containing a muon candidate with a poorly measured charge-to-momentum ratio of $\frac{\sigma(q/p)}{|q/p|} > 0.2$ are rejected. Events are required not to contain any candidate muon with large transverse (d_0) and longitudinal (z_0) impact parameter, $|z_0| > 1$ mm or $|d_0| > 0.2$ mm, to reduce contributions from those originating from cosmic rays. The efficiencies for electrons and muons to satisfy the reconstruction, identification, and isolation criteria are measured using samples of leptonic Z and J/ψ decays, and corrections are applied to the simulated samples to reproduce the efficiencies observed in data [73, 74].

The reconstruction of hadronically decaying τ -leptons is based on information from tracks in the ID and three-dimensional clusters in the EM and hadronic calorimeters. The τ -lepton reconstruction algorithm is seeded by jets reconstructed from topological clusters of energy deposits in the calorimeter and uses a looser requirement of $p_T > 10$ GeV and $|\eta| < 2.5$. The reconstructed energies of the hadronically decaying τ -lepton candidates are corrected from the local hadron topocluster scale to the τ -lepton energy scale, which is calibrated based on simulation and in situ measurements using $Z \rightarrow \tau\tau$ decays [75]. Hadronically decaying τ -lepton candidates are required to have one or three associated charged-particle tracks (prongs) and the total electric charge of those tracks must be ± 1 times the electron charge. To improve the discrimination between hadronically decaying τ -leptons and jets, electrons, or muons, multivariate algorithms are used [76]. A recurrent neural network discriminant is used to reject jets that do not originate from a hadronically decaying τ -lepton, with a “medium” or “tight” working point as described in Ref. [77]. The medium (tight) working point has an efficiency of 75% (60%) for 1-prong τ -leptons and 60% (45%) for 3-prong τ -leptons, based on $\gamma^* \rightarrow \tau\tau$ MC simulation. The background rejection factor for the medium (tight) working point is 35 (70) for 1-prong τ -leptons and 240 (700) for 3-prong τ -leptons, based on dijet MC simulation. A boosted decision tree is used to discriminate 1-prong τ -leptons against electrons. This discriminant is built using information from the EM calorimeter and the tracking detector. This requirement has about 95% efficiency, and a rejection factor from 10 to 50 depending on the η range. The τ -leptons are required to have $p_T > 20$ GeV and $|\eta| < 2.47$, and must lie outside the transition region between the barrel and endcap calorimeters ($1.37 < |\eta| < 1.52$).

The MC simulation is corrected for differences in the efficiencies of the τ -lepton identification at both trigger and reconstruction level between data and simulation. For hadronically decaying τ -leptons originating from prompt gauge boson decays, the corrections are calculated with a *tag-and-probe* method in a sample of $Z \rightarrow \tau\tau$ events where one τ -lepton decays hadronically and the other leptonically into a muon and two neutrinos [78].

The measured $\mathbf{p}_T^{\text{miss}}$, and its magnitude E_T^{miss} , is defined as the negative vectorial sum of the \mathbf{p}_T of all identified jets, τ -leptons, electrons, photons, muons, and an additional soft term. The soft term is

constructed from all tracks that are associated with the primary vertex but not with any identified particle or jet [79, 80].

To avoid the possible double counting of reconstructed objects, an overlap removal procedure is used, following these steps. The τ -leptons that are close to electron or muon candidates ($\Delta R < 0.2$, where $\Delta R = \sqrt{(\Delta y)^2 + (\Delta\phi)^2}$) are removed, as are electrons that share a track with a muon. For electrons close to a jet ($\Delta R < 0.4$), the electron is removed, except when $\Delta R < 0.2$ and the jet is not b -tagged, in which case the jet is removed. Any remaining jet close to a muon or τ -lepton ($\Delta R < 0.4$) is removed.

5 General analysis strategy and event variables

Events for all scenarios are required to have at least two hadronically decaying τ -leptons. Different signal regions (SRs) are defined to target the specific SUSY scenario, using kinematic variables that provide a good signal-to-background separation, described in this section. For τ -leptons, kinematic variables are calculated from the visible decay products. The event selections and background estimates are described for Direct stau production SRs in Section 6, for the Intermediate stau channel SRs in Section 7, and for the Intermediate Wh channel SRs in Section 8.

The main SM backgrounds are estimated by normalizing MC simulation samples to data in dedicated control regions (CRs); backgrounds resulting from non-prompt and misidentified leptons are derived from data, while sub-dominant backgrounds are estimated by using MC simulation only. To validate the modelling of the SM backgrounds, the yields and shapes of key kinematic variables are compared with data in dedicated validation regions (VRs). SRs are designed for the best expected sensitivity to the simplified SUSY signal models studied. Where appropriate, looser, or merged SRs are used to enhance discovery prospects or to set model-independent limits.

The observed number of events in the CRs and SRs are used in a combined profile likelihood fit to determine the expected SM background yields. The statistical interpretation of the results is performed using the profile likelihood method implemented in the HistFitter framework [81]. Systematic uncertainties are included as nuisance parameters in the likelihood fits and are assumed to follow a Gaussian distribution with a width determined from the size of the uncertainty. Correlations of systematic uncertainties between control and signal regions, and between background processes are taken into account with common nuisance parameters. The fit parameters are determined by maximising the product of the Poisson probability functions and the constraints for the nuisance parameters.

To constrain the SM backgrounds normalized to data in CRs, a *background-only* fit is used. This uses the observed yields in the CRs with the expected SM contributions (other than multi-jet) in the CRs and SRs, and the corresponding background transfer factors described in Section 6.2.1. The free parameters in the fit are the normalizations of the SM processes. To estimate the SM background in the SRs (or VRs), a combined fit is performed that includes the observed data in the CRs and SRs (or VRs) with the SM background estimates, and accounts for correlations between CRs and SRs (or VRs), as well as between background processes. The presence of BSM signal in any CR, SR, or VR is assumed to be zero in the combined and background-only fits.

To assess the possibility of the presence of any BSM events in each SR, a *model-independent* fit is used. This uses the observed yields in both the CRs and SRs with the SM background estimates to test whether any BSM events could be present in the SR. The presence of BSM signal in any CR is assumed to be zero in the model-independent fit. The significance of a possible excess of observed events over the SM

prediction is quantified by the one-sided probability, $p(\text{signal} = 0)$ denoted by p_0 , of the background alone to fluctuate to the observed number of events or higher using the asymptotic formula described in Ref. [82]. The upper limit on the visible cross-section of BSM events in an SR, σ_{vis}^{95} , is also calculated, which includes the acceptance and efficiency effect of any BSM signal possibly present.

Finally, to assess the compatibility of the signal scenarios with the data observation, a *model-dependent* fit is used, which accounts for the SUSY signal in all CRs and SRs scaled by a floating signal normalization factor. The background normalization factors are also determined simultaneously in the fit. A SUSY scenario is rejected if the upper limit at 95 % confidence level (CL) of the signal normalization factor obtained in this fit is smaller than the predicted cross-section of the scenario [83].

The following variables are used to discriminate SUSY signals from the SM background:

- m_T , the transverse mass values obtained from a reconstructed lepton with the $\mathbf{p}_T^{\text{miss}}$, defined by

$$m_T(\mathbf{p}_T, \mathbf{p}_T^{\text{miss}}) = \sqrt{2(|\mathbf{p}_T||\mathbf{p}_T^{\text{miss}}| - \mathbf{p}_T \cdot \mathbf{p}_T^{\text{miss}})},$$

where \mathbf{p}_T is the transverse momenta of the lepton. The transverse mass calculated using light leptons only (e or μ) is denoted by $m_{T,\ell}$.

- $m_{T\text{sum}}$, the sum of the transverse mass values of the two highest- p_T τ -lepton candidates with the $\mathbf{p}_T^{\text{miss}}$. For Intermediate Wh scenarios, $m_{T,\ell}$ is also added to $m_{T\text{sum}}$.
- m_{T2} , the ‘‘stransverse mass,’’ which has a kinematic endpoint for events where two massive particles are pair produced, then each particle decays into a detected object (the lepton) and an undetected object (the neutralino) [84, 85]. It is defined as:

$$m_{T2} = \min_{\mathbf{q}_T} \left[\max \left(m_T(\mathbf{p}_{T1}, \mathbf{q}_T), m_T(\mathbf{p}_{T2}, \mathbf{p}_T^{\text{miss}} - \mathbf{q}_T) \right) \right],$$

where \mathbf{p}_{T1} and \mathbf{p}_{T2} are the transverse momenta of the two leptons and \mathbf{q}_T is the transverse vector chosen to minimise the larger of the two transverse masses. In this case, \mathbf{q}_T or $\mathbf{p}_T^{\text{miss}} - \mathbf{q}_T$ replaces $\mathbf{p}_T^{\text{miss}}$ in the calculation of m_T . In events with more than two τ -lepton candidates, the pair that maximises m_{T2} is used. Similarly, in the Intermediate Wh analysis, the pairing of $e\tau$, $\mu\tau$, or $\tau\tau$ that maximises m_{T2} is used. For $t\bar{t}$ and WW events, the m_{T2} distribution has a kinematic endpoint at the W boson mass, but the distribution for SUSY scenarios extends significantly beyond this endpoint if the mass difference between the produced SUSY particle and the $\tilde{\chi}_1^0$ is large. The $\tilde{\chi}_1^0$ is assumed to be massless in the calculation of m_{T2} .

- m_{eff} , the effective mass, is defined as the scalar sum of the E_T^{miss} and the p_T of the two highest- p_T τ -leptons. The effective mass for SUSY processes is typically higher than for SM processes.
- $\Delta R(\tau_1, \tau_2) = \sqrt{(\Delta\eta(\tau_1, \tau_2))^2 + \Delta\phi(\tau_1, \tau_2)^2}$, the angular distance between the two highest- p_T τ -leptons. An upper requirement on this variable is used to discriminate against back-to-back objects in SM events.
- $m(\tau_1, \tau_2)$: the invariant mass of the two highest- p_T τ -leptons. A similar variable is also used for the invariant mass of a τ -lepton and a muon, $m(\tau, \mu)$.
- $|\Delta\phi(\tau_1, \tau_2)|$: the absolute value of the difference of azimuthal angle around the z -axis between the two highest- p_T τ -lepton candidates. A similar variable is also used for the $\mathbf{p}_T^{\text{miss}}$ and τ -leptons, e.g., $|\Delta\phi(\tau, \mathbf{p}_T^{\text{miss}})|$.

- $|\Delta\eta(\tau_1, \tau_2)|$: the absolute value of the difference of pseudorapidity between the two highest- p_T τ -leptons.

6 Direct stau production

The Direct stau analysis targets the production of $\tilde{\tau}_L \tilde{\tau}_L$ and $\tilde{\tau}_R \tilde{\tau}_R$, with the stau decaying into a τ -lepton and a $\tilde{\chi}_1^0$, as shown in Figure 1(a). This analysis aims to improve upon previous results, particularly for moderate mass splittings between the stau and $\tilde{\chi}_1^0$, and for $\tilde{\tau}_R \tilde{\tau}_R$ production. Multiple Boosted Decision Trees (BDTs) are trained for sensitivity to different areas of the $\tilde{\tau} - \tilde{\chi}_1^0$ phase space. The event selection and BDT training are described in Section 6.1, followed by the background estimate in Section 6.2.

6.1 Event selection

Events are selected using an asymmetric di- τ trigger, where the first τ -lepton must satisfy $p_T > 95$ GeV and the second τ -lepton must satisfy $p_T > 60$ (75) GeV for 2015–2017 (2018) data-taking. The τ -lepton p_T thresholds applied are to ensure the trigger efficiencies are in the plateau region.

Four BDTs are trained using the LightGBM [86] package on four groupings of signal scenarios chosen for their different $\tilde{\tau}$ masses and $\Delta m(\tilde{\tau}, \tilde{\chi}_1^0)$. Events used in training have at least two OS medium τ -leptons, no electron, muon, or b -tagged jet candidates and satisfy loose selections on kinematic variables, as shown in Table 1. Three BDT SRs (SR-BDT1, SR-BDT2, SR-BDT3) have two bins in their BDT score, while the fourth BDT has only one bin (SR-BDT4) due to the low statistics available. The binned regions are used for setting exclusion limits in simplified models, while inclusive regions that merge each of the two bins in the binned regions are used to enhance discovery prospects and set model-independent limits. The single-bin region, SR-BDT4, is unchanged when used for setting exclusion limits and model-independent limits. The events selected by the four BDT SRs significantly overlap, thus the SR with the best expected sensitivity is chosen for interpretations.

The BDT training uses inputs including E_T^{miss} , the p_T , and m_T of the two τ -leptons, $\Delta\phi(\tau_1, \mathbf{p}_T^{\text{miss}})$, $\Delta\phi(\tau_2, \mathbf{p}_T^{\text{miss}})$, $\Delta\eta(\tau_1, \tau_2)$, $m(\tau_1, \tau_2)$, m_{eff} , and $m_{T\text{sum}}$. Cross-validation is used with three equal folds for a training, validation, and test set. To improve the reliability of the background modelling during training, input variables are binned such that the statistical error on the MC simulated background is less than 30% per bin. Furthermore, the maximum depth of the individual decision trees is restricted to one so that each tree makes only one selection on a variable. To avoid over-fitting, early-stopping is used, where trees cease to be added during training if performance on the relevant validation set does not improve after ten trees. The fitting procedure is further constrained to avoid over-fitting by using regularisation techniques, where BDT2 and BDT4 use a higher amount of regularisation than BDT1 and BDT3, and consequently, BDT2 and BDT4 occupy a smaller fraction of the total BDT score range compared with the others.

6.2 Background estimate

The main backgrounds contributing to the Direct stau SRs are from multi-jet production with misidentified τ -leptons, W and Z boson production in association with jets, multi-boson production, and events containing at least one top quark, referred to as *Top* background. Top quark background events originate mostly

Table 1: Summary of the selection requirements for the stau pair production SRs.

	BDT Training Preselection							
N medium τ	≥ 2							
Charge combination	OS							
Trigger	asymm. di- τ							
N e/μ	$= 0$							
N b -jets	$= 0$							
E_T^{miss} [GeV]	> 20							
m_{τ_2} [GeV]	> 30							
$m(\tau_1, \tau_2)$ [GeV]	> 120							
$\Delta R(\tau_1, \tau_2)$	< 4							
	SR-BDT1		SR-BDT2		SR-BDT3		SR-BDT4	
	Bin 1	Bin 2	Bin 1	Bin 2	Bin 1	Bin 2		
Target scenario	Low $m(\tilde{\tau})$ Small $\Delta m(\tilde{\tau}, \tilde{\chi}_1^0)$		Mid $m(\tilde{\tau})$ Large $\Delta m(\tilde{\tau}, \tilde{\chi}_1^0)$		Mid $m(\tilde{\tau})$ Small $\Delta m(\tilde{\tau}, \tilde{\chi}_1^0)$		High $m(\tilde{\tau})$	
N medium τ	$= 2$							
BDT1 score	$\in (0.73, 0.78)$	> 0.78	–	–	–	–	–	
BDT2 score	–	–	$\in (0.78, 0.82)$	> 0.82	–	–	–	
BDT3 score	–	–	–	–	$\in (0.79, 0.86)$	> 0.86	–	
BDT4 score	–	–	–	–	–	–	> 0.64	

from $t\bar{t}$ production in association with additional jets or an additional W or Z boson. The dominant SM backgrounds, W +jets, Z +jets, and top quark processes, are estimated by using MC simulation normalized to data in dedicated control regions. The multi-jet background yield is estimated from data using the so-called ABCD method, described below, and MC simulation is used for all other minor SM backgrounds. The normalization factors obtained from control regions are applied for backgrounds in the BDT training, as is the data-driven multi-jet estimate.

6.2.1 Multi-jet background estimate

Background events contain a combination of ‘real’ τ -leptons, defined as correctly identified τ -leptons, or ‘misidentified’ τ -leptons, which can originate from a misidentified light-flavor quark or gluon jet, an electron, or a muon. Selected events from multi-jet production contain mostly misidentified τ -leptons originating from misidentified jets.

The multi-jet contribution is estimated by using a data-driven ABCD method, which is common to both the Direct stau channel and the Intermediate stau channel described in Section 7. Orthogonal regions are defined using two approximately uncorrelated discriminating variables, as shown schematically in Figure 2. The number of multi-jet events in region D, N_D , can be calculated from that in region A, N_A , multiplied by the transfer factor $T = N_C/N_B$, where region D corresponds to one of the SRs and regions A–C are CRs. Intermediate VRs are defined to verify the reliability of the transfer factor obtained from the ABCD estimate and to estimate the systematic uncertainty from the residual correlation between the discriminating variables. Non-multi-jet SM contributions are subtracted from data in each region using MC simulation, and in the case of the Direct stau channel, the W +jets, Z +jets, and top quark backgrounds are subtracted after their normalization to data in their dedicated CRs.

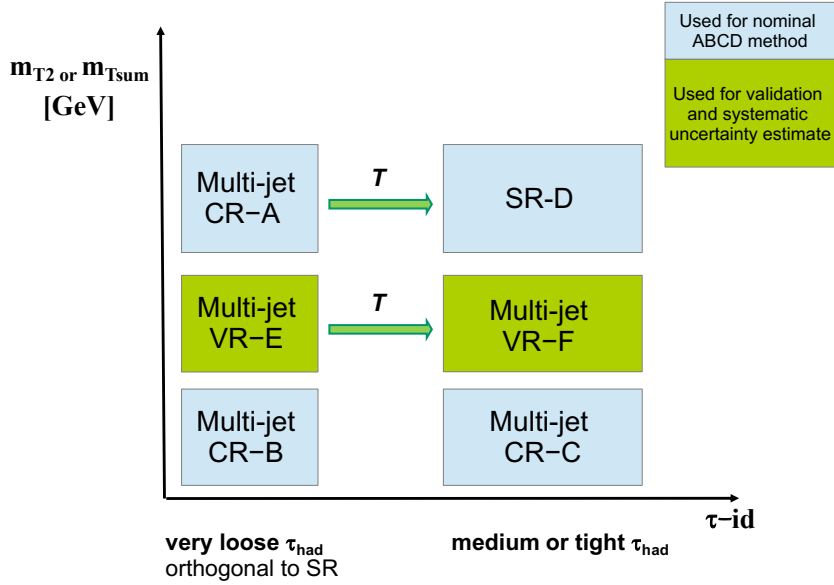


Figure 2: Illustration of the ABCD method for the multi-jet background determination. The control regions A, B, and C and signal region D are drawn as light blue boxes. Shown in green and labeled as VR are the regions E and F, which are used to validate the ABCD method and to estimate the systematic uncertainty.

The discriminating variables used here are the τ -lepton identification (“very loose” τ -leptons as described in Ref.[77], that fail to meet either the medium criterion or OS requirement) and m_{T2} ($10 < m_{T2} < 20$ GeV for regions B and C, $20 < m_{T2} < 30$ GeV for regions E and F, $m_{T2} > 30$ GeV for A and D). The τ -lepton p_T thresholds to ensure high triggering efficiency are not applied, effectively lowering the τ -lepton p_T thresholds to the online thresholds of 80 GeV and 50 GeV (60 GeV) for 2015–2017 (2018) data-taking. This increases the statistics available and reduces the statistical uncertainty without affecting the transfer factor within statistical uncertainties.

Agreement between data and the estimated SM background is found in VR-F, within statistical uncertainties. A validation region (MJVR), with higher multi-jet purity and with the τ -lepton p_T thresholds applied (see Table 2), is also checked. Good agreement is seen, as shown in Figure 3, and a discussion of the systematic uncertainties of the total SM background can be seen in Section 9. The correlation between the τ -lepton identification and the kinematic variables is verified by studying the variation of the transfer factor as a function of the kinematic variables used and is found to be negligible.

The signal contamination in a certain region is defined as the ratio of the number of signal events to the sum of the number of signal events and SM background processes. A significant signal contamination in SM CRs can affect the model-dependent fit and reduce the sensitivity to SUSY scenarios. Thus the CRs (and VRs) are designed to have negligible signal contamination for the SUSY scenarios considered in this paper, particularly for the SUSY particle mass ranges not excluded by previous searches.

6.2.2 W +jets background estimate

The production of W +jets events with at least one misidentified τ -lepton is an important background, composing up to 50% of the expected SM background in the Direct stau SRs. To correct the misidentified

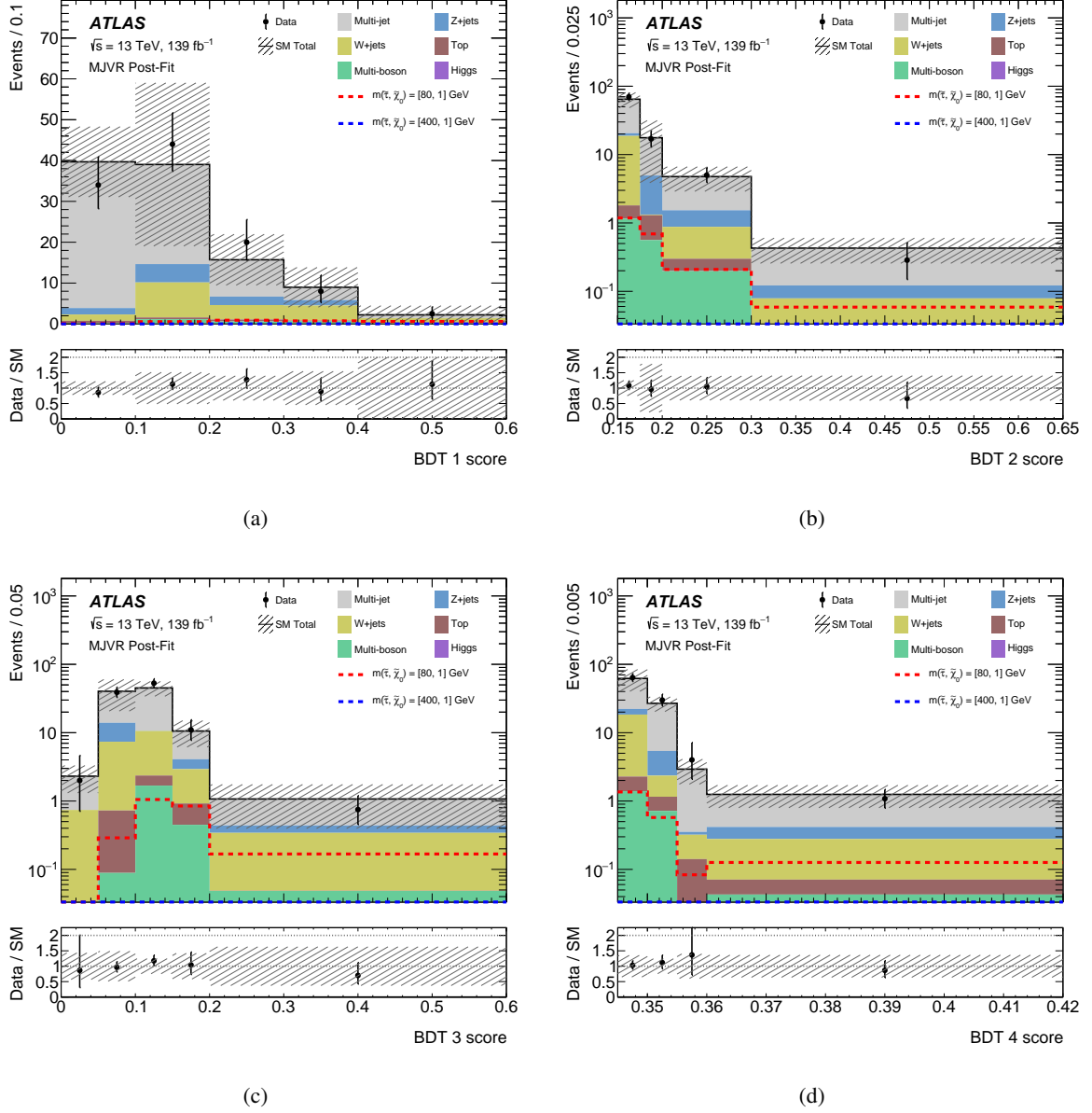


Figure 3: The BDT score distributions for the Direct stau multi-jet background in MJVR after the background-only fit, showing the scores for (a) BDT1, (b) BDT2, (c) BDT3, and (d) BDT4. A reduced range of BDT2 in (b) and BDT4 score in (d) are shown as they populate only a narrow range of the full score allowed. Representative SUSY scenarios are overlaid for illustration. The hatched bands represent the combined statistical and systematic uncertainties of the total SM background. The lower panels show the ratio of data to the total SM background estimate.

Table 2: The definition of the control and validation regions for the Direct stau channel.

Process	W+jets		Top	
Region	WCR	WVR	TCR	TVR
Charge combination	OS			
N medium τ	= 1		= 1	= 2
N tight τ	= 0		-	-
N e/μ	= 1 μ		= 1 μ	= 0
N b -jets	= 0		≥ 1	≥ 1
Trigger	single μ		single μ	asymm. di- τ
$p_T(\tau_1)$ [GeV]	-		-	> 95
$p_T(\tau_2)$ [GeV]	-		-	> 65
$\max[p_T(\tau), p_T(\mu)]$ [GeV]	> 95		> 95	-
$\min[p_T(\tau), p_T(\mu)]$ [GeV]	> 60		> 60	-
E_T^{miss} [GeV]	> 20		> 20	> 20
$m_{T,\mu}$ [GeV]	$\in (50, 150]$		$\in (50, 150]$	-
m_{T2} [GeV]	> 30		> 30	> 30
$m(\tau, \mu)$ [GeV]	> 120		> 120	-
$m(\tau_1, \tau_2)$ [GeV]	-		-	> 120
BDT score	All < 0.5	Any > 0.5		-

Process	Z+jets		Multi-boson	Multi-jet	Inclusive
Region	ZCR	ZVR	MBVR	MJVR	InclVR
Charge combination	OS				
N medium τ	= 2		= 2	= 2	= 2
N e/μ	= 0		= 0	= 0	= 0
N b -jets	= 0		= 0	= 0	= 0
Trigger	asymm. di- τ		asymm. di- τ	asymm. di- τ	asymm. di- τ
E_T^{miss} [GeV]	-		> 20	< 50	> 20
m_{T2} [GeV]	> 30		> 30	> 30	> 30
$m(\tau_1, \tau_2)$ [GeV]	< 120		< 120	> 120	> 120
$\Delta R(\tau_1, \tau_2)$	< 4		< 4	> 3	< 4
BDT1 score	≤ 0.10	> 0.10	-		≤ 0.60
BDT2 score	-	-	-		≤ 0.70
BDT3 score	-	-	-		≤ 0.70
BDT4 score	≤ 0.60	≤ 0.60	> 0.61		≤ 0.60

τ -lepton MC modelling and reduce the theoretical uncertainty from the W +jets background, dedicated control regions pure in W bosons decaying into $\mu\nu$ (WCR) are used to normalize the W +jets MC estimate to data.

Events are required to satisfy a single-muon trigger with increasing p_T thresholds of 21 – 27 GeV throughout data-taking to ensure the trigger efficiencies are in the plateau region [87]. Events must contain exactly one isolated μ matching the trigger signature and one τ -lepton with the same charge selection as the signal regions. The τ -lepton is required to satisfy the medium ID criterion, but fail to meet the tight criterion, to allow future searches targeting direct stau production using one leptonically decaying τ -lepton and one hadronically decaying τ -lepton. The contribution from events with top quarks is suppressed by rejecting events containing b -tagged jets. The contributions from Z +jets, top-quark and multi-boson production are reduced with m_T requirements.

Thresholds on $E_{\text{T}}^{\text{miss}}$ and lepton p_{T} are applied to select events with kinematics similar to the SR definition. Events in the *WCR* are selected by requiring all four BDT scores to be low, while the modelling is checked using a *WVR* with any one of the four BDT scores being high. The definitions of the *WCR* and *WVR* are given in Table 2. The purity of the selection in *W*+jets events is around 83% in the control and validation regions. The signal contamination in the *WCR* and *WVR* is negligible due to the requirement of an isolated muon in these regions.

6.2.3 Z+jets background estimate

The production of *Z*+jets where the *Z* boson decays into two τ -leptons is an irreducible background in the Direct stau SRs, composing 7 – 50% of the total SM background. The *Z*+jets background is estimated by using MC simulation normalized to data in a control region, *ZCR*, which is similar to the SRs, but reverses the selection on $m(\tau_1, \tau_2)$. Events with a low BDT4 score are selected to avoid overlap with the validation region for multi-bosons (Section 6.2.5). A selection on the score for BDT1 is used to create an orthogonal validation region *ZVR* to check the modelling of the normalized *Z*+jets background. The purity of the selection in *Z*+jets events is around 85 – 90% in the control and validation regions. The definitions of the *ZCR* and *ZVR* are shown in Table 2.

6.2.4 Top quark background estimate

Events containing one or more top quarks also contribute significantly to the total background in the Direct stau SRs at 7 – 30%. The top quark background is estimated by using MC simulation normalized to data in a control region, *TCR*, which, like the *WCR*, contains one isolated muon and one medium τ -lepton, but additionally requires a *b*-tagged jet. A validation region, *TVR*, is used to check the modelling of the top quark background in events closer to the signal regions with two medium τ -leptons and a *b*-tagged jet. The purity of the selection in top quark events is around 80 – 92% in the control and validation regions. The definitions of the *TCR* and *TVR* are shown in Table 2.

6.2.5 Multiboson background estimate

Events with more than one SM *W*/*Z* boson are the dominant background in SR-BDT2 and SR-BDT4, with very small contributions from processes involving Higgs bosons in all SRs. These processes produce two real τ -leptons and $E_{\text{T}}^{\text{miss}}$, and this irreducible background is taken from MC simulation. The modelling is checked using two validation regions. The first targets multi-boson production (*MBVR*) using a similar selection to SR-BDT4 but with the selection on $m(\tau_1, \tau_2)$ reversed. The second is a more inclusive validation region (*InclVR*) that checks the overall background estimate strategy and the modelling of the BDT score distributions. The definitions of these regions are shown in Table 2. The background estimate is seen to model the data well in these two regions and the agreement in the BDT score distributions in *InclVR* is shown in Figure 4.

Overall, the background estimate strategy is seen to model the data well in all validation regions used for the Direct stau channel. The yields for the estimated SM background and data are shown in Figure 5 after the background-only fit to data is applied, as described in Section 10.

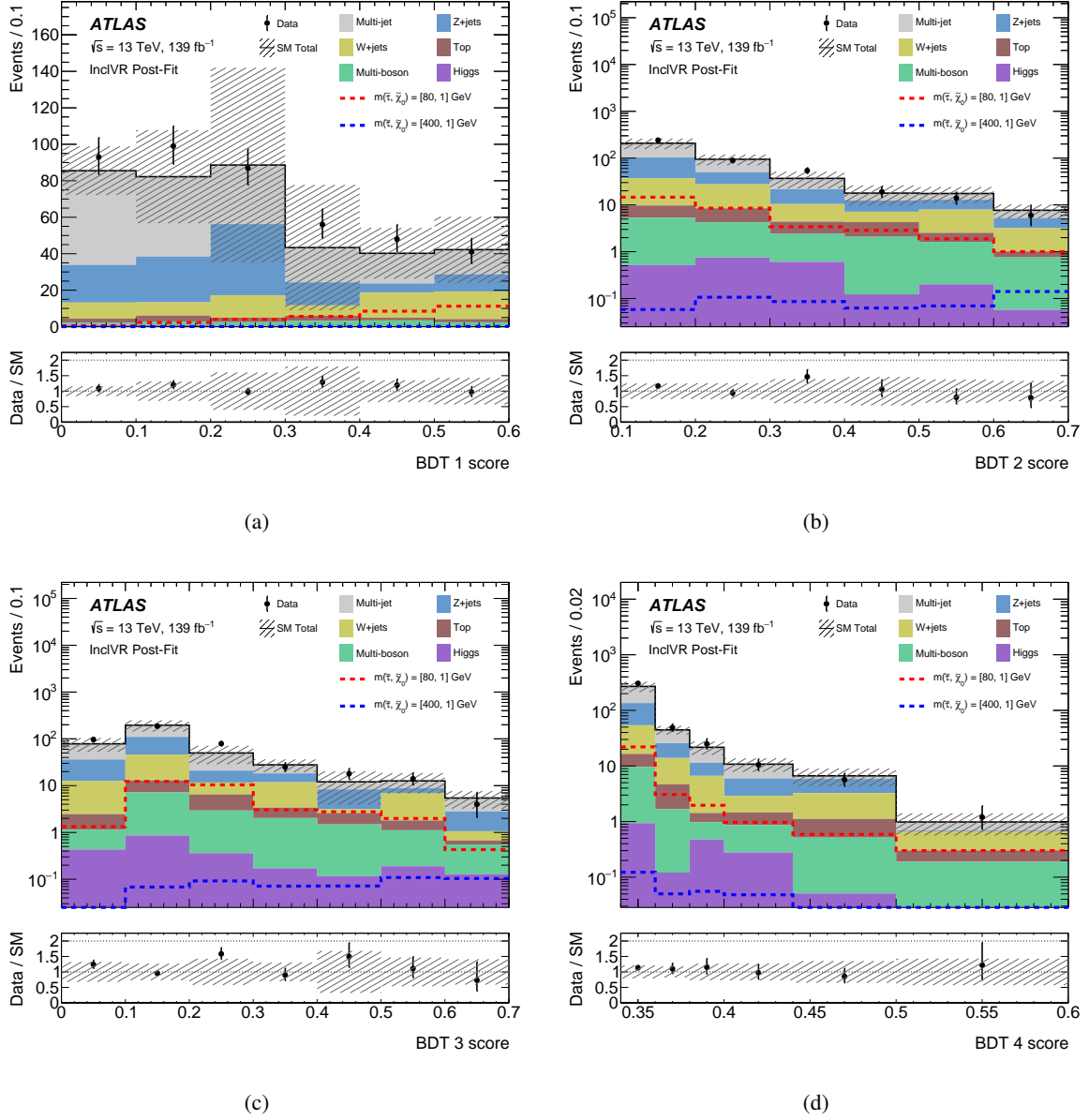


Figure 4: The BDT score distributions for the Direct stau channel in InclVR after the background-only fit, showing the scores for (a) BDT1, (b) BDT2, (c) BDT3, and (d) BDT4. Representative SUSY scenarios are overlaid for illustration. The hatched bands represent the combined statistical and systematic uncertainties of the total SM background. Large uncertainties are seen in some bins due to a few highly weighted Z+jets MC simulation events migrating across bins when considering systematic variations. The lower panels show the ratio of data to the total SM background estimate.

7 Intermediate stau channel

The Intermediate stau channel targets two different production mechanisms, mass-degenerate $\tilde{\chi}_1^\pm \tilde{\chi}_2^0$ (C1N2) and $\tilde{\chi}_1^+ \tilde{\chi}_1^-$ (C1C1), with decays into the lightest neutralino only through intermediate stau and τ -sneutrinos, as shown in Figure 1(b) and Figure 1(c). The C1N2 analysis is then sub-divided into final states where

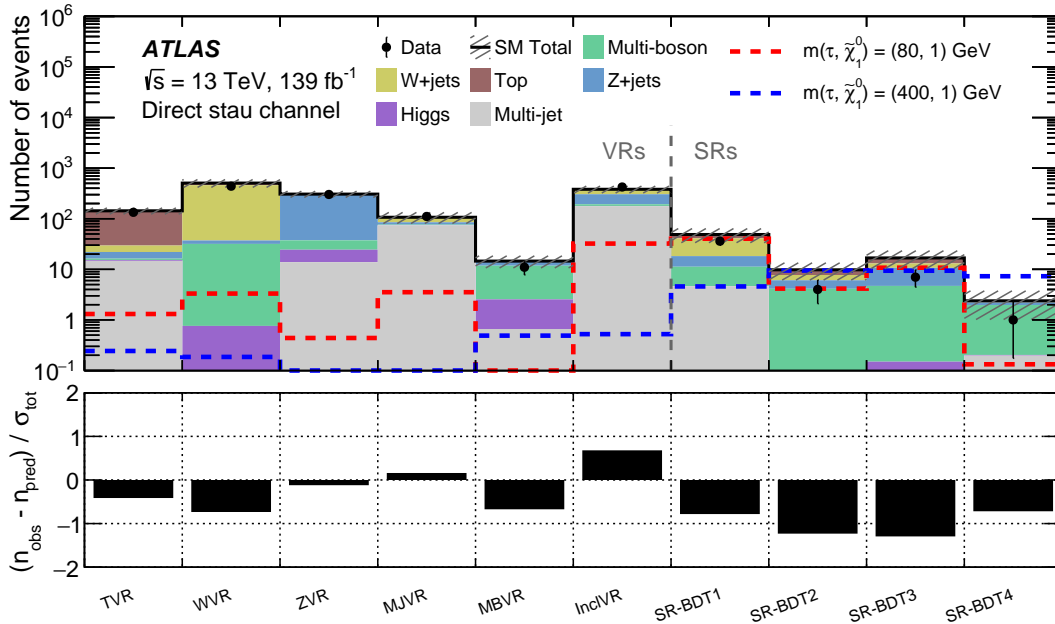


Figure 5: Comparison of the observed and expected event yields in all VRs and SRs after the background-only fit for the Direct stau channel. Representative SUSY scenarios are overlaid for illustration. The hatched band represents the combined statistical and systematic uncertainties of the total SM background. The lower panel shows the significance of any difference between the data and total SM background estimate yields.

the two highest- p_T τ -lepton candidates have opposite sign (OS) charge (C1N2OS) or have same-sign (SS) charge (C1N2SS). The SRs are separated into low-mass (LM) and high-mass (HM) regions to target respectively low or high $\tilde{\chi}_1^\pm/\tilde{\chi}_2^0$ mass regions. The high-mass regions target SUSY scenarios with masses above that probed by the partial Run 2 result from the ATLAS Collaboration [14], and the low-mass regions target SUSY scenarios with smaller mass splittings. The event selections of C1C1, C1N2OS and C1N2SS analyses are described in Section 7.1, and the background estimates are described in Section 7.2.

7.1 Event selection

The SRs are optimised by varying the kinematic selection criteria resulting in six SRs defined to cover LM and HM regions for C1C1, C1N2OS and C1N2SS channels. Events used in this channel must satisfy the same di- τ trigger described in Section 6.1, or a combined di- $\tau + E_T^{\text{miss}}$ trigger. To ensure the trigger efficiencies are in the plateau region, events that satisfy the di- $\tau + E_T^{\text{miss}}$ trigger for 2015–2017 (2018) data sample must have a τ -lepton with $p_T > 50$ (75) GeV, a second τ -lepton with $p_T > 40$ GeV (both matching the trigger signature), and the reconstructed $E_T^{\text{miss}} > 150$ GeV.

For the C1N2OS (C1N2SS) channels, events are required to have at least two medium τ -leptons with OS (SS), while for the C1C1 channel, events are required to have exactly two medium τ -leptons with OS. In the LM signal regions, SR-C1C1-LM and SR-C1N2OS-LM, at least one of the τ -leptons must satisfy a tighter identification criteria, referred to as a tight τ -lepton [77], to suppress quark or gluon jets misidentified as τ -leptons in the lower E_T^{miss} region. Additionally, $E_T^{\text{miss}} > 60$ GeV is required in these two SRs to further suppress background from misidentified τ -leptons.

To discriminate the SUSY signal events from SM background processes, additional requirements are applied, as outlined in Table 3. Background processes producing τ -lepton pairs from low-mass resonances, or from Z or Higgs bosons, are suppressed using high $m(\tau_1, \tau_2)$ selections, while top quark processes are suppressed with a b -jet veto. Contributions from $t\bar{t}$ and WW events are reduced using lower bounds on m_{T2} and $m_{T\text{sum}}$.

Table 3: Summary of the selection requirements for the $\tilde{\chi}_1^+ \tilde{\chi}_1^- / \tilde{\chi}_1^\pm \tilde{\chi}_2^0$ pair production SRs for the Intermediate stau channel.

SR-	C1C1-LM	C1N2OS-LM	C1N2SS-LM	C1C1-HM	C1N2OS-HM	C1N2SS-HM
Trigger	asymm. di- τ			di- $\tau + E_T^{\text{miss}}$		
E_T^{miss} [GeV]	< 150			> 150		
N medium τ	= 2	≥ 2	≥ 2	= 2	≥ 2	≥ 2
N tight τ	≥ 1	≥ 1	–	–	–	–
Charge combination	OS	OS	SS	OS	OS	SS
N b -jets	= 0	= 0	= 0	= 0	= 0	= 0
N jets	–	< 3	< 3	–	–	–
$ \Delta\phi(\tau_1, \tau_2) $	> 1.6	–	> 1.5	–	–	–
$m(\tau_1, \tau_2)$ [GeV]	> 120	> 120	–	> 120	> 120	–
E_T^{miss} [GeV]	> 60	> 60	–	–	–	–
$m_{T\text{sum}}$ [GeV]	–	–	> 200	> 400	> 400	> 450
m_{T2} [GeV]	> 80	> 70	> 80	> 85	> 85	> 80

7.2 Background estimate

The dominant backgrounds in the Intermediate stau SRs are multi-jet production with misidentified τ -leptons, W +jets and Z +jets, multi-boson production, and top quark backgrounds. The multi-jet background accounts for 28–48 % (<17 %) of the total SM yield in high-mass SRs (low-mass SRs) for all three scenarios, while W +jets accounts for 4–16 % of the total background. The multi-jet and W +jets background estimates are presented in Section 7.2.1 and Section 7.2.2, respectively, and use the same methods described in Sections 6.2.1 and 6.2.2. A dedicated CR is used to estimate the top quark backgrounds for the SS final state, where misidentified τ -lepton contributions are a dominant source, as described in Section 7.2.3.

Multi-boson production contributes mainly through events containing real τ -leptons resulting from WW and ZZ decaying into a $\tau\tau\nu\nu$ final state in C1C1 and C1N2OS scenarios, while in the C1N2SS scenario, the main process is WZ decaying into a $\tau\tau\nu$ final state. The contribution from real τ -leptons exceeds 85–90% in Z +jets and diboson production. Additionally, the real τ -lepton contribution exceeds 80% in backgrounds containing top quarks in OS final states. The estimation of the Top, multiboson, and Z +jets backgrounds is described in Section 7.2.4.

7.2.1 Multi-jet background estimate

The same approach for the multi-jet background estimate described in Section 6.2.1 is used for the Intermediate stau channels, with the following changes. The sign of the electric charge of the two τ -leptons (OS or SS), and m_{T2} and $m_{T\text{sum}}$ are used to define the control regions and validation regions, as shown in Table 4. In the C1C1 and C1N2OS scenarios, the m_{T2} variable is used to distinguish the regions of the ABCD method, while $m_{T\text{sum}}$ is used for the C1N2SS channel. In all validation regions and both

sets of CR-B and CR-C, the events are required to satisfy a di- τ trigger, instead of the di- $\tau + E_T^{\text{miss}}$ trigger in the Intermediate stau channel to increase the statistics from the lower E_T^{miss} requirements. The offline $E_T^{\text{miss}} > 150$ GeV requirement is also removed. The di- τ trigger requires the identification of two hadronically decaying τ -leptons with transverse momenta exceeding the same set of thresholds for the di- $\tau + E_T^{\text{miss}}$ trigger, such that no bias on the τ -leptons is introduced.

Table 4: The definition of the ABCD regions for all channels in the Intermediate stau scenarios. Only those requirements that differ between the CRs/VRs and the SRs are listed.

Channel	variable	CR-B / CR-C	VR-E / VR-F	CR-A / SR
C1C1-LM	m_{T2} [GeV]	$\in (15, 35]$	$\in (35, 80]$	> 80
	E_T^{miss} [GeV]	$\in (10, 150]$	$\in (10, 150]$	$\in (60, 150]$
C1C1-HM	m_{T2} [GeV]	$\in (35, 60]$	$\in (60, 85]$	> 85
	$m_{T\text{sum}}$ [GeV]	$\in (100, 300]$	$\in (200, 400]$	> 400
	E_T^{miss} [GeV]	> 50	> 50	> 150
C1N2OS-LM	m_{T2} [GeV]	$\in (15, 35]$	$\in (35, 70]$	> 70
	E_T^{miss} [GeV]	$\in (10, 150]$	$\in (10, 150]$	$\in (60, 150]$
C1N2OS-HM	m_{T2} [GeV]	$\in (35, 60]$	$\in (60, 85]$	> 85
	$m_{T\text{sum}}$ [GeV]	$\in (150, 300]$	$\in (200, 400]$	> 400
	E_T^{miss} [GeV]	> 50	> 50	> 150
C1N2SS-LM	$m_{T\text{sum}}$ [GeV]	< 100	$\in (100, 200]$	> 200
	$ \Delta\phi(\tau_1, \tau_2) $	< 1.5	< 1.5	> 1.5
C1N2SS-HM	$m_{T\text{sum}}$ [GeV]	$\in (100, 200]$	$\in (200, 450]$	> 450
	E_T^{miss} [GeV]	> 50	> 50	> 150

The estimated SM background is found to agree with the data for the m_{T2} and $m_{T\text{sum}}$ distributions in the validation regions, as shown in Figure 6. Several signal reference points targeting sensitivity to LM and HM SRs are also shown to highlight the small signal contamination in the VRs.

7.2.2 W +jets background estimate

The W +jets background is an important background for the Intermediate stau channel. A similar approach as in Section 6.2.2 is used and definitions for the W +jet CRs and VRs (W CR and W VVR) for OS/SS selections are shown in Table 5. Top quark background events in the OS final state are labeled as “top-tagged” if they satisfy a dedicated selection; these events are vetoed in the W CR to suppress top quark background processes. Events are top-tagged using the contranverse mass variable [88], m_{CT} , to identify events that are kinematically compatible with $t\bar{t}$ pair production. Furthermore, top-tagged events must have at least two jets and the scalar sum of the p_T of at least one combination of two jets and the two leptons in the event must exceed 100 GeV. The orthogonality of the W CRs and W VVRs is ensured using $m_{T2}(\tau, \mu)$ selections. The purity of the selection in W +jets events is 73–85 % in all W control and validation regions. The signal contamination in the W CR and W VVR is negligible due to the requirement of a muon in the event.

The multi-jet contribution in the W CRs and W VVRs is small and is estimated using the lack of correlation of the charge of the faked muon and τ -lepton in multi-jet production, resulting in equal SS and OS lepton contributions. This is not the case for other processes like W +jets production, which is dominated by g_u/g_d -initiated processes that often give rise to a jet originating from a quark, the charge of which is

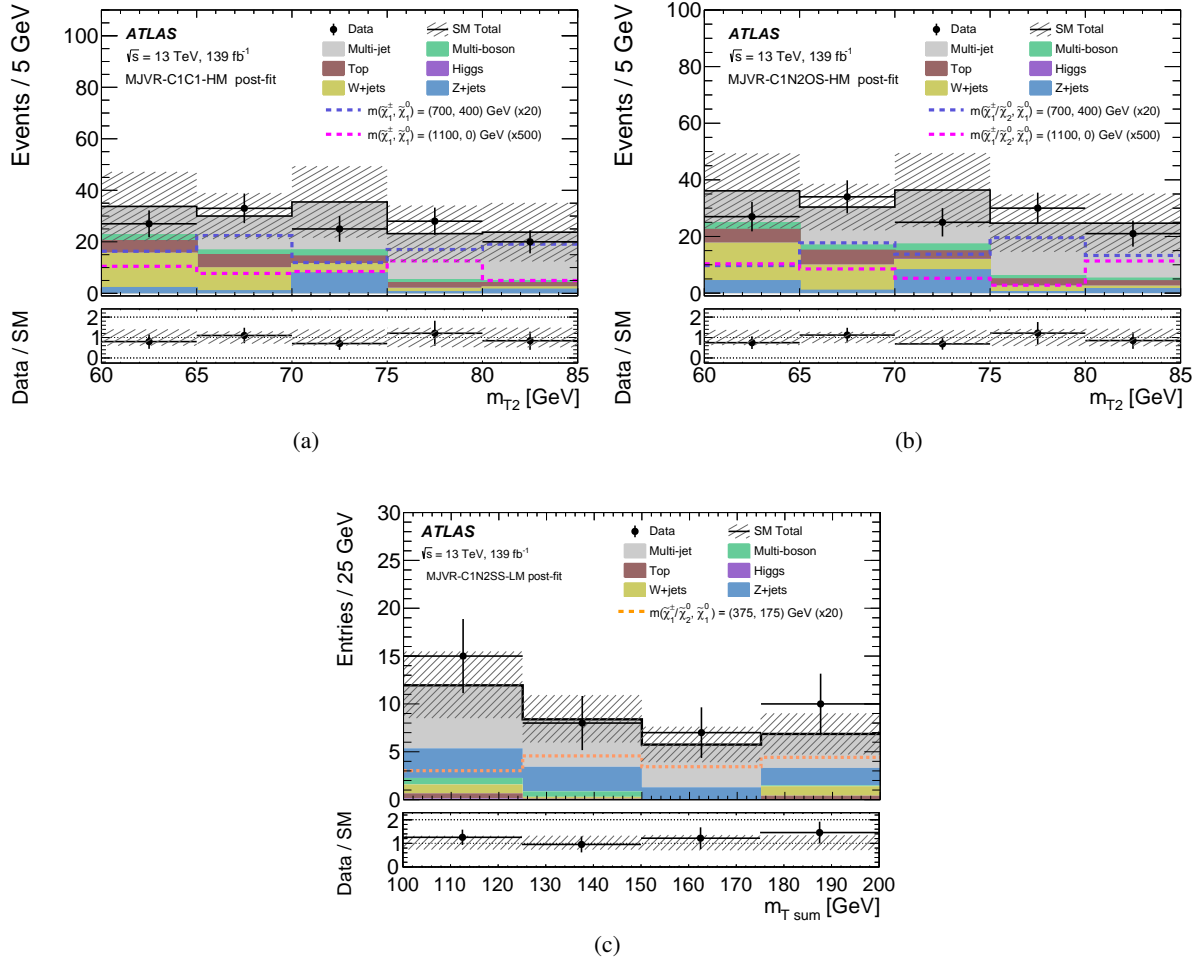


Figure 6: The kinematic distributions of m_{T2} and $m_{T\text{sum}}$ in the multi-jet background VR-F after the background-only fit for (a) SR-C1C1-HM (MJVR-C1C1-HM), (b) SR-C1N2OS-HM (MJVR-C1N2OS-HM) and (c) SR-C1N2SS-LM (MJVR-C1N2SS-LM), respectively. Representative SUSY scenarios are overlaid for illustration and scaled appropriately for improved visibility. The hatched bands represent the combined statistical and systematic uncertainties of the total SM background. The lower panels show the ratio of data to the total SM background estimate.

anti-correlated with the W -boson charge. The contribution from multi-jet production in the W CRs and W VRs is estimated using data in regions selected with the same requirements as the CR/VR but requiring the electric charge of the two leptons to be different, i.e. SS for OS CR/VR, and OS for SS CR/VR. Event yields from SM processes other than multi-jet production are subtracted from the data in these regions using MC simulation, leaving only the multi-jet estimate, which is assumed to be equal to that in the CR/VR. Based on studies with simulated samples, a conservative systematic uncertainty of 100 % is assigned to the estimate of the multi-jet event yield in the W +jets CRs and VRs.

Table 5: The definition of the control and validation regions for the Intermediate stau channel.

Process	W+jets				Top			
Region	WCR-OS	WVR-OS	WCR-SS	WVR-SS	TCR-SS-HM	TVR-SS-HM	TVR-OS-LM	TVR-OS-HM
Charge combination	OS		SS		SS		OS	
Trigger	single μ				di- $\tau + E_T^{\text{miss}}$		asymm. di- τ di- $\tau + E_T^{\text{miss}}$	
N medium τ	= 1				< 2		≥ 2	
N tight τ	-				-		≥ 1	
N loose τ	-				≥ 1		-	
N “very loose” τ	-				≥ 2		-	
N e/μ	= 1 μ				-		-	
N b -jets	= 0				≥ 1		≥ 1 = 0	
$p_T(\tau)$ [GeV]	> 50				-		-	
$p_T(\mu)$ [GeV]	> 40				-		-	
Top tagged	veto		-		-		-	
$m_{T,\mu}$ [GeV]	< 140		$\in (50, 150]$		-		-	
$m_{T,\mu} + m_{T,\tau}$ [GeV]	-		> 80		-		-	
E_T^{miss} [GeV]	> 60		> 50		> 150		$\in (20, 150]$ > 150	
$m(\tau_1, \tau_2)$ [GeV]	-		-		-		> 120 > 120	
m_{T2} [GeV]	$\in (40, 70]$	> 70	< 60	> 60	-	-	> 40	> 30
$m_{T\text{sum}}$ [GeV]	-	-	-	-	< 400	> 400	> 150	> 150
$ \Delta\phi(\tau_1, \tau_2) $	-	-	-	-	-	-	> 1.0	> 1.0

Process	Z+jets		Multi-bosons		
Region	ZVR-OS-LM	ZVR-OS-HM	MBVR-OS-LM	MBVR-OS-HM	MBVR-SS
Charge combination	OS		OS		SS
Trigger	asymm. di- τ di- $\tau + E_T^{\text{miss}}$		asymm. di- τ di- $\tau + E_T^{\text{miss}}$		single μ
N medium τ	≥ 2		≥ 2		= 1
N tight τ	≥ 1		≥ 1		-
N μ	-		-		= 2
N b -jets	= 0		= 0		= 0
E_T^{miss} [GeV]	$\in (40, 150]$	> 150	$\in (70, 150]$	> 150	> 100
$m(\tau_1, \tau_2)$ [GeV]	< 70	< 60	< 80	< 90	-
$\Delta R(\tau_1, \tau_2)$	< 1.0	< 1.0	< 1.2	< 1.2	-
$ \Delta\phi(\tau_1, \tau_2) $	-	-	< 1.0	< 1.0	-
$ \Delta\phi(\tau_1, \mathbf{p}_T^{\text{miss}}) $	-	-	-	-	≤ 1.75
$m_{T\text{sum}}$ [GeV]	-	-	> 180	> 180	-
m_{T2} [GeV]	< 60	< 60	> 60	> 60	-

7.2.3 Top quark background estimate for C1N2SS

The top quark background in SR-C1N2SS-LM is very small (<1%) and mostly composed of two real τ -leptons, and hence is estimated from MC simulation. However, the top quark background is a dominant contribution in SR-C1N2SS-HM and mostly consists of one or two misidentified τ -leptons from $t\bar{t}$ and Wt production. To estimate this background in SR-C1N2SS-HM, a data-driven approach is used to normalize the top quark background MC simulation to data using a dedicated top-enriched CR (TCR-SS-HM) and validated in a top-enriched VR (TVR-SS-HM), described in Table 5. The τ -lepton identification working point was loosened to increase the statistics in these regions, while high E_T^{miss} is required to suppress the contribution from multi-jet processes. The top quark background purity in the top quark CR and VR for SR-C1N2SS-HM (TCR-SS-HM and TVR-SS-HM) is high and exceeds 83% in both regions.

7.2.4 Top, multiboson, and Z+jets background estimates

Additional irreducible SM backgrounds are estimated from MC simulation and checked in dedicated VRs. The top quark background contributions in OS final states are small and amount to about 7–14% of the

total background in all SRs. Two regions enriched in top-quark events are defined to validate the top quark modelling in OS events, TVR -OS-LM and TVR -OS-HM for the low and high-mass SR kinematics, respectively, and are defined in Table 5.

The Z +jets contribution is 16–21 % of the total background in all OS SRs and mainly arises from $Z \rightarrow \tau\tau$ decays. The multi-boson background accounts for 25–50 % of the total SM contribution in the SRs and mainly arises from $WW \rightarrow \tau\nu\tau\nu$ and $ZZ \rightarrow \tau\tau\nu\nu$ events. Over 96 % of τ -leptons from Z +jets and multi-bosons events in the SRs are real. To validate the MC modelling and normalization of the Z +jets and multi-boson processes, four dedicated VRs are defined: ZVR -OS-LM ($MBVR$ -OS-LM) is defined to validate Z +jets (multi-boson) MC modelling in the low-mass SRs, while ZVR -OS-HM ($MBVR$ -OS-HM) is defined to validate the MC modelling in the high-mass SRs, as shown in Table 5.

The purity of the selection in $t\bar{t}$ and Z +jets events is in the range of 81–99 % in the respective validation regions, and the purity of the selection in multi-boson events is 41–68 % in the OS $MBVR$ s. The signal contamination in the VRs is small due to the b -jet requirement in the top-quark VRs and the $m(\tau_1, \tau_2)$ upper thresholds in the Z +jets and multi-boson VRs.

In the SS final state, the multi-boson background is estimated from MC simulation and validated in a dedicated VR, $MBVR$ -SS, also defined in Table 5. The selection is enriched in multi-boson production, resulting in a multi-boson purity of 73%.

The agreement between data and the SM prediction is shown in all validation and signal regions for the Intermediate stau channels in Figure 7 after the background-only fit to data is applied, as described in Section 10.

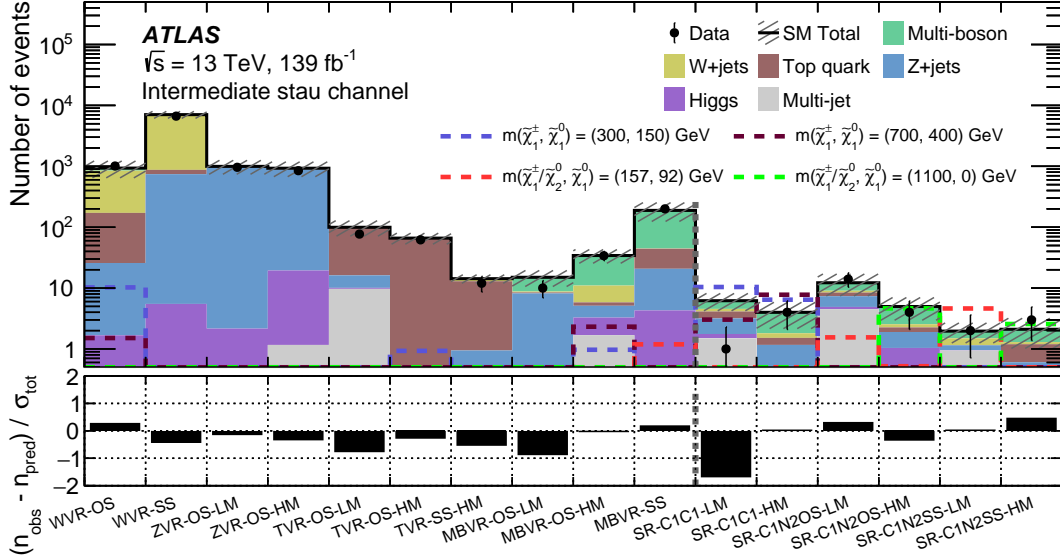


Figure 7: Comparison of the observed and expected event yields in all VRs and SRs after the background-only fit for the signal regions targeting chargino/neutralino production and decay via intermediate staus. Representative SUSY scenarios are overlaid for illustration. The hatched band represents the combined statistical and systematic uncertainties of the total SM background. The lower panel shows the significance of any difference between the data and total SM background estimate yields.

8 Intermediate Wh channel

The search for the production of mass-degenerate $\tilde{\chi}_1^\pm \tilde{\chi}_2^0$ decaying via an intermediate W and h boson, as shown in Figure 1(d), is described in this section. The analysis targets the leptonic decay of the W boson to an electron or muon, and the decay of the Higgs boson to two OS τ -leptons. The event selection of the Intermediate Wh channel is described in Section 8.1 and the background estimates are described in Section 8.2.

8.1 Event selection

Events for the Intermediate Wh channel must have at least two hadronically decaying τ -leptons with OS and exactly one light lepton (e or μ). The selected light lepton must satisfy the signal electron or muon requirements described in Section 4 and also satisfy the single electron or single muon trigger with a threshold of $p_T > 27$ GeV to ensure the triggering efficiency is in the plateau region. Two SRs are defined to cover low-mass (SR-Wh-LM) and high-mass (SR-Wh-HM) $\tilde{\chi}_1^\pm \tilde{\chi}_2^0$ production, with an overlapping selection, as shown in Table 6. To set limits in a SUSY scenario, the SR with the best expected sensitivity is used. The invariant mass of the two τ -leptons, $m(\tau_1, \tau_2)$, is required to be compatible with the Higgs boson mass, while the b -jet veto and $|\Delta R(\tau_1, \tau_2)|$ requirements suppress the top quark and fake τ -lepton backgrounds, respectively. High m_{T2} , $m_{T,\ell}$ and $m_{T\text{sum}}$ requirements provide good discrimination between SUSY signal events and SM background.

Table 6: Summary of selection requirements for the SRs of $\tilde{\chi}_1^\pm \tilde{\chi}_2^0$ pair production decaying into an intermediate Wh for low-mass and high-mass regions. The two SRs are not orthogonal.

	SR-Wh-LM	SR-Wh-HM
Trigger	Single e or μ	
N medium τ	≥ 2	
N e/μ	$= 1$	
Charge combination	OS	
N b -jets	$= 0$	
$ \Delta\phi(\tau_1, \tau_2) $	< 3	
$\Delta R(\tau_1, \tau_2)$	–	< 2.2
$m(\tau_1, \tau_2)$ [GeV]	$\in [90, 130]$	$\in [80, 160]$
m_{T2} [GeV]	> 100	> 80
$m_{T,\ell}$ [GeV]	–	> 80
$m_{T\text{sum}}$ [GeV]	–	> 450

8.2 Background estimate

The SM backgrounds for a final state with two hadronically decaying τ -leptons from a Higgs boson decay and one light lepton from a W -boson decay can be separated into two groups. The first group is composed of events with a real light lepton and two real τ -leptons, and is dominated by multi-boson processes that are estimated by using MC simulation, as described in Section 8.2.3. The second group includes processes with one or two τ -leptons from misidentified jets. Events with a single misidentified τ -lepton are dominated by events with a top quark, which is estimated by using MC normalized to data in a dedicated CR and described in Section 8.2.2. Events with two misidentified τ -leptons are mostly from W +jets events and are

estimated by using a data-driven technique – the fake factor method – as described in Section 8.2.1. All other SM backgrounds are estimated directly from MC simulation. Overall, the dominant background contributions in both SRs are from top quark and multi-boson processes, and account for 89%–90% of the total background.

8.2.1 Misidentified τ -lepton background estimate

The W +jets process dominates the background with two misidentified τ -leptons, with less than 7% contribution from other processes. The fake factor method estimates all processes with two misidentified τ -leptons using a control data sample (FFCR) with τ -leptons that fail to meet the nominal τ -lepton identification requirement. This estimate is obtained as the product of the number of FFCR events and the fake factor (FF), which relates the number of events with looser τ -lepton candidates to the number where τ -leptons meet the nominal identification criteria.

To compute the FF, an anti- τ -lepton (\bar{T}) is defined that satisfies a looser set of identification criteria, but fails to meet the medium identification criteria of τ -leptons (T). The FF value is the ratio of T events to \bar{T} events. To estimate the two misidentified τ -lepton contributions, three control regions are defined using the identification criteria applied to the two highest- p_T τ -leptons: $\bar{T}\bar{T}$, $T\bar{T}$, and TT . The estimate of the contribution from processes with two misidentified τ -leptons (N_{fakes}) can be written as the product of the two fake factors ($\text{FF}_{\tau i}^{\text{CR}}$) and the number of events from the $\bar{T}\bar{T}$ region ($N_{\bar{T}\bar{T}, \text{fake bkg}}$):

$$N_{\text{fakes}} = N_{\bar{T}\bar{T}, \text{fakes}} \times \text{FF}_{\tau 1}^{\text{CR}} \times \text{FF}_{\tau 2}^{\text{CR}}, \quad (1)$$

where the individual fake factors for the two τ -leptons are written as:

$$\text{FF}_{\tau 1}^{\text{CR}} = \frac{N_{\text{data}, T\bar{T}} - N_{\text{MC}, T\bar{T}}^{\geq 1 \text{ truth } \tau}}{N_{\text{data}, \bar{T}\bar{T}} - N_{\text{MC}, \bar{T}\bar{T}}^{\geq 1 \text{ truth } \tau}} \quad \text{and} \quad (2)$$

$$\text{FF}_{\tau 2}^{\text{CR}} = \frac{N_{\text{data}, TT} - N_{\text{MC}, TT}^{\geq 1 \text{ truth } \tau}}{N_{\text{data}, T\bar{T}} - N_{\text{MC}, T\bar{T}}^{\geq 1 \text{ truth } \tau}}. \quad (3)$$

The contamination from events with at least one real τ -lepton ($N_{\text{MC}}^{\geq 1 \text{ truth } \tau}$) is estimated from MC simulation and subtracted when calculating the ratio.

The fake factors are calculated in a W -enriched control region (FFCR-Wh), which maximises available statistics by loosening kinematic selection requirements and remains orthogonal to the SRs by inverting the OS requirement, as summarised in Table 7.

The fake factor dependencies on the parameters of the τ -leptons, such as the number of tracks, p_T and $|\eta|$, are studied and are found to be minimal except for the number of tracks (1-prong or 3-prong τ -leptons). The fake factors are measured in bins of p_T and $|\eta|$, separately for 1-prong and 3-prong τ -leptons, with the binning optimised based on the available statistics. The fake factor for the two highest- p_T τ -leptons is similar at around 0.4 (0.1) for the 1-prong (3-prong) τ -leptons. The fake factor estimate is validated in a misidentified τ -lepton dominated VR (FFVR-Wh) with a selection similar to the SR-Wh-LM with loosened selections on $m(\tau_1, \tau_2)$ and m_{T2} , as shown in Table 7. The kinematic distributions in FFVR-Wh are shown in Figure 8 and good agreement between data and SM prediction is observed.

Table 7: The definition of the fake factor control and validation regions, FFCR-Wh and FFVR-Wh, respectively.

	FFCR-Wh	FFVR-Wh
N medium τ	–	≥ 2
N “very loose” τ	≥ 2	–
Charge combination	SS	OS
$N e/\mu$		$= 1$
$N b$ -jets		$= 0$
$ \Delta\phi(\tau_1, \tau_2) $		< 3
$m(\tau_1, \tau_2)$ [GeV]	> 20	$\in [40, 160]$
m_{T2} [GeV]	> 20	> 30

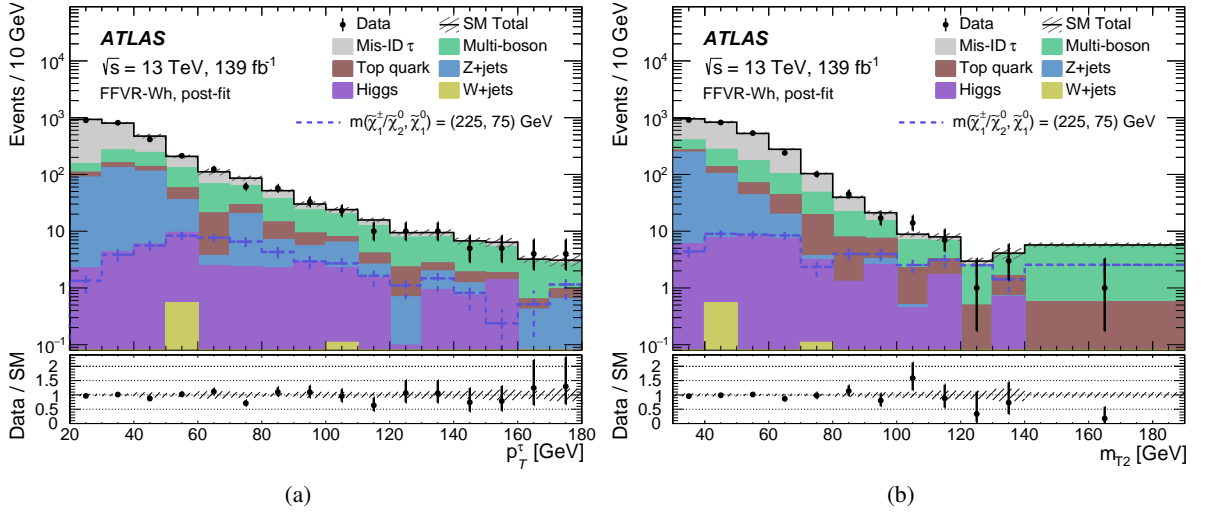


Figure 8: The distributions of (a) the highest- p_T τ -lepton transverse momentum p_T^τ and (b) m_{T2} variables in FFVR-Wh after the background-only fit. The misidentified contribution with at least two misidentified τ -leptons (Mis-ID τ) is estimated from data using the fake factor method. Representative SUSY scenarios are overlaid for illustration. The hatched bands represent the combined statistical and systematic uncertainties of the total SM background. The lower panels show the ratio of data to the total SM background estimate.

8.2.2 Top quark background estimate

The top quark background is small in SR-Wh-HM and is accounted for in the estimate with the FF method since it is dominated by two misidentified τ -leptons. However, in SR-Wh-LM the top quark background is more important and is comprised mainly of $t\bar{t}$ events with one W -boson decaying into an electron or muon, and the other into a τ -lepton – the second τ -lepton typically originates from a misidentified jet. The top quark background is estimated from MC and normalized to data using a top quark enriched control region (TCR-Wh) and validated in a top-quark VR (TVR-Wh), as defined in Table 8. MC simulation shows the top quark background composition is similar across the CR, VR and SR. The selection for the control and validation region are similar to the SR selection, but with one or two b -jets required to be orthogonal to the SR. To increase the statistics, the OS requirement is removed and the $m(\tau_1, \tau_2)$ requirement is also loosened, and to improve the purity of the top quark background, high $m_{T\text{sum}}$ is required. The top quark background purity is between 73%–81% in the CR and VR.

Table 8: The definition of the top quark and multi-boson control and validation regions for the Intermediate Wh channel.

Process	Top		Multi-boson
Region	TCR-Wh	TVR-Wh	MBVR-Wh
N medium τ	≥ 2		
Charge combination	OS		
$N e/\mu$	$= 1$		
Trigger	single e/μ		
$ \Delta\phi(\tau_1, \tau_2) $	< 3		
$N b$ -jets	$\in [1, 2]$		$= 0$
$p_{T\tau_2}$ [GeV]	-		> 30
$m_{T,l}$ [GeV]	-		> 70
$m(\tau_1, \tau_2)$ [GeV]	$\in (40, 160]$		$\in (40, 70]$
$m_{T\text{sum}}$ [GeV]	> 250		-
m_{T2} [GeV]	$\in (20, 80]$	> 80	< 80

8.2.3 Multi-boson background estimate

Multi-boson production is the dominant SM contribution in both the Intermediate Wh SRs. The main contribution is WZ production with both the bosons decaying leptonically, giving one light lepton and two real τ -leptons in the SRs. Smaller contributions in SR-Wh-LM stem from ZZ or WW production decaying into one light lepton, one real τ -lepton, and one misidentified τ -lepton.

The multi-boson background is estimated from MC simulation and validated in a multi-boson enriched region, MBVR-Wh, defined in Table 8. The selection on the invariant mass of the τ -leptons is lowered compared with the SRs, and an upper threshold on m_{T2} of 80 GeV is required. The multi-boson purity is found to be 61% in MBVR-Wh. The good agreement between data and the SM prediction is shown in the validation and signal regions for the Intermediate Wh channels in Figure 9.

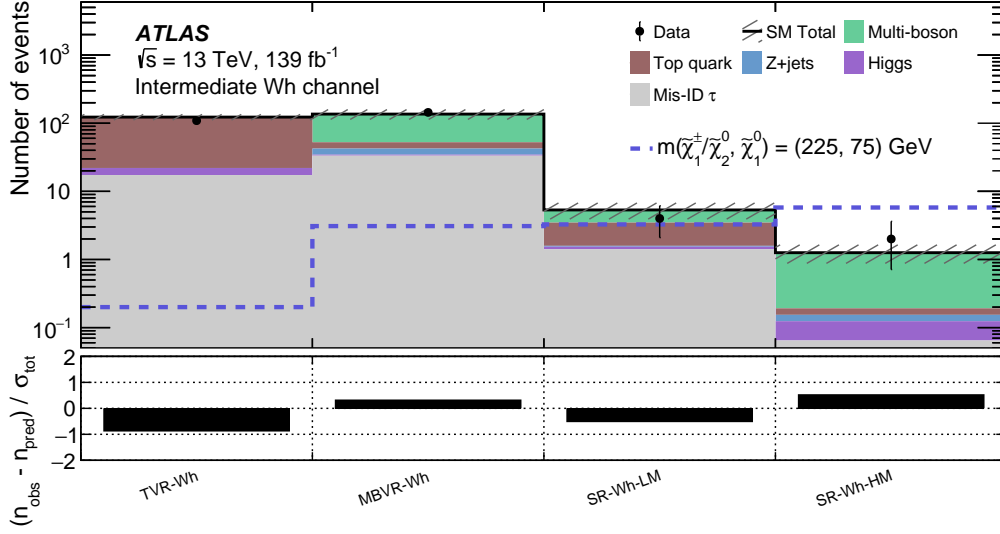


Figure 9: Comparison of the observed and expected event yields in the TVRs and MBVRs and two SRs after the background-only fit. Representative SUSY scenarios are overlaid for illustration. The hatched band represents the combined statistical and systematic uncertainties of the total SM background. The lower panel shows the significance of any difference between the data and total SM background estimate yields.

9 Systematic uncertainties

Systematic uncertainties have an impact on the background and signal estimates in the control and signal regions. Uncertainties arising from experimental effects and theoretical sources are considered. The main sources of experimental systematic uncertainty in the SM background estimates include τ -lepton and jet energy calibrations and resolution, τ -lepton identification, systematic effects due to the presence of pileup events, and uncertainties related to the modelling of E_T^{miss} in the simulation. The uncertainties in the energy and momentum scale of each of the objects entering the E_T^{miss} calculation are estimated, as well as the uncertainties in the soft-term resolution and scale [89]. A variation in the pileup reweighting of the MC simulated event samples is included to cover the uncertainty in the ratio of the predicted and measured inelastic cross-section [90]. The uncertainty in the combined 2015–2018 integrated luminosity was measured to be 1.7% [91], obtained using the LUCID-2 detector [92] for the primary luminosity measurements.

Theoretical uncertainties affecting the main irreducible backgrounds W +jets, Z +jets, top quark processes, and dibosons, are estimated by varying the generator parameters: renormalization and factorisation scales, as well as PDFs, following the PDF4LHC recommendations [93]. Uncertainties due to the choice of renormalization and factorisation scales are included by varying the scales from their nominal values by a factor of two or one half – the two scale variations are taken as uncorrelated and the additional coherent up/down variation of the two scales is also considered. Additionally, cross-section uncertainties are assigned to be included in the normalization of the signal and the background processes taken directly from MC simulation.

Several sources of uncertainty are considered for the ABCD method used to determine the multi-jet background estimate for Direct stau channel and the Intermediate stau channel, they include: the correlation between the τ -lepton identification and the kinematic variables m_{T2} , the limited number of events in

the CRs, and the subtraction of other SM backgrounds. The systematic uncertainty in the correlation is estimated by using the transfer factor from VR-E to VR-F instead of that from CR-B to CR-C. The systematic uncertainty in the non-multi-jet background subtraction in the control regions is estimated by considering the total uncertainties of the MC estimates of the non-multi-jet background in the CRs. The systematic uncertainty due to the limited number of events in the control regions is estimated by taking the statistical uncertainty of the event yields in these control regions. The statistical uncertainty from the data yields in every CR is propagated to the uncertainty on the background estimation in the SRs.

The different sources of uncertainty considered for the fake factor method used to determine the misidentified background with at least two misidentified τ -leptons in the Intermediate Wh channel are as follows. The fake factor values are varied up and down by their statistical uncertainties and the difference is used as a source of uncertainty. A further 30% systematic uncertainty in the subtracted MC processes is used as a conservative estimate on the systematic uncertainty from MC subtractions in the FFCR-Wh. The difference between the quark/gluon contributions in the fake factor control regions and signal regions was studied and found to be negligible compared with the uncertainties placed on the overall normalization and statistical contributions. The systematic uncertainties and their sizes in each SR are summarized in Figure 10.

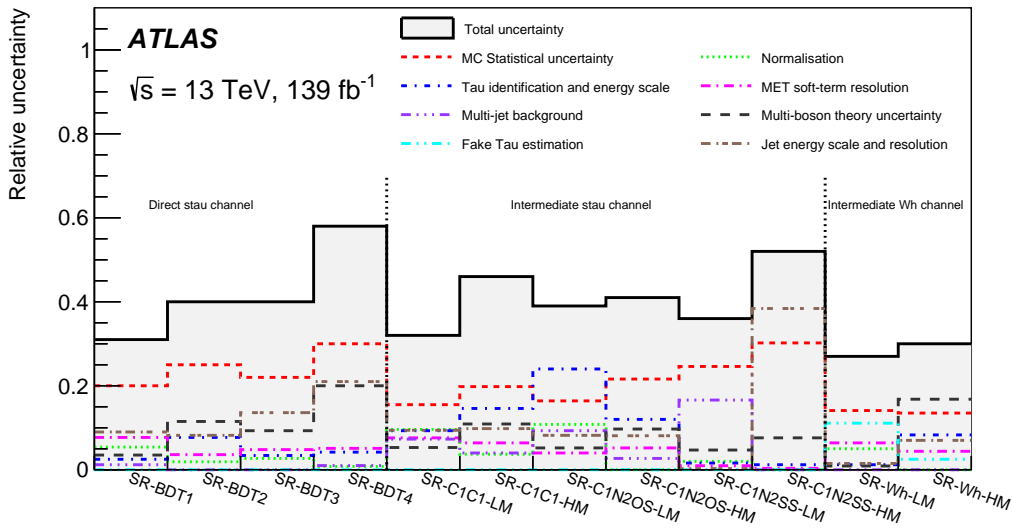


Figure 10: Summary of the total uncertainty in the predictions of the background event yields of each SR in the three search channels. The dominant systematic contributions are indicated by individual dashed/dot-dashed/dotted lines. The total uncertainty in each SR is denoted by the solid black line. For simplicity, the individual uncertainties are added in quadrature for each category, without accounting for correlations. Theoretical uncertainties in the multiboson MC simulation-based estimates are grouped under the “Multi-boson theory uncertainty” category, while the “Normalisation” category includes the statistical uncertainties of the data counts in the CRs and the uncertainty from the fitted normalization factors.

The dominant contributions of systematic uncertainties in all scenarios are mainly from the statistics of the MC samples, the normalization uncertainties of the multi-jet background, the τ -lepton identification and the energy scale, jet energy scale and resolution. In the Intermediate stau channel, uncertainties in the multi-jet estimate are also important. In the Direct stau and Intermediate Wh channels, multi-boson theory uncertainties represent a major contribution to the systematics.

10 Results

The results of the Direct stau, Intermediate stau, and Intermediate Wh channels are presented in this section as background-only combined fits to the control and signal regions, along with model-dependent and model-independent fits for BSM signal exclusion.

10.1 Direct stau production analysis

The expected and observed numbers of events in the Direct stau signal regions are shown in Table 9, where the observations are consistent with the SM expectations. The distributions of the four BDT scores are shown in Figure 11. All the SR-BDT strongly overlap and show a common deficit of significance $0.7 - 1.3 \sigma$. For example, the single event in data selected by SR-BDT4 is also selected by the other three SR-BDT, while the four events in SR-BDT2 are also selected by SR-BDT3. The W +jets, Z +jets, and top quark backgrounds are normalized to data in their respective control regions, obtaining normalization factors of 0.93 ± 0.11 , 0.91 ± 0.07 , and 0.85 ± 0.05 , respectively, as shown in Table 10.

The model-dependent fits using the results from the signal and control regions are used to place exclusion limits at 95% CL on Direct stau production. SR-BDT4 has a low predicted yield, so 10,000 pseudoexperiments are used to calculate the exclusion limits. Since the four main SR-BDT overlap, the SR with the lowest expected CLs value for each signal scenario is used to set the limit, statistically combining the two bins each within SR-BDT1, SR-BDT2, and SR-BDT3 as two distinct regions. The exclusion limits for mass-degenerate $\tilde{\tau}_{L,R}$ production are shown in Figure 12(a), where stau masses up to 500 GeV are excluded for massless $\tilde{\chi}_1^0$. The limits are improved relative to previous results, particularly towards smaller $\tilde{\tau}$ - $\tilde{\chi}_1^0$ mass splittings, as well as at higher $\tilde{\tau}$ masses. The observed limits are stronger than the expected limit due to the small observed deficit. The feature in the observed limit around stau masses of 250 – 300 GeV is due to a transition from one SR-BDT to another being used to set the limit (a similar effect is also seen for Figures 12(b)-12(c)).

The exclusion limits for $\tilde{\tau}_L$ and $\tilde{\tau}_R$ production separately are shown in Figure 12(b) and Figure 12(c), respectively. Similar improvements are seen in the sensitivity to $\tilde{\tau}_L$ production as in the mass-degenerate case, with stau masses excluded up to 425 GeV. Sensitivity to $\tilde{\tau}_R$ production is obtained for the first time at ATLAS, with masses excluded up to 350 GeV.

10.2 Intermediate stau analysis

The observed number of events in each SR and the expected contributions from SM processes are given in Table 11. The contributions of multi-jet, W +jets and top quark events are scaled with the normalization factors obtained from the background-only fit. The multi-jet normalization with respect to the prediction from the ABCD method in all SRs is compatible with unity and has an uncertainty of 29–40% (4%), due to the small number of observed events in the multi-jet CR-A in C1C1 and C1N2OS (C1N2SS) scenarios. The W +jets normalization factor is measured to be 0.98 ± 0.12 (1.04 ± 0.09) in C1C1 and C1N2OS (C1N2SS) scenarios and the top quark background normalization factor is found to be 0.71 ± 0.11 in the C1N2SS scenario. The normalization factors are summarised in Table 10. The m_{T2} distributions of events in the signal regions are shown in Figure 13. In all SRs, observations and background predictions are found to be compatible within uncertainties. The one-sided p_0 -values, and the observed and expected 95% CL upper limits on the visible non-SM cross-section (σ_{vis}^{95}) are shown in Table 11.

Table 9: Observed and expected numbers of events after the background-only fit in the signal regions targeting direct stau production. The uncertainties correspond to the sum of statistical and systematic uncertainties. The correlation of systematic uncertainties among control regions and among background processes is taken into account. The one-sided p_0 -value, and the observed and expected 95 % CL upper limits on the visible non-SM cross-section (σ_{vis}^{95}) from the model-independent fit are given for the unbinned SRs. Values of $p_0 > 0.5$ are truncated to $p_0 = 0.5$.

SM process	SR-BDT1	SR-BDT1_bin0	SR-BDT1_bin1	SR-BDT2	SR-BDT2_bin0	SR-BDT2_bin1
Multi-boson	6.6 ± 3.1	3.3 ± 1.9	3.3 ± 1.7	4.1 ± 2.0	1.7 ± 0.9	2.3 ± 1.2
W+jets	23 ± 10	12 ± 7	11 ± 4	$1.6^{+1.7}_{-1.6}$	$1.6^{+1.6}_{-1.6}$	$0.09^{+0.09}_{-0.09}$
Top	7.8 ± 2.6	3.3 ± 1.7	4.5 ± 1.9	2.1 ± 1.2	1.0 ± 0.9	1.0 ± 0.7
Z+jets	7 ± 7	4 ± 4	2.8 ± 2.6	2.0 ± 0.9	1.6 ± 0.8	0.40 ± 0.20
Higgs	–	$0.004^{+0.006}_{-0.004}$	–	$0.02^{+0.14}_{-0.02}$	$0.02^{+0.13}_{-0.02}$	$0.004^{+0.018}_{-0.004}$
Multi-jet	4.6 ± 2.8	2.2 ± 1.6	2.4 ± 2.3	< 1.0	< 1.0	< 0.16
SM total	49 ± 15	25 ± 10	24 ± 8	10 ± 4	5.9 ± 2.8	3.9 ± 1.6
Observed	36	22	14	4	3	1
$m(\tilde{\tau}, \tilde{\chi}_1^0) = (80, 1)$ GeV	40 ± 9	14 ± 4	27 ± 6	4.2 ± 2.0	3.4 ± 1.4	0.7 ± 0.7
$m(\tilde{\tau}, \tilde{\chi}_1^0) = (400, 1)$ GeV	4.6 ± 0.9	1.2 ± 0.4	3.4 ± 0.8	9.5 ± 1.1	2.1 ± 0.4	7.4 ± 0.9
p_0	0.5	–	–	0.5	–	–
Expected σ_{vis}^{95} [fb]	0.22	–	–	0.06	–	–
Observed σ_{vis}^{95} [fb]	0.18	–	–	0.04	–	–

SM process	SR-BDT3	SR-BDT3_bin0	SR-BDT3_bin1	SR-BDT4
Multi-boson	4.6 ± 2.2	2.0 ± 1.2	2.5 ± 1.3	1.8 ± 1.0
W+jets	2^{+4}_{-2}	2^{+4}_{-2}	0.5 ± 0.5	< 0.7
Top	3.7 ± 1.3	2.7 ± 1.1	1.0 ± 0.9	$0.16^{+0.19}_{-0.16}$
Z+jets	6 ± 4	$1.9^{+2.7}_{-1.9}$	4.1 ± 2.6	$0.2^{+0.9}_{-0.2}$
Higgs	$0.13^{+0.15}_{-0.13}$	$0.13^{+0.14}_{-0.13}$	$0.001^{+0.012}_{-0.001}$	< 0.015
Multi-jet	< 1.1	< 1.0	< 0.26	$0.20^{+0.28}_{-0.20}$
SM total	17 ± 7	9 ± 6	8.2 ± 3.3	2.4 ± 1.4
Observed	7	6	1	1
$m(\tilde{\tau}, \tilde{\chi}_1^0) = (80, 1)$ GeV	11 ± 4	8.6 ± 3.0	2.2 ± 1.4	$0.13^{+0.22}_{-0.13}$
$m(\tilde{\tau}, \tilde{\chi}_1^0) = (400, 1)$ GeV	9.4 ± 1.4	3.7 ± 0.7	5.7 ± 1.1	7.3 ± 0.9
p_0	0.5	–	–	0.5
Expected σ_{vis}^{95} [fb]	0.07	–	–	0.03
Observed σ_{vis}^{95} [fb]	0.04	–	–	0.03

In the absence of a significant excess over the expected SM background, the observed and expected numbers of events in the signal regions are used to place exclusion limits at 95 % CL using the model-dependent fit. SR-C1C1-LM and SR-C1C1-HM are statistically combined to derive limits on $\tilde{\chi}_1^+ \tilde{\chi}_1^-$ production, and SR-C1N2OS-LM, SR-C1N2OS-HM, SR-C1N2SS-LM and SR-C1N2SS-HM are combined to derive limits for the production of $\tilde{\chi}_1^+ \tilde{\chi}_1^-$ and $\tilde{\chi}_1^\pm \tilde{\chi}_2^0$. The exclusion limits for simplified models are shown in Figure 14.

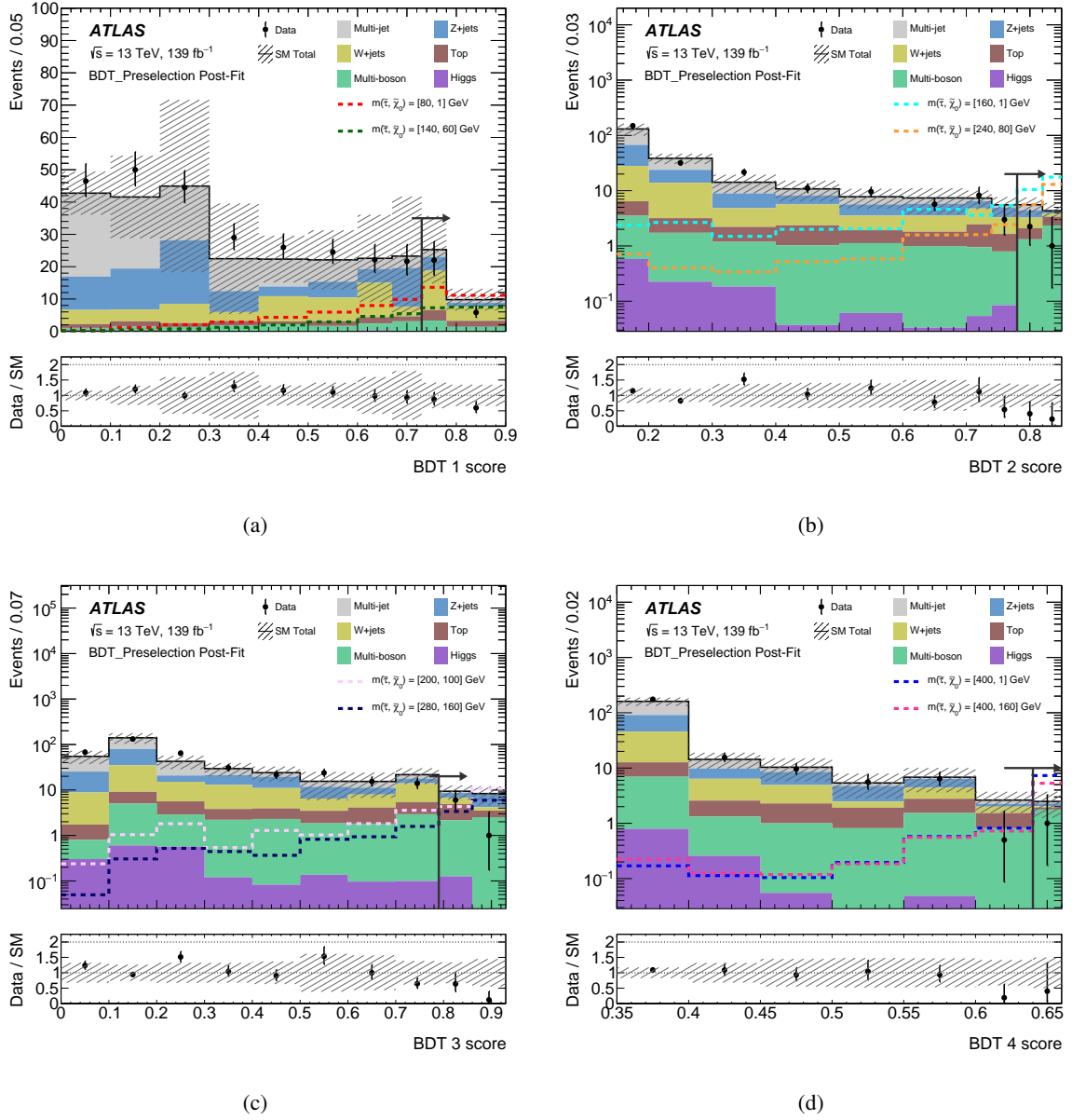


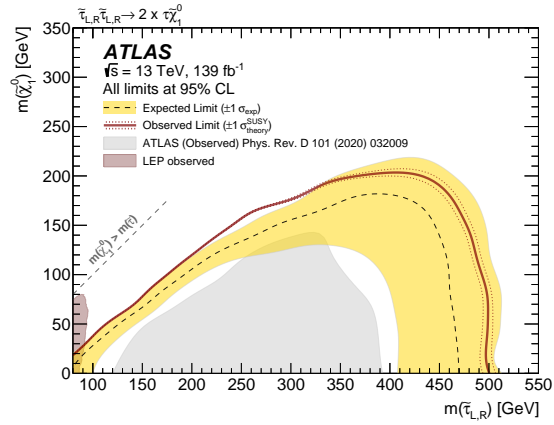
Figure 11: The BDT score distributions for the Direct stau channel after the background-only fit, showing the scores for (a) BDT1, (b) BDT2, (c) BDT3, and (d) BDT4, before the selections on the BDT scores are made. The black arrow depicts the BDT score selection for the SR-BDT. A few example SUSY scenarios targeted by each BDT are overlaid for illustration. The hashed bands represent the combined statistical and systematic uncertainties of the total SM background. The lower panels show the ratio of data to the total SM background estimate.

Only $\tilde{\chi}_1^+ \tilde{\chi}_1^-$ production is assumed for Figure 14 (a), whereas both production processes are considered simultaneously for the Figure 14 (b) and (c). The C1N2SS channel contributes significantly to the combination in the lower mass regions where this channel does not contain significant SM backgrounds.

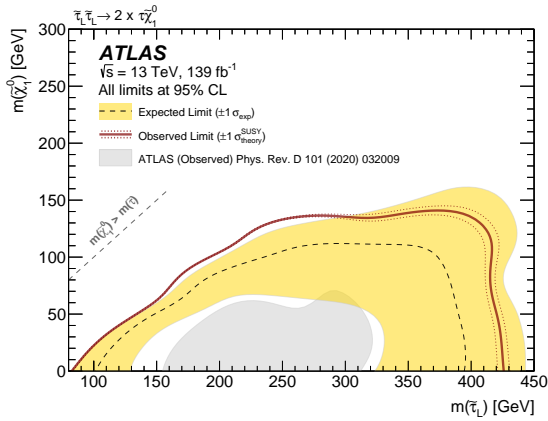
Chargino masses up to 970 GeV are excluded for decays into a massless neutralino in the direct production of chargino pairs. For production of chargino pairs of mass-degenerate charginos and next-to-lightest

Table 10: Normalization factors from the background-only fit in each scenario for the Direct stau, Intermediate stau, and Intermediate Wh channels. The normalization factors include corrections to the misidentified τ -lepton efficiency in addition to the cross-section and acceptance effects.

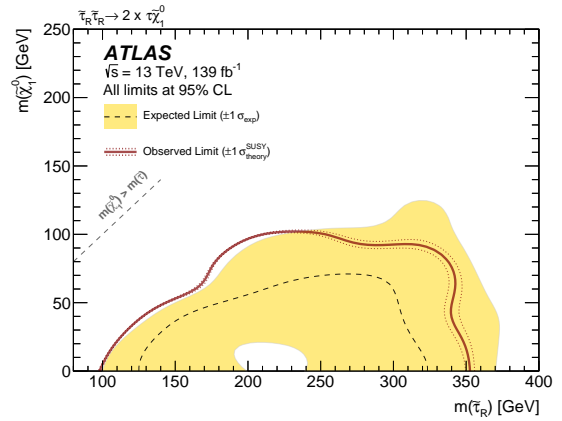
Channel	Direct stau	Intermediate stau			Intermediate Wh
Normalization factor	$\tilde{\tau}\tilde{\tau}$	C1C1	C1N2OS	C1N2SS	C1N2Wh
μW +jets	0.93 ± 0.11	0.98 ± 0.12	0.98 ± 0.12	1.04 ± 0.09	–
μZ +jets	0.91 ± 0.07	–	–	–	–
μ Top	0.85 ± 0.05	–	–	0.71 ± 0.11	1.00 ± 0.14
μ Multi-jet	–	1.0 ± 0.4	1.00 ± 0.29	1.00 ± 0.04	–



(a)



(b)



(c)

Figure 12: The 95% CL exclusion contours for simplified models of (a) $\tilde{\tau}_{L,R}\tilde{\tau}_{L,R}$ production, (b) $\tilde{\tau}_L\tilde{\tau}_L$ production, and (c) $\tilde{\tau}_R\tilde{\tau}_R$ production. The solid (dashed) lines show the observed (expected) exclusion contours. The band around the expected limit shows the $\pm 1\sigma$ variations, including all uncertainties except theoretical uncertainties in the signal cross-section. The expected exclusion contour from the previous ATLAS result in Ref. [15] is shown as a gray-filled contour in (a) and (b). The observed contour from LEP in Ref. [94] is shown as a brown-filled contour in (a).

Table 11: Observed and expected numbers of events for the background-only fit in the signal regions targeting chargino/neutralino production and decay via intermediate staus. Expected event yields for a few SUSY reference points are also shown. The uncertainties correspond to the sum in quadrature of statistical and systematic uncertainties. The correlation of systematic uncertainties among control regions and among background processes is taken into account. The one-sided p_0 -values, and the observed and expected 95 % CL upper limits on the visible non-SM cross-section (σ_{vis}^{95}) from the model-independent fit are given.

SM process	SR-C1C1-LM	SR-C1C1-HM	SR-C1N2OS-LM	SR-C1N2OS-HM
Multi-boson	1.6 ± 0.6	2.2 ± 1.6	3.2 ± 1.2	2.4 ± 1.6
W +jets	0.4 ± 0.4	$0.29^{+0.35}_{-0.29}$	$0.6^{+2.2}_{-0.6}$	$0.29^{+0.35}_{-0.29}$
Top quark	1.0 ± 0.5	0.36 ± 0.13	$1.1^{+1.2}_{-1.1}$	0.36 ± 0.14
Z +jets	$1.4^{+1.5}_{-1.4}$	0.78 ± 0.34	2.5 ± 1.7	0.9 ± 0.4
Higgs	0.27 ± 0.06	$0.01^{+0.13}_{-0.01}$	0.40 ± 0.22	0.73 ± 0.23
Multi-jet	1.5 ± 0.5	0.37 ± 0.21	4.5 ± 1.0	0.31 ± 0.17
SM total	6.2 ± 2.0	4.0 ± 1.8	12.2 ± 4.8	5.0 ± 2.0
Observed	1	4	14	4
$m(\tilde{\chi}_1^\pm, \tilde{\chi}_1^0) = (700, 400)$ GeV	3.0 ± 0.6	7.8 ± 1.6	4.7 ± 1.0	14.1 ± 2.8
$m(\tilde{\chi}_1^\pm/\tilde{\chi}_2^0, \tilde{\chi}_1^0) = (1100, 0)$ GeV	0.20 ± 0.05	3.1 ± 0.6	0.39 ± 0.11	4.6 ± 1.0
p_0	0.5	0.5	0.4	0.5
Expected σ_{vis}^{95} [fb]	0.04	0.05	0.10	0.05
Observed σ_{vis}^{95} [fb]	0.02	0.05	0.10	0.05

SM process	SR-C1N2SS-LM	SR-C1N2SS-HM
Multi-boson	0.47 ± 0.20	0.8 ± 0.4
W +jets	0.33 ± 0.25	0.10 ± 0.05
Top quark	$0.01^{+0.02}_{-0.01}$	0.59 ± 0.20
Z +jets	0.20 ± 0.15	$0.6^{+0.8}_{-0.6}$
Higgs	< 0.01	0.02 ± 0.01
Multi-jet	0.9 ± 0.5	0.00 ± 0.00
SM total	2.0 ± 0.7	2.1 ± 1.1
Observed	2	3
$m(\tilde{\chi}_1^\pm/\tilde{\chi}_2^0, \tilde{\chi}_1^0) = (157, 92)$ GeV	4.6 ± 1.3	0.00 ± 0.00
$m(\tilde{\chi}_1^\pm/\tilde{\chi}_2^0, \tilde{\chi}_1^0) = (900, 300)$ GeV	0.84 ± 0.07	6.23 ± 0.21
p_0	0.4	0.3
Expected σ_{vis}^{95} [fb]	0.03	0.04
Observed σ_{vis}^{95} [fb]	0.03	0.04

neutralinos, chargino masses up to 1160 GeV are excluded for a massless neutralino. Both the limits apply to scenarios where the neutralinos and charginos decay solely via intermediate staus and τ -sneutrinos. These limits significantly extend previous results [14, 18] in the high $\tilde{\chi}_1^\pm/\tilde{\chi}_2^0$ mass region. The improvement

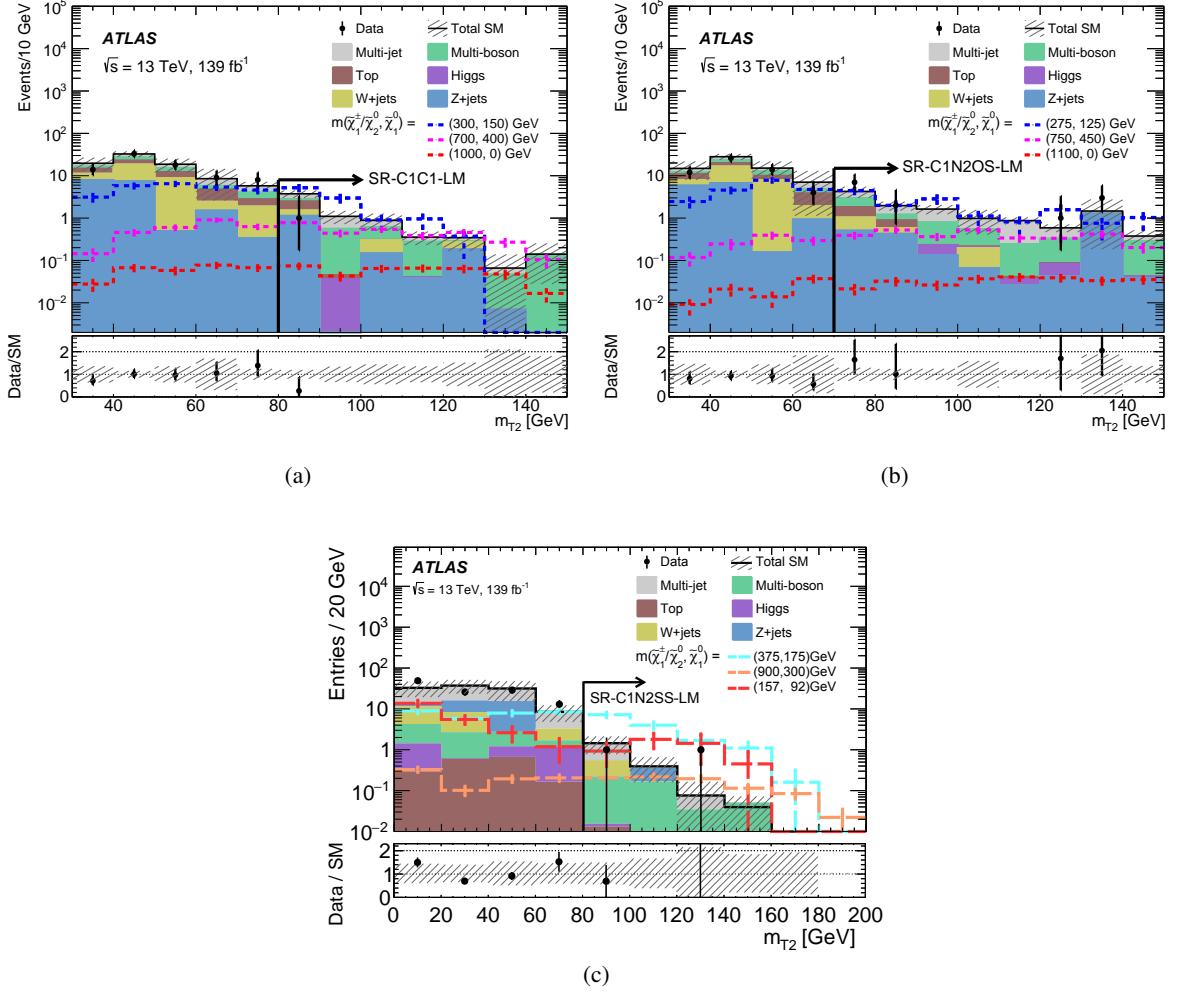
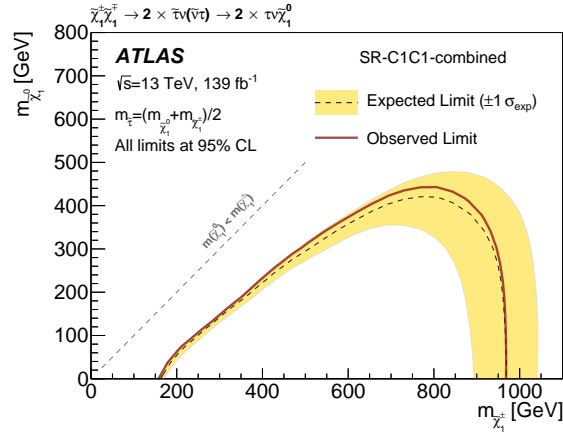


Figure 13: The kinematic distributions for the Intermediate stau channel after the background-only fit, showing the m_{T2} distribution in (a) SR-C1C1-LM, (b) SR-C1N2OS-LM, and (c) SR-C1N2SS-LM before the selection on m_{T2} is made. The black arrow depicts the selection for the signal region. An example SUSY scenario is overlaid for illustration. The hashed bands represent the combined statistical and systematic uncertainties of the total SM background. The lower panels show the ratio of data to the total SM background estimate.

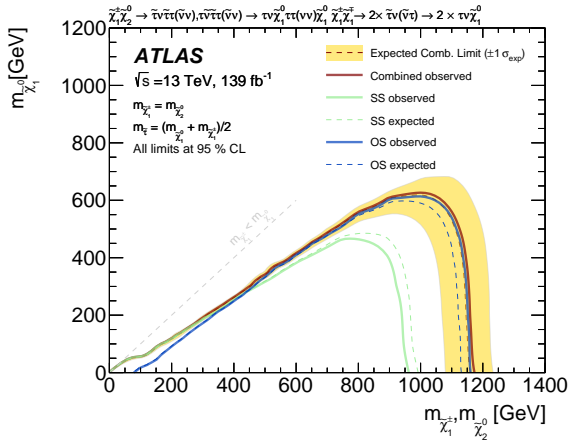
at compressed and low $\tilde{\chi}_1^\pm/\tilde{\chi}_2^0$ masses is mainly driven by the C1N2SS analysis.

10.3 Intermediate Wh analysis

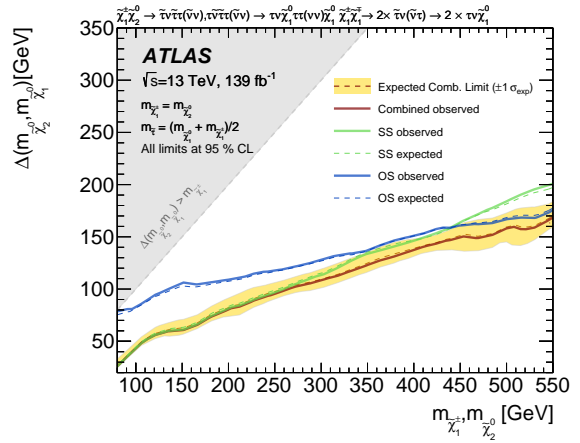
The observed number of events in the two SRs and the expected contributions from SM processes are given in Table 12. The contribution of top quark background events is scaled with the normalization factor obtained from the background-only fit. The top quark background normalization factor is fitted to be 1.00 ± 0.14 . Kinematic distributions of events in the signal regions are shown in Figure 15. In all SRs, the observed number of events from data and the background predictions are found to be compatible within uncertainties. The one-sided p_0 -values, the observed and expected 95 % CL upper limits on the visible non-SM cross-section (σ_{vis}^{95}) are shown in Table 12.



(a)



(b)



(c)

Figure 14: The 95 % CL exclusion contours for simplified models of (a) $\tilde{\chi}_1^{\pm} \tilde{\chi}_1^{\mp}$ production, and of (b-c) $\tilde{\chi}_1^{\pm} \tilde{\chi}_1^{\mp}$ and $\tilde{\chi}_1^{\pm} \tilde{\chi}_2^0$ production. The solid (dashed) lines show the observed (expected) exclusion contours. The band around the expected limit shows the $\pm 1\sigma$ variations, including all uncertainties except theoretical uncertainties in the signal cross-section. The green curves are from the contribution of C1N2SS scenario, while the blue curves are from the contribution of C1C1 and C1N2OS scenarios, and the red curves are the combination of the channels. The gray solid area in (c) shows the forbidden area where $m(\tilde{\chi}_1^0) > m(\tilde{\chi}_2^0)$.

Since no significant excess over the expected SM background is observed, the observed and expected number of events in the SRs are used to place exclusion limits at 95 % CL using the model-dependent fit. The SR with the best expected limit from SR-Wh-LM and SR-Wh-HM is used to derive limits on $\tilde{\chi}_1^{\pm} \tilde{\chi}_2^0$ production decaying via an intermediate Wh , and are shown in Figure 16. The slightly weaker observed limits than expected for $\tilde{\chi}_1^{\pm} / \tilde{\chi}_2^0$ masses above 250 GeV are driven by the results in SR-Wh-HM, as seen in Table 12. Chargino and next-to-lightest neutralino masses up to 330 GeV are excluded for a massless lightest neutralino.

Table 12: Observed and expected numbers of events for the background-only fit in the signal regions targeting chargino-neutralino production and decay via Wh . Expected event yields for a few SUSY reference points are also shown. The uncertainties correspond to the sum in quadrature of statistical and systematic uncertainties. The correlation of systematic uncertainties among control regions and among background processes is fully taken into account. The one-sided p_0 -values, and the observed and expected 95 % CL upper limits on the visible non-SM cross-section (σ_{vis}^{95}) from the model-independent fit are given.

SM process	SR-Wh-LM	SR-Wh-HM
Multi-boson	1.85 ± 0.5	1.1 ± 0.4
Misidentified processes	1.4 ± 0.6	0.06 ± 0.03
Top quark	1.9 ± 0.6	$0.04^{+0.06}_{-0.04}$
Z+jets	0.05 ± 0.02	0.03 ± 0.01
Higgs	$0.13^{+0.99}_{-0.13}$	0.06 ± 0.02
SM total	5.3 ± 1.4	1.3 ± 0.4
Observed	4	2
$m(\tilde{\chi}_1^\pm/\tilde{\chi}_2^0, \tilde{\chi}_1^0) = (225, 75) \text{ GeV}$	5.8 ± 1.5	3.3 ± 0.9
p_0	0.5	0.3
Expected σ_{vis}^{95} [fb]	0.05	0.03
Observed σ_{vis}^{95} [fb]	0.04	0.03

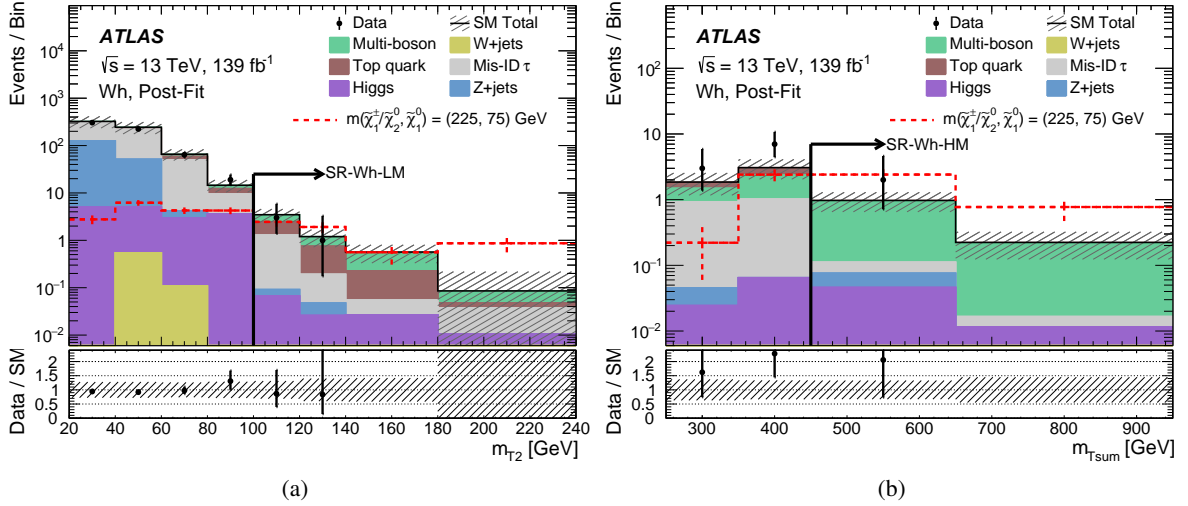


Figure 15: The kinematic distributions for the Intermediate Wh channel after the background-only fit, showing (a) m_{T2} in SR-Wh-LM and (b) $m_{T\text{sum}}$ in SR-Wh-HM, before the selection on that kinematic is made. The black arrow depicts the selection for the signal region. An example SUSY scenario is overlaid for illustration. The hashed bands represent the combined statistical and systematic uncertainties of the total SM background. The lower panels show the ratio of data to the total SM background estimate.

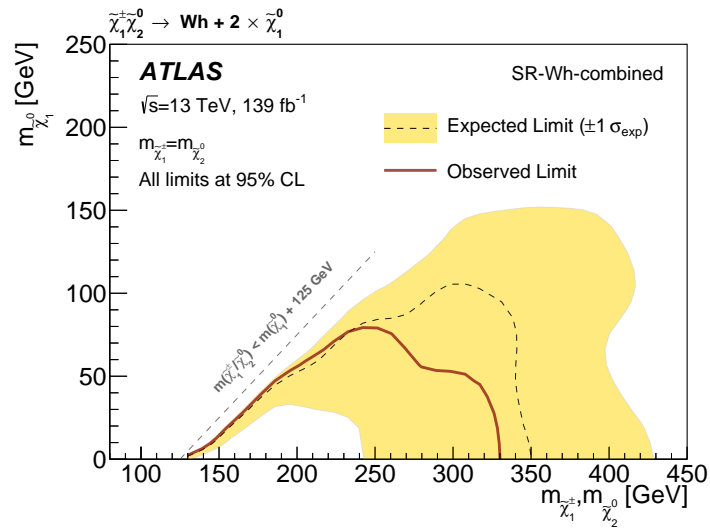


Figure 16: The 95 % CL exclusion contours for simplified models of $\tilde{\chi}_1^\pm \tilde{\chi}_2^0$ production decaying via an intermediate Wh . The solid (dashed) lines show the observed (expected) exclusion contours. The band around the expected limit shows the $\pm 1\sigma$ variations, including all uncertainties except theoretical uncertainties in the signal cross-section. The best expected limits for SR-Wh-LM and SR-Wh-HM are used.

11 Summary

Searches for direct τ -slepton (stau) production and direct wino pair production decaying via an intermediate stau or Wh with at least two hadronically decaying τ -leptons in the final state are presented. The searches use 139 fb^{-1} of integrated luminosity of pp collisions at $\sqrt{s} = 13 \text{ TeV}$ collected by the ATLAS detector from 2015 to 2018. Agreement between data and SM expectation is observed in all signal regions and the results are used to set limits on the visible cross-section for processes beyond the Standard Model. Exclusion limits at 95% CL are also placed on simplified models of direct stau production, excluding mass-degenerate $\tilde{\tau}_{L,R}$ up to 500 GeV, $\tilde{\tau}_L$ up to 425 GeV, and $\tilde{\tau}_R$ up to 350 GeV. The sensitivity to $\tilde{\tau}_R \tilde{\tau}_R$ production obtained here is the first time for this process reported by ATLAS, achieved with a Boosted Decision Tree for improved signal-background separation.

In the scenario of direct production of wino-like chargino pairs decaying into the lightest neutralino via an intermediate on-shell stau, exclusion limits are placed for chargino masses up to 970 GeV for a massless lightest neutralino. In the case of the associated production of pairs of charginos and of mass-degenerate charginos and next-to-lightest neutralinos, masses up to 1160 GeV are excluded for a massless lightest neutralino. These limits improve upon previous results by 340–400 GeV, mainly due to an increased amount of integrated luminosity and improvements in the recurrent neural network τ -lepton identification. The sensitivity for more compressed mass scenarios is also improved by the addition of the same-sign τ -lepton channel. For pairs of degenerate charginos and next-to-lightest neutralinos decaying via intermediate W and h bosons, chargino and next-to-lightest neutralino masses up to 330 GeV are excluded for a massless lightest neutralino.

Acknowledgements

We thank CERN for the very successful operation of the LHC and its injectors, as well as the support staff at CERN and at our institutions worldwide without whom ATLAS could not be operated efficiently.

The crucial computing support from all WLCG partners is acknowledged gratefully, in particular from CERN, the ATLAS Tier-1 facilities at TRIUMF/SFU (Canada), NDGF (Denmark, Norway, Sweden), CC-IN2P3 (France), KIT/GridKA (Germany), INFN-CNAF (Italy), NL-T1 (Netherlands), PIC (Spain), RAL (UK) and BNL (USA), the Tier-2 facilities worldwide and large non-WLCG resource providers. Major contributors of computing resources are listed in Ref. [95].

We gratefully acknowledge the support of ANPCyT, Argentina; YerPhI, Armenia; ARC, Australia; BMWFW and FWF, Austria; ANAS, Azerbaijan; CNPq and FAPESP, Brazil; NSERC, NRC and CFI, Canada; CERN; ANID, Chile; CAS, MOST and NSFC, China; Minciencias, Colombia; MEYS CR, Czech Republic; DNRF and DNSRC, Denmark; IN2P3-CNRS and CEA-DRF/IRFU, France; SRNSFG, Georgia; BMBF, HGF and MPG, Germany; GSRI, Greece; RGC and Hong Kong SAR, China; ISF and Benozziyo Center, Israel; INFN, Italy; MEXT and JSPS, Japan; CNRST, Morocco; NWO, Netherlands; RCN, Norway; MEiN, Poland; FCT, Portugal; MNE/IFA, Romania; MESTD, Serbia; MSSR, Slovakia; ARRS and MIZŠ, Slovenia; DSI/NRF, South Africa; MICINN, Spain; SRC and Wallenberg Foundation, Sweden; SERI, SNSF and Cantons of Bern and Geneva, Switzerland; MOST, Taipei; TENMAK, Türkiye; STFC, United Kingdom; DOE and NSF, United States of America.

Individual groups and members have received support from BCKDF, CANARIE, CRC and DRAC, Canada; COST, ERC, ERDF, Horizon 2020, ICSC-NextGenerationEU and Marie Skłodowska-Curie Actions,

European Union; Investissements d’Avenir Labex, Investissements d’Avenir Idex and ANR, France; DFG and AvH Foundation, Germany; Herakleitos, Thales and Aristeia programmes co-financed by EU-ESF and the Greek NSRF, Greece; BSF-NSF and MINERVA, Israel; Norwegian Financial Mechanism 2014-2021, Norway; NCN and NAWA, Poland; La Caixa Banking Foundation, CERCA Programme Generalitat de Catalunya and PROMETEO and GenT Programmes Generalitat Valenciana, Spain; Göran Gustafssons Stiftelse, Sweden; The Royal Society and Leverhulme Trust, United Kingdom.

In addition, individual members wish to acknowledge support from Chile: Agencia Nacional de Investigación y Desarrollo (FONDECYT 1190886, FONDECYT 1210400, FONDECYT 1230987); China: National Natural Science Foundation of China (NSFC - 12175119, NSFC 12275265); European Union: European Research Council (ERC - 948254), Horizon 2020 Framework Programme (MUCCA - CHIST-ERA-19-XAI-00), Italian Center for High Performance Computing, Big Data and Quantum Computing (ICSC, NextGenerationEU), Marie Skłodowska-Curie Actions (EU H2020 MSC IF GRANT NO 101033496); France: Agence Nationale de la Recherche (ANR-20-CE31-0013, ANR-21-CE31-0013, ANR-21-CE31-0022), Investissements d’Avenir Idex (ANR-11-LABX-0012), Investissements d’Avenir Labex (ANR-11-LABX-0012); Germany: Baden-Württemberg Stiftung (BW Stiftung-Postdoc Eliteprogramme), Deutsche Forschungsgemeinschaft (DFG - CR 312/5-1); Italy: Istituto Nazionale di Fisica Nucleare (FELLINI G.A. n. 754496, ICSC, NextGenerationEU); Japan: Japan Society for the Promotion of Science (JSPS KAKENHI 22H01227, JSPS KAKENHI JP21H05085, JSPS KAKENHI JP22H04944); Netherlands: Netherlands Organisation for Scientific Research (NWO Veni 2020 - VI.Veni.202.179); Norway: Research Council of Norway (RCN-314472); Poland: Polish National Agency for Academic Exchange (PPN/PPO/2020/1/00002/U/00001), Polish National Science Centre (NCN 2021/42/E/ST2/00350, NCN UMO-2019/34/E/ST2/00393, UMO-2020/37/B/ST2/01043, UMO-2021/40/C/ST2/00187); Slovenia: Slovenian Research Agency (ARIS grant J1-3010); Spain: BBVA Foundation (LEO22-1-603), Generalitat Valenciana (Artemisa, FEDER, IDIFEDER/2018/048), La Caixa Banking Foundation (LCF/BQ/PI20/11760025), Ministry of Science and Innovation (RYC2019-028510-I, RYC2020-030254-I), PROMETEO and GenT Programmes Generalitat Valenciana (CIDEAGENT/2019/023, CIDEAGENT/2019/027); Sweden: Swedish Research Council (VR 2022-03845, VR 2022-04683), Knut and Alice Wallenberg Foundation (KAW 2017.0100, KAW 2018.0157, KAW 2019.0447); Switzerland: Swiss National Science Foundation (SNSF - PCEFP2_194658); United Kingdom: Leverhulme Trust (Leverhulme Trust RPG-2020-004); United States of America: Neubauer Family Foundation.

References

- [1] Y. Golfand and E. Likhtman, *Extension of the Algebra of Poincare Group Generators and Violation of P Invariance*, JETP Lett. **13** (1971) 323, [Pisma Zh. Eksp. Teor. Fiz. **13** (1971) 452].
- [2] D. Volkov and V. Akulov, *Is the neutrino a goldstone particle?*, Phys. Lett. B **46** (1973) 109.
- [3] J. Wess and B. Zumino, *Supergauge transformations in four dimensions*, Nucl. Phys. B **70** (1974) 39.
- [4] J. Wess and B. Zumino, *Supergauge invariant extension of quantum electrodynamics*, Nucl. Phys. B **78** (1974) 1.
- [5] S. Ferrara and B. Zumino, *Supergauge invariant Yang-Mills theories*, Nucl. Phys. B **79** (1974) 413.
- [6] A. Salam and J. Strathdee, *Super-symmetry and non-Abelian gauges*, Phys. Lett. B **51** (1974) 353.

- [7] S. P. Martin, *A Supersymmetry Primer*, *Adv. Ser. Direct. High Energy Phys.* **18** (1998) 1, arXiv: [hep-ph/9709356](#).
- [8] G. R. Farrar and P. Fayet, *Phenomenology of the production, decay, and detection of new hadronic states associated with supersymmetry*, *Phys. Lett. B* **76** (1978) 575.
- [9] H. Goldberg, *Constraint on the Photino Mass from Cosmology*, *Phys. Rev. Lett.* **50** (1983) 1419, Erratum: *Phys. Rev. Lett.* **103** (2009) 099905.
- [10] J. Ellis, J. Hagelin, D. V. Nanopoulos, K. A. Olive and M. Srednicki, *Supersymmetric relics from the big bang*, *Nucl. Phys. B* **238** (1984) 453.
- [11] D. Albornoz Vásquez, G. Bélanger and C. Boehm, *Revisiting light neutralino scenarios in the MSSM*, *Phys. Rev. D* **84** (2011) 095015, arXiv: [1108.1338](#) [[hep-ph](#)].
- [12] ATLAS Collaboration, *Search for the direct production of charginos, neutralinos and staus in final states with at least two hadronically decaying taus and missing transverse momentum in pp collisions at $\sqrt{s} = 8$ TeV with the ATLAS detector*, *JHEP* **10** (2014) 096, arXiv: [1407.0350](#) [[hep-ex](#)].
- [13] ATLAS Collaboration, *Search for the electroweak production of supersymmetric particles in $\sqrt{s} = 8$ TeV pp collisions with the ATLAS detector*, *Phys. Rev. D* **93** (2016) 052002, arXiv: [1509.07152](#) [[hep-ex](#)].
- [14] ATLAS Collaboration, *Search for the direct production of charginos and neutralinos in final states with tau leptons in $\sqrt{s} = 13$ TeV pp collisions with the ATLAS detector*, *Eur. Phys. J. C* **78** (2018) 154, arXiv: [1708.07875](#) [[hep-ex](#)].
- [15] ATLAS Collaboration, *Search for direct stau production in events with two hadronic τ -leptons in $\sqrt{s} = 13$ TeV pp collisions with the ATLAS detector*, *Phys. Rev. D* **101** (2020) 032009, arXiv: [1911.06660](#) [[hep-ex](#)].
- [16] CMS Collaboration, *Searches for electroweak production of charginos, neutralinos, and sleptons decaying to leptons and W, Z, and Higgs bosons in pp collisions at 8 TeV*, *Eur. Phys. J. C* **74** (2014) 3036, arXiv: [1405.7570](#) [[hep-ex](#)].
- [17] CMS Collaboration, *Search for direct pair production of supersymmetric partners of τ leptons in the final state with two hadronically decaying τ leptons and missing transverse momentum in proton–proton collisions at $\sqrt{s} = 13$ TeV*, (2023), arXiv: [2207.02254](#) [[hep-ex](#)].
- [18] CMS Collaboration, *Search for electroweak production of charginos and neutralinos in proton–proton collisions at $\sqrt{s} = 13$ TeV*, *JHEP* **04** (2022) 147, arXiv: [2106.14246](#) [[hep-ex](#)].
- [19] ATLAS Collaboration, *The ATLAS Experiment at the CERN Large Hadron Collider*, *JINST* **3** (2008) S08003.
- [20] ATLAS Collaboration, *Operation of the ATLAS trigger system in Run 2*, *JINST* **15** (2020) P10004, arXiv: [2007.12539](#) [[hep-ex](#)].
- [21] ATLAS Collaboration, *The ATLAS Collaboration Software and Firmware*, ATL-SOFT-PUB-2021-001, 2021, URL: <https://cds.cern.ch/record/2767187>.
- [22] ATLAS Collaboration, *ATLAS data quality operations and performance for 2015–2018 data-taking*, *JINST* **15** (2020) P04003, arXiv: [1911.04632](#) [[physics.ins-det](#)].
- [23] T. Sjöstrand, S. Mrenna and P. Skands, *A brief introduction to PYTHIA 8.1*, *Comput. Phys. Commun.* **178** (2008) 852, arXiv: [0710.3820](#) [[hep-ph](#)].

- [24] ATLAS Collaboration, *The Pythia 8 A3 tune description of ATLAS minimum bias and inelastic measurements incorporating the Donnachie–Landshoff diffractive model*, ATL-PHYS-PUB-2016-017, 2016, URL: <https://cds.cern.ch/record/2206965>.
- [25] NNPDF Collaboration, R. D. Ball et al., *Parton distributions with LHC data*, *Nucl. Phys. B* **867** (2013) 244, arXiv: [1207.1303](https://arxiv.org/abs/1207.1303) [hep-ph].
- [26] D. J. Lange, *The EvtGen particle decay simulation package*, *Nucl. Instrum. Meth. A* **462** (2001) 152.
- [27] ATLAS Collaboration, *The ATLAS Simulation Infrastructure*, *Eur. Phys. J. C* **70** (2010) 823, arXiv: [1005.4568](https://arxiv.org/abs/1005.4568) [physics.ins-det].
- [28] S. Agostinelli et al., *GEANT4 – a simulation toolkit*, *Nucl. Instrum. Meth. A* **506** (2003) 250.
- [29] ATLAS Collaboration, *Performance of the Fast ATLAS Tracking Simulation (FATRAS) and the ATLAS Fast Calorimeter Simulation (FastCaloSim) with single particles*, ATL-SOFT-PUB-2014-001, 2014, URL: <https://cds.cern.ch/record/1669341>.
- [30] S. Frixione, G. Ridolfi and P. Nason, *A positive-weight next-to-leading-order Monte Carlo for heavy flavour hadroproduction*, *JHEP* **09** (2007) 126, arXiv: [0707.3088](https://arxiv.org/abs/0707.3088) [hep-ph].
- [31] P. Nason, *A new method for combining NLO QCD with shower Monte Carlo algorithms*, *JHEP* **11** (2004) 040, arXiv: [hep-ph/0409146](https://arxiv.org/abs/hep-ph/0409146).
- [32] S. Frixione, P. Nason and C. Oleari, *Matching NLO QCD computations with parton shower simulations: the POWHEG method*, *JHEP* **11** (2007) 070, arXiv: [0709.2092](https://arxiv.org/abs/0709.2092) [hep-ph].
- [33] S. Alioli, P. Nason, C. Oleari and E. Re, *A general framework for implementing NLO calculations in shower Monte Carlo programs: the POWHEG BOX*, *JHEP* **06** (2010) 043, arXiv: [1002.2581](https://arxiv.org/abs/1002.2581) [hep-ph].
- [34] ATLAS Collaboration, *ATLAS Pythia 8 tunes to 7 TeV data*, ATL-PHYS-PUB-2014-021, 2014, URL: <https://cds.cern.ch/record/1966419>.
- [35] M. Beneke, P. Falgari, S. Klein and C. Schwinn, *Hadronic top-quark pair production with NNLL threshold resummation*, *Nucl. Phys. B* **855** (2012) 695, arXiv: [1109.1536](https://arxiv.org/abs/1109.1536) [hep-ph].
- [36] M. Cacciari, M. Czakon, M. Mangano, A. Mitov and P. Nason, *Top-pair production at hadron colliders with next-to-next-to-leading logarithmic soft-gluon resummation*, *Phys. Lett. B* **710** (2012) 612, arXiv: [1111.5869](https://arxiv.org/abs/1111.5869) [hep-ph].
- [37] P. Bärnreuther, M. Czakon and A. Mitov, *Percent-Level-Precision Physics at the Tevatron: Next-to-Next-to-Leading Order QCD Corrections to $q\bar{q} \rightarrow t\bar{t} + X$* , *Phys. Rev. Lett.* **109** (2012) 132001, arXiv: [1204.5201](https://arxiv.org/abs/1204.5201) [hep-ph].
- [38] M. Czakon and A. Mitov, *NNLO corrections to top-pair production at hadron colliders: the all-fermionic scattering channels*, *JHEP* **12** (2012) 054, arXiv: [1207.0236](https://arxiv.org/abs/1207.0236) [hep-ph].
- [39] M. Czakon and A. Mitov, *NNLO corrections to top pair production at hadron colliders: the quark-gluon reaction*, *JHEP* **01** (2013) 080, arXiv: [1210.6832](https://arxiv.org/abs/1210.6832) [hep-ph].

- [40] M. Czakon, P. Fiedler and A. Mitov,
Total Top-Quark Pair-Production Cross Section at Hadron Colliders Through $O(\alpha_S^4)$,
Phys. Rev. Lett. **110** (2013) 252004, arXiv: [1303.6254 \[hep-ph\]](#).
- [41] M. Czakon and A. Mitov,
Top++: A program for the calculation of the top-pair cross-section at hadron colliders,
Comput. Phys. Commun. **185** (2014) 2930, arXiv: [1112.5675 \[hep-ph\]](#).
- [42] M. Aliev et al., *HATHOR – HAdronic Top and Heavy quarks crOss section calculatoR,*
Comput. Phys. Commun. **182** (2011) 1034, arXiv: [1007.1327 \[hep-ph\]](#).
- [43] P. Kant et al., *HatHor for single top-quark production: Updated predictions and uncertainty estimates for single top-quark production in hadronic collisions,*
Comput. Phys. Commun. **191** (2015) 74, arXiv: [1406.4403 \[hep-ph\]](#).
- [44] J. Alwall et al., *The automated computation of tree-level and next-to-leading order differential cross sections, and their matching to parton shower simulations,* *JHEP* **07** (2014) 079,
arXiv: [1405.0301 \[hep-ph\]](#).
- [45] A. Lazopoulos, T. McElmurry, K. Melnikov and F. Petriello,
Next-to-leading order QCD corrections to $t\bar{t}Z$ production at the LHC, *Phys. Lett. B* **666** (2008) 62,
arXiv: [0804.2220 \[hep-ph\]](#).
- [46] J. M. Campbell and R. K. Ellis, *$t\bar{t}W^\pm$ production and decay at NLO,* *JHEP* **07** (2012) 052,
arXiv: [1204.5678 \[hep-ph\]](#).
- [47] T. Gleisberg et al., *Event generation with SHERPA 1.1,* *JHEP* **02** (2009) 007,
arXiv: [0811.4622 \[hep-ph\]](#).
- [48] S. Höche, F. Krauss, M. Schönherr and F. Siegert,
QCD matrix elements + parton showers. The NLO case, *JHEP* **04** (2013) 027,
arXiv: [1207.5030 \[hep-ph\]](#).
- [49] T. Gleisberg and S. Höche, *Comix, a new matrix element generator,* *JHEP* **12** (2008) 039,
arXiv: [0808.3674 \[hep-ph\]](#).
- [50] F. Cascioli, P. Maierhöfer and S. Pozzorini, *Scattering Amplitudes with Open Loops,*
Phys. Rev. Lett. **108** (2012) 111601, arXiv: [1111.5206 \[hep-ph\]](#).
- [51] A. Denner, S. Dittmaier and L. Hofer,
COLLIER: A fortran-based complex one-loop library in extended regularizations,
Comput. Phys. Commun. **212** (2017) 220, arXiv: [1604.06792 \[hep-ph\]](#).
- [52] S. Schumann and F. Krauss,
A parton shower algorithm based on Catani–Seymour dipole factorisation, *JHEP* **03** (2008) 038,
arXiv: [0709.1027 \[hep-ph\]](#).
- [53] NNPDF Collaboration, R. D. Ball et al., *Parton distributions for the LHC run II,*
JHEP **04** (2015) 040, arXiv: [1410.8849 \[hep-ph\]](#).
- [54] S. Catani, L. Cieri, G. Ferrera, D. de Florian and M. Grazzini, *Vector Boson Production at Hadron Colliders: A Fully Exclusive QCD Calculation at Next-to-Next-to-Leading Order,*
Phys. Rev. Lett. **103** (2009) 082001, arXiv: [0903.2120 \[hep-ph\]](#).
- [55] S. Catani, F. Krauss, B. R. Webber and R. Kuhn, *QCD Matrix Elements + Parton Showers,*
JHEP **11** (2001) 063, arXiv: [hep-ph/0109231](#).

- [56] S. Höche, F. Krauss, S. Schumann and F. Siegert, *QCD matrix elements and truncated showers*, *JHEP* **05** (2009) 053, arXiv: [0903.1219 \[hep-ph\]](#).
- [57] D. de Florian et al., *Handbook of LHC Higgs Cross Sections: 4. Deciphering the Nature of the Higgs Sector*, (2016), arXiv: [1610.07922 \[hep-ph\]](#).
- [58] L. Lönnblad and S. Prestel, *Matching tree-level matrix elements with interleaved showers*, *JHEP* **03** (2012) 019, arXiv: [1109.4829 \[hep-ph\]](#).
- [59] B. Fuks, M. Klasen, D. R. Lamprea and M. Rothering, *Gaugino production in proton-proton collisions at a center-of-mass energy of 8 TeV*, *JHEP* **10** (2012) 081, arXiv: [1207.2159 \[hep-ph\]](#).
- [60] B. Fuks, M. Klasen, D. R. Lamprea and M. Rothering, *Precision predictions for electroweak superpartner production at hadron colliders with RESUMMINO*, *Eur. Phys. J. C* **73** (2013) 2480, arXiv: [1304.0790 \[hep-ph\]](#).
- [61] C. Borschensky et al., *Squark and gluino production cross sections in pp collisions at $\sqrt{s} = 13, 14, 33$ and 100 TeV*, *Eur. Phys. J. C* **74** (2014) 3174, arXiv: [1407.5066 \[hep-ph\]](#).
- [62] ATLAS Collaboration, *Vertex Reconstruction Performance of the ATLAS Detector at $\sqrt{s} = 13$ TeV*, ATL-PHYS-PUB-2015-026, 2015, URL: <https://cds.cern.ch/record/2037717>.
- [63] ATLAS Collaboration, *Jet reconstruction and performance using particle flow with the ATLAS Detector*, *Eur. Phys. J. C* **77** (2017) 466, arXiv: [1703.10485 \[hep-ex\]](#).
- [64] M. Cacciari, G. P. Salam and G. Soyez, *The anti- k_t jet clustering algorithm*, *JHEP* **04** (2008) 063, arXiv: [0802.1189 \[hep-ph\]](#).
- [65] M. Cacciari, G. P. Salam and G. Soyez, *FastJet user manual*, *Eur. Phys. J. C* **72** (2012) 1896, arXiv: [1111.6097 \[hep-ph\]](#).
- [66] ATLAS Collaboration, *Jet energy measurement with the ATLAS detector in proton–proton collisions at $\sqrt{s} = 7$ TeV*, *Eur. Phys. J. C* **73** (2013) 2304, arXiv: [1112.6426 \[hep-ex\]](#).
- [67] ATLAS Collaboration, *Jet Calibration and Systematic Uncertainties for Jets Reconstructed in the ATLAS Detector at $\sqrt{s} = 13$ TeV*, ATL-PHYS-PUB-2015-015, 2015, URL: <https://cds.cern.ch/record/2037613>.
- [68] M. Cacciari and G. P. Salam, *Pileup subtraction using jet areas*, *Phys. Lett. B* **659** (2008) 119, arXiv: [0707.1378](#).
- [69] ATLAS Collaboration, *Performance of pile-up mitigation techniques for jets in pp collisions at $\sqrt{s} = 8$ TeV using the ATLAS detector*, *Eur. Phys. J. C* **76** (2016) 581, arXiv: [1510.03823 \[hep-ex\]](#).
- [70] ATLAS Collaboration, *Selection of jets produced in 13 TeV proton–proton collisions with the ATLAS detector*, ATLAS-CONF-2015-029, 2015, URL: <https://cds.cern.ch/record/2037702>.
- [71] ATLAS Collaboration, *ATLAS b-jet identification performance and efficiency measurement with $t\bar{t}$ events in pp collisions at $\sqrt{s} = 13$ TeV*, *Eur. Phys. J. C* **79** (2019) 970, arXiv: [1907.05120 \[hep-ex\]](#).

- [72] ATLAS Collaboration, *ATLAS flavour-tagging algorithms for the LHC Run 2 pp collision dataset*, *Eur. Phys. J. C* **83** (2023) 681, arXiv: 2211.16345 [physics.data-an].
- [73] ATLAS Collaboration, *Electron and photon performance measurements with the ATLAS detector using the 2015–2017 LHC proton–proton collision data*, *JINST* **14** (2019) P12006, arXiv: 1908.00005 [hep-ex].
- [74] ATLAS Collaboration, *Muon reconstruction and identification efficiency in ATLAS using the full Run 2 pp collision data set at $\sqrt{s} = 13$ TeV*, *Eur. Phys. J. C* **81** (2021) 578, arXiv: 2012.00578 [hep-ex].
- [75] ATLAS Collaboration, *Measurement of the tau lepton reconstruction and identification performance in the ATLAS experiment using pp collisions at $\sqrt{s} = 13$ TeV*, ATLAS-CONF-2017-029, 2017, URL: <https://cds.cern.ch/record/2261772>.
- [76] ATLAS Collaboration, *Reconstruction, Energy Calibration, and Identification of Hadronically Decaying Tau Leptons in the ATLAS Experiment for Run-2 of the LHC*, ATL-PHYS-PUB-2015-045, 2015, URL: <https://cds.cern.ch/record/2064383>.
- [77] ATLAS Collaboration, *Identification of hadronic tau lepton decays using neural networks in the ATLAS experiment*, ATL-PHYS-PUB-2019-033, 2019, URL: <https://cds.cern.ch/record/2688062>.
- [78] ATLAS Collaboration, *Identification and energy calibration of hadronically decaying tau leptons with the ATLAS experiment in pp collisions at $\sqrt{s} = 8$ TeV*, *Eur. Phys. J. C* **75** (2015) 303, arXiv: 1412.7086 [hep-ex].
- [79] ATLAS Collaboration, *Expected performance of missing transverse momentum reconstruction for the ATLAS detector at $\sqrt{s} = 13$ TeV*, ATL-PHYS-PUB-2015-023, 2015, URL: <https://cds.cern.ch/record/2037700>.
- [80] ATLAS Collaboration, *Performance of missing transverse momentum reconstruction with the ATLAS detector in the first proton–proton collisions at $\sqrt{s} = 13$ TeV*, ATL-PHYS-PUB-2015-027, 2015, URL: <https://cds.cern.ch/record/2037904>.
- [81] M. Baak et al., *HistFitter software framework for statistical data analysis*, *Eur. Phys. J. C* **75** (2015) 153, arXiv: 1410.1280 [hep-ex].
- [82] G. Cowan, K. Cranmer, E. Gross and O. Vitells, *Asymptotic formulae for likelihood-based tests of new physics*, *Eur. Phys. J. C* **71** (2011) 1554, [Erratum: *Eur. Phys. J. C* **73** (2013) 2501], arXiv: 1007.1727 [physics.data-an], [Erratum: *Eur. Phys. J. C* **73** (2013) 2501].
- [83] A. L. Read, *Presentation of search results: the CL_s technique*, *J. Phys. G* **28** (2002) 2693.
- [84] C. G. Lester and D. J. Summers, *Measuring masses of semi-invisibly decaying particle pairs produced at hadron colliders*, *Phys. Lett. B* **463** (1999) 99, arXiv: hep-ph/9906349.
- [85] A. Barr, C. Lester and P. Stephens, *A variable for measuring masses at hadron colliders when missing energy is expected; m_{T2} : the truth behind the glamour*, *J. Phys. G* **29** (2003) 2343, arXiv: hep-ph/0304226.
- [86] G. Ke et al., *LightGBM: A Highly Efficient Gradient Boosting Decision Tree*, NIPS'17 (2017) 3149.
- [87] ATLAS Collaboration, *Performance of the ATLAS muon triggers in Run 2*, *JINST* **15** (2020) P09015, arXiv: 2004.13447 [physics.ins-det].

- [88] D. Tovey,
On measuring the masses of pair-produced semi-invisibly decaying particles at hadron colliders,
JHEP **04** (2008) 034, arXiv: [0802.2879](https://arxiv.org/abs/0802.2879).
- [89] ATLAS Collaboration,
 E_T^{miss} performance in the ATLAS detector using 2015–2016 LHC pp collisions,
ATLAS-CONF-2018-023, 2018, URL: <https://cds.cern.ch/record/2625233>.
- [90] ATLAS Collaboration, *Measurement of the Inelastic Proton-Proton Cross Section at $\sqrt{s} = 13$ TeV with the ATLAS Detector at the LHC*, **Phys. Rev. Lett.** **117** (2016) 182002,
arXiv: [1606.02625](https://arxiv.org/abs/1606.02625) [[hep-ex](#)].
- [91] ATLAS Collaboration,
Luminosity determination in pp collisions at $\sqrt{s} = 13$ TeV using the ATLAS detector at the LHC,
ATLAS-CONF-2019-021, 2019, URL: <https://cds.cern.ch/record/2677054>.
- [92] G. Avoni et al., *The new LUCID-2 detector for luminosity measurement and monitoring in ATLAS*,
JINST **13** (2018) P07017.
- [93] J. Butterworth et al., *PDF4LHC recommendations for LHC Run II*, **J. Phys. G** **43** (2016) 023001,
arXiv: [1510.03865](https://arxiv.org/abs/1510.03865) [[hep-ex](#)].
- [94] The LEP SUSY Working Group and the ALEPH, DELPHI, L3 and OPAL experiments,
notes LEPSUSYWG/01-03.1, 04-01.1,
URL: <http://lepsusy.web.cern.ch/lepsusy/Welcome.html>.
- [95] ATLAS Collaboration, *ATLAS Computing Acknowledgements*, ATL-SOFT-PUB-2023-001, 2023,
URL: <https://cds.cern.ch/record/2869272>.

The ATLAS Collaboration

G. Aad ¹⁰², B. Abbott ¹²⁰, K. Abeling ⁵⁵, N.J. Abicht ⁴⁹, S.H. Abidi ²⁹, A. Aboulhorma ^{35e}, H. Abramowicz ¹⁵¹, H. Abreu ¹⁵⁰, Y. Abulaiti ¹¹⁷, B.S. Acharya ^{69a,69b,m}, C. Adam Bourdarios ⁴, L. Adamczyk ^{86a}, L. Adamek ¹⁵⁵, S.V. Addepalli ²⁶, M.J. Addison ¹⁰¹, J. Adelman ¹¹⁵, A. Adiguzel ^{21c}, T. Adye ¹³⁴, A.A. Affolder ¹³⁶, Y. Afik ³⁶, M.N. Agaras ¹³, J. Agarwala ^{73a,73b}, A. Aggarwal ¹⁰⁰, C. Agheorghiesei ^{27c}, A. Ahmad ³⁶, F. Ahmadov ^{38,y}, W.S. Ahmed ¹⁰⁴, S. Ahuja ⁹⁵, X. Ai ^{62a}, G. Aielli ^{76a,76b}, A. Aikot ¹⁶³, M. Ait Tamlah ^{35e}, B. Aitbenchikh ^{35a}, I. Aizenberg ¹⁶⁹, M. Akbiyik ¹⁰⁰, T.P.A. Åkesson ⁹⁸, A.V. Akimov ³⁷, D. Akiyama ¹⁶⁸, N.N. Akolkar ²⁴, K. Al Khoury ⁴¹, G.L. Alberghi ^{23b}, J. Albert ¹⁶⁵, P. Albicocco ⁵³, G.L. Albouy ⁶⁰, S. Alderweireldt ⁵², M. Aleksa ³⁶, I.N. Aleksandrov ³⁸, C. Alexa ^{27b}, T. Alexopoulos ¹⁰, F. Alfonsi ^{23b}, M. Algren ⁵⁶, M. Alhroob ¹²⁰, B. Ali ¹³², H.M.J. Ali ⁹¹, S. Ali ¹⁴⁸, S.W. Alibocus ⁹², M. Aliev ¹⁴⁵, G. Alimonti ^{71a}, W. Alkakhri ⁵⁵, C. Allaire ⁶⁶, B.M.M. Allbrooke ¹⁴⁶, J.F. Allen ⁵², C.A. Allendes Flores ^{137f}, P.P. Allport ²⁰, A. Aloisio ^{72a,72b}, F. Alonso ⁹⁰, C. Alpigiani ¹³⁸, M. Alvarez Estevez ⁹⁹, A. Alvarez Fernandez ¹⁰⁰, M. Alves Cardoso ⁵⁶, M.G. Alviggi ^{72a,72b}, M. Aly ¹⁰¹, Y. Amaral Coutinho ^{83b}, A. Ambler ¹⁰⁴, C. Amelung ³⁶, M. Ameri ¹⁰¹, C.G. Ames ¹⁰⁹, D. Amidei ¹⁰⁶, S.P. Amor Dos Santos ^{130a}, K.R. Amos ¹⁶³, V. Ananiev ¹²⁵, C. Anastopoulos ¹³⁹, T. Andeen ¹¹, J.K. Anders ³⁶, S.Y. Andreev ^{47a,47b}, A. Andreatta ^{71a,71b}, S. Angelidakis ⁹, A. Angerami ^{41,ab}, A.V. Anisenkov ³⁷, A. Annovi ^{74a}, C. Antel ⁵⁶, M.T. Anthony ¹³⁹, E. Antipov ¹⁴⁵, M. Antonelli ⁵³, F. Anulli ^{75a}, M. Aoki ⁸⁴, T. Aoki ¹⁵³, J.A. Aparisi Pozo ¹⁶³, M.A. Aparo ¹⁴⁶, L. Aperio Bella ⁴⁸, C. Appelt ¹⁸, A. Apyan ²⁶, N. Aranzabal ³⁶, C. Arcangeletti ⁵³, A.T.H. Arce ⁵¹, E. Arena ⁹², J-F. Arguin ¹⁰⁸, S. Argyropoulos ⁵⁴, J.-H. Arling ⁴⁸, O. Arnaez ⁴, H. Arnold ¹¹⁴, G. Artoni ^{75a,75b}, H. Asada ¹¹¹, K. Asai ¹¹⁸, S. Asai ¹⁵³, N.A. Asbah ⁶¹, K. Assamagan ²⁹, R. Astalos ^{28a}, S. Atashi ¹⁶⁰, R.J. Atkin ^{33a}, M. Atkinson ¹⁶², H. Atmani ^{35f}, P.A. Atmasiddha ¹⁰⁶, K. Augsten ¹³², S. Auricchio ^{72a,72b}, A.D. Auriol ²⁰, V.A. Austrup ¹⁰¹, G. Avolio ³⁶, K. Axiotis ⁵⁶, G. Azuelos ^{108,ag}, D. Babal ^{28b}, H. Bachacou ¹³⁵, K. Bachas ^{152,p}, A. Bachiu ³⁴, F. Backman ^{47a,47b}, A. Badea ⁶¹, P. Bagnaia ^{75a,75b}, M. Bahmani ¹⁸, A.J. Bailey ¹⁶³, V.R. Bailey ¹⁶², J.T. Baines ¹³⁴, L. Baines ⁹⁴, C. Bakalis ¹⁰, O.K. Baker ¹⁷², E. Bakos ¹⁵, D. Bakshi Gupta ⁸, V. Balakrishnan ¹²⁰, R. Balasubramanian ¹¹⁴, E.M. Baldin ³⁷, P. Balek ^{86a}, E. Ballabene ^{23b,23a}, F. Balli ¹³⁵, L.M. Baltes ^{63a}, W.K. Balunas ³², J. Balz ¹⁰⁰, E. Banas ⁸⁷, M. Bandieramonte ¹²⁹, A. Bandyopadhyay ²⁴, S. Bansal ²⁴, L. Barak ¹⁵¹, M. Barakat ⁴⁸, E.L. Barberio ¹⁰⁵, D. Barberis ^{57b,57a}, M. Barbero ¹⁰², M.Z. Barel ¹¹⁴, K.N. Barends ^{33a}, T. Barillari ¹¹⁰, M-S. Barisits ³⁶, T. Barklow ¹⁴³, P. Baron ¹²², D.A. Baron Moreno ¹⁰¹, A. Baroncelli ^{62a}, G. Barone ²⁹, A.J. Barr ¹²⁶, J.D. Barr ⁹⁶, L. Barranco Navarro ^{47a,47b}, F. Barreiro ⁹⁹, J. Barreiro Guimarães da Costa ^{14a}, U. Barron ¹⁵¹, M.G. Barros Teixeira ^{130a}, S. Barsov ³⁷, F. Bartels ^{63a}, R. Bartoldus ¹⁴³, A.E. Barton ⁹¹, P. Bartos ^{28a}, A. Basan ¹⁰⁰, M. Baselga ⁴⁹, A. Bassalat ^{66,b}, M.J. Basso ^{156a}, C.R. Basson ¹⁰¹, R.L. Bates ⁵⁹, S. Batlamous ^{35e}, J.R. Batley ³², B. Batool ¹⁴¹, M. Battaglia ¹³⁶, D. Battulga ¹⁸, M. Bause ^{75a,75b}, M. Bauer ³⁶, P. Bauer ²⁴, L.T. Bazzano Hurrell ³⁰, J.B. Beacham ⁵¹, T. Beau ¹²⁷, P.H. Beauchemin ¹⁵⁸, F. Becherer ⁵⁴, P. Bechtel ²⁴, H.P. Beck ^{19,o}, K. Becker ¹⁶⁷, A.J. Beddall ⁸², V.A. Bednyakov ³⁸, C.P. Bee ¹⁴⁵, L.J. Beemster ¹⁵, T.A. Beermann ³⁶, M. Begalli ^{83d}, M. Begel ²⁹, A. Behera ¹⁴⁵, J.K. Behr ⁴⁸, J.F. Beirer ⁵⁵, F. Beisiegel ²⁴, M. Belfkir ¹⁵⁹, G. Bella ¹⁵¹, L. Bellagamba ^{23b}, A. Bellerive ³⁴, P. Bellos ²⁰, K. Beloborodov ³⁷, D. Benchebroun ^{35a}, F. Bendebba ^{35a}, Y. Benhammou ¹⁵¹, M. Benoit ²⁹, J.R. Bensinger ²⁶, S. Bentvelsen ¹¹⁴, L. Beresford ⁴⁸, M. Beretta ⁵³, E. Bergeas Kuutmann ¹⁶¹,

N. Berger ⁴, B. Bergmann ¹³², J. Beringer ^{17a}, G. Bernardi ⁵, C. Bernius ¹⁴³,
 F.U. Bernlochner ²⁴, F. Bernon ^{36,102}, T. Berry ⁹⁵, P. Berta ¹³³, A. Berthold ⁵⁰, I.A. Bertram ⁹¹,
 S. Bethke ¹¹⁰, A. Betti ^{75a,75b}, A.J. Bevan ⁹⁴, M. Bhamjee ^{33c}, S. Bhatta ¹⁴⁵,
 D.S. Bhattacharya ¹⁶⁶, P. Bhattarai ¹⁴³, V.S. Bhopatkar ¹²¹, R. Bi ^{29,ai}, R.M. Bianchi ¹²⁹,
 G. Bianco ^{23b,23a}, O. Biebel ¹⁰⁹, R. Bielski ¹²³, M. Biglietti ^{77a}, M. Bindi ⁵⁵, A. Bingul ^{21b},
 C. Bini ^{75a,75b}, A. Biondini ⁹², C.J. Birch-sykes ¹⁰¹, G.A. Bird ^{20,134}, M. Birman ¹⁶⁹,
 M. Biros ¹³³, S. Biryukov ¹⁴⁶, T. Bisanz ⁴⁹, E. Bisceglie ^{43b,43a}, J.P. Biswal ¹³⁴, D. Biswas ¹⁴¹,
 A. Bitadze ¹⁰¹, K. Bjørke ¹²⁵, I. Bloch ⁴⁸, C. Blocker ²⁶, A. Blue ⁵⁹, U. Blumenschein ⁹⁴,
 J. Blumenthal ¹⁰⁰, G.J. Bobbink ¹¹⁴, V.S. Bobrovnikov ³⁷, M. Boehler ⁵⁴, B. Boehm ¹⁶⁶,
 D. Bogavac ³⁶, A.G. Bogdanchikov ³⁷, C. Bohm ^{47a}, V. Boisvert ⁹⁵, P. Bokan ⁴⁸, T. Bold ^{86a},
 M. Bomben ⁵, M. Bona ⁹⁴, M. Boonekamp ¹³⁵, C.D. Booth ⁹⁵, A.G. Borbély ⁵⁹,
 I.S. Bordulev ³⁷, H.M. Borecka-Bielska ¹⁰⁸, G. Borissov ⁹¹, D. Bortoletto ¹²⁶, D. Boscherini ^{23b},
 M. Bosman ¹³, J.D. Bossio Sola ³⁶, K. Bouaouda ^{35a}, N. Bouchhar ¹⁶³, J. Boudreau ¹²⁹,
 E.V. Bouhova-Thacker ⁹¹, D. Boumediene ⁴⁰, R. Bouquet ⁵, A. Boveia ¹¹⁹, J. Boyd ³⁶,
 D. Boye ²⁹, I.R. Boyko ³⁸, J. Bracinek ²⁰, N. Brahimi ^{62d}, G. Brandt ¹⁷¹, O. Brandt ³²,
 F. Braren ⁴⁸, B. Brau ¹⁰³, J.E. Brau ¹²³, R. Brenner ¹⁶⁹, L. Brenner ¹¹⁴, R. Brenner ¹⁶¹,
 S. Bressler ¹⁶⁹, D. Britton ⁵⁹, D. Britzger ¹¹⁰, I. Brock ²⁴, G. Brooijmans ⁴¹, W.K. Brooks ^{137f},
 E. Brost ²⁹, L.M. Brown ¹⁶⁵, L.E. Bruce ⁶¹, T.L. Bruckler ¹²⁶, P.A. Bruckman de Renstrom ⁸⁷,
 B. Brüers ⁴⁸, A. Bruni ^{23b}, G. Bruni ^{23b}, M. Bruschi ^{23b}, N. Brusino ^{75a,75b}, T. Buanes ¹⁶,
 Q. Buat ¹³⁸, D. Buchin ¹¹⁰, A.G. Buckley ⁵⁹, O. Bulekov ³⁷, B.A. Bullard ¹⁴³, S. Burdin ⁹²,
 C.D. Burgard ⁴⁹, A.M. Burger ⁴⁰, B. Burghgrave ⁸, O. Burlayenko ⁵⁴, J.T.P. Burr ³²,
 C.D. Burton ¹¹, J.C. Burzynski ¹⁴², E.L. Busch ⁴¹, V. Büscher ¹⁰⁰, P.J. Bussey ⁵⁹,
 J.M. Butler ²⁵, C.M. Buttar ⁵⁹, J.M. Butterworth ⁹⁶, W. Buttinger ¹³⁴, C.J. Buxo Vazquez ¹⁰⁷,
 A.R. Buzykaev ³⁷, S. Cabrera Urbán ¹⁶³, L. Cadamuro ⁶⁶, D. Caforio ⁵⁸, H. Cai ¹²⁹,
 Y. Cai ^{14a,14e}, V.M.M. Cairo ³⁶, O. Cakir ^{3a}, N. Calace ³⁶, P. Calafiura ^{17a}, G. Calderini ¹²⁷,
 P. Calfayan ⁶⁸, G. Callea ⁵⁹, L.P. Caloba ^{83b}, D. Calvet ⁴⁰, S. Calvet ⁴⁰, T.P. Calvet ¹⁰²,
 M. Calvetti ^{74a,74b}, R. Camacho Toro ¹²⁷, S. Camarda ³⁶, D. Camarero Munoz ²⁶,
 P. Camarri ^{76a,76b}, M.T. Camerlingo ^{72a,72b}, D. Cameron ³⁶, C. Camincher ¹⁶⁵, M. Campanelli ⁹⁶,
 A. Camplani ⁴², V. Canale ^{72a,72b}, A. Canesse ¹⁰⁴, J. Cantero ¹⁶³, Y. Cao ¹⁶², F. Capocasa ²⁶,
 M. Capua ^{43b,43a}, A. Carbone ^{71a,71b}, R. Cardarelli ^{76a}, J.C.J. Cardenas ⁸, F. Cardillo ¹⁶³,
 T. Carli ³⁶, G. Carlino ^{72a}, J.I. Carlotto ¹³, B.T. Carlson ^{129,q}, E.M. Carlson ^{165,156a},
 L. Carminati ^{71a,71b}, A. Carnelli ¹³⁵, M. Carnesale ^{75a,75b}, S. Caron ¹¹³, E. Carquin ^{137f},
 S. Carrá ^{71a}, G. Carratta ^{23b,23a}, F. Carrio Argos ^{33g}, J.W.S. Carter ¹⁵⁵, T.M. Carter ⁵²,
 M.P. Casado ^{13,i}, M. Caspar ⁴⁸, E.G. Castiglia ¹⁷², F.L. Castillo ⁴, L. Castillo Garcia ¹³,
 V. Castillo Gimenez ¹⁶³, N.F. Castro ^{130a,130e}, A. Catinaccio ³⁶, J.R. Catmore ¹²⁵, V. Cavaliere ²⁹,
 N. Cavalli ^{23b,23a}, V. Cavalinni ^{74a,74b}, Y.C. Cekmecelioglu ⁴⁸, E. Celebi ^{21a}, F. Celli ¹²⁶,
 M.S. Centonze ^{70a,70b}, V. Cepaitis ⁵⁶, K. Cerny ¹²², A.S. Cerqueira ^{83a}, A. Cerri ¹⁴⁶,
 L. Cerrito ^{76a,76b}, F. Cerutti ^{17a}, B. Cervato ¹⁴¹, A. Cervelli ^{23b}, G. Cesarini ⁵³, S.A. Cetin ⁸²,
 Z. Chadi ^{35a}, D. Chakraborty ¹¹⁵, J. Chan ¹⁷⁰, W.Y. Chan ¹⁵³, J.D. Chapman ³², E. Chapon ¹³⁵,
 B. Chargeishvili ^{149b}, D.G. Charlton ²⁰, T.P. Charman ⁹⁴, M. Chatterjee ¹⁹, C. Chauhan ¹³³,
 S. Chekanov ⁶, S.V. Chekulaev ^{156a}, G.A. Chelkov ^{38,a}, A. Chen ¹⁰⁶, B. Chen ¹⁵¹, B. Chen ¹⁶⁵,
 H. Chen ^{14c}, H. Chen ²⁹, J. Chen ^{62c}, J. Chen ¹⁴², M. Chen ¹²⁶, S. Chen ¹⁵³, S.J. Chen ^{14c},
 X. Chen ^{62c,135}, X. Chen ^{14b,af}, Y. Chen ^{62a}, C.L. Cheng ¹⁷⁰, H.C. Cheng ^{64a}, S. Cheong ¹⁴³,
 A. Cheplakov ³⁸, E. Cheremushkina ⁴⁸, E. Cherepanova ¹¹⁴, R. Cherkaoui El Moursli ^{35e},
 E. Cheu ⁷, K. Cheung ⁶⁵, L. Chevalier ¹³⁵, V. Chiarella ⁵³, G. Chiarelli ^{74a}, N. Chiedde ¹⁰²,
 G. Chiodini ^{70a}, A.S. Chisholm ²⁰, A. Chitan ^{27b}, M. Chitishvili ¹⁶³, M.V. Chizhov ³⁸,
 K. Choi ¹¹, A.R. Chomont ^{75a,75b}, Y. Chou ¹⁰³, E.Y.S. Chow ¹¹⁴, T. Chowdhury ^{33g},

K.L. Chu [id](#)¹⁶⁹, M.C. Chu [id](#)^{64a}, X. Chu [id](#)^{14a,14e}, J. Chudoba [id](#)¹³¹, J.J. Chwastowski [id](#)⁸⁷, D. Cieri [id](#)¹¹⁰,
 K.M. Ciesla [id](#)^{86a}, V. Cindro [id](#)⁹³, A. Ciocio [id](#)^{17a}, F. Ciroto [id](#)^{72a,72b}, Z.H. Citron [id](#)^{169,k}, M. Citterio [id](#)^{71a},
 D.A. Ciubotaru [id](#)^{27b}, B.M. Ciungu [id](#)¹⁵⁵, A. Clark [id](#)⁵⁶, P.J. Clark [id](#)⁵², J.M. Clavijo Columbie [id](#)⁴⁸,
 S.E. Clawson [id](#)⁴⁸, C. Clement [id](#)^{47a,47b}, J. Clercx [id](#)⁴⁸, Y. Coadou [id](#)¹⁰², M. Cobal [id](#)^{69a,69c},
 A. Coccaro [id](#)^{57b}, R.F. Coelho Barrue [id](#)^{130a}, R. Coelho Lopes De Sa [id](#)¹⁰³, S. Coelli [id](#)^{71a}, H. Cohen [id](#)¹⁵¹,
 A.E.C. Coimbra [id](#)^{71a,71b}, B. Cole [id](#)⁴¹, J. Collot [id](#)⁵⁰, P. Conde Muiño [id](#)^{130a,130g}, M.P. Connell [id](#)^{33c},
 S.H. Connell [id](#)^{33c}, I.A. Connelly [id](#)⁵⁹, E.I. Conroy [id](#)¹²⁶, F. Conventi [id](#)^{72a,ah}, H.G. Cooke [id](#)²⁰,
 A.M. Cooper-Sarkar [id](#)¹²⁶, A. Cordeiro Oudot Choi [id](#)¹²⁷, F. Cormier [id](#)¹⁶⁴, L.D. Corpe [id](#)⁴⁰,
 M. Corradi [id](#)^{75a,75b}, F. Corriveau [id](#)^{104,w}, A. Cortes-Gonzalez [id](#)¹⁸, M.J. Costa [id](#)¹⁶³, F. Costanza [id](#)⁴,
 D. Costanzo [id](#)¹³⁹, B.M. Cote [id](#)¹¹⁹, G. Cowan [id](#)⁹⁵, K. Cranmer [id](#)¹⁷⁰, D. Cremonini [id](#)^{23b,23a},
 S. Crépe-Renaudin [id](#)⁶⁰, F. Crescioli [id](#)¹²⁷, M. Cristinziani [id](#)¹⁴¹, M. Cristoforetti [id](#)^{78a,78b}, V. Croft [id](#)¹¹⁴,
 J.E. Crosby [id](#)¹²¹, G. Crosetti [id](#)^{43b,43a}, A. Cueto [id](#)⁹⁹, T. Cuhadar Donszelmann [id](#)¹⁶⁰, H. Cui [id](#)^{14a,14e},
 Z. Cui [id](#)⁷, W.R. Cunningham [id](#)⁵⁹, F. Curcio [id](#)^{43b,43a}, P. Czodrowski [id](#)³⁶, M.M. Czurylo [id](#)^{63b},
 M.J. Da Cunha Sargedas De Sousa [id](#)^{57b,57a}, J.V. Da Fonseca Pinto [id](#)^{83b}, C. Da Via [id](#)¹⁰¹,
 W. Dabrowski [id](#)^{86a}, T. Dado [id](#)⁴⁹, S. Dahbi [id](#)^{33g}, T. Dai [id](#)¹⁰⁶, D. Dal Santo [id](#)¹⁹, C. Dallapiccola [id](#)¹⁰³,
 M. Dam [id](#)⁴², G. D'amen [id](#)²⁹, V. D'Amico [id](#)¹⁰⁹, J. Damp [id](#)¹⁰⁰, J.R. Dandoy [id](#)¹²⁸, M.F. Daneri [id](#)³⁰,
 M. Danninger [id](#)¹⁴², V. Dao [id](#)³⁶, G. Darbo [id](#)^{57b}, S. Darmora [id](#)⁶, S.J. Das [id](#)^{29,ai}, S. D'Auria [id](#)^{71a,71b},
 C. David [id](#)^{156b}, T. Davidek [id](#)¹³³, B. Davis-Purcell [id](#)³⁴, I. Dawson [id](#)⁹⁴, H.A. Day-hall [id](#)¹³², K. De [id](#)⁸,
 R. De Asmundis [id](#)^{72a}, N. De Biase [id](#)⁴⁸, S. De Castro [id](#)^{23b,23a}, N. De Groot [id](#)¹¹³, P. de Jong [id](#)¹¹⁴,
 H. De la Torre [id](#)¹¹⁵, A. De Maria [id](#)^{14c}, A. De Salvo [id](#)^{75a}, U. De Sanctis [id](#)^{76a,76b}, A. De Santo [id](#)¹⁴⁶,
 J.B. De Vivie De Regie [id](#)⁶⁰, D.V. Dedovich [id](#)³⁸, J. Degens [id](#)¹¹⁴, A.M. Deiana [id](#)⁴⁴, F. Del Corso [id](#)^{23b,23a},
 J. Del Peso [id](#)⁹⁹, F. Del Rio [id](#)^{63a}, F. Deliot [id](#)¹³⁵, C.M. Delitzsch [id](#)⁴⁹, M. Della Pietra [id](#)^{72a,72b},
 D. Della Volpe [id](#)⁵⁶, A. Dell'Acqua [id](#)³⁶, L. Dell'Asta [id](#)^{71a,71b}, M. Delmastro [id](#)⁴, P.A. Delsart [id](#)⁶⁰,
 S. Demers [id](#)¹⁷², M. Demichev [id](#)³⁸, S.P. Denisov [id](#)³⁷, L. D'Eramo [id](#)⁴⁰, D. Derendarz [id](#)⁸⁷, F. Derue [id](#)¹²⁷,
 P. Dervan [id](#)⁹², K. Desch [id](#)²⁴, C. Deutsch [id](#)²⁴, F.A. Di Bello [id](#)^{57b,57a}, A. Di Ciaccio [id](#)^{76a,76b},
 L. Di Ciaccio [id](#)⁴, A. Di Domenico [id](#)^{75a,75b}, C. Di Donato [id](#)^{72a,72b}, A. Di Girolamo [id](#)³⁶,
 G. Di Gregorio [id](#)³⁶, A. Di Luca [id](#)^{78a,78b}, B. Di Micco [id](#)^{77a,77b}, R. Di Nardo [id](#)^{77a,77b}, C. Diaconu [id](#)¹⁰²,
 M. Diamantopoulou [id](#)³⁴, F.A. Dias [id](#)¹¹⁴, T. Dias Do Vale [id](#)¹⁴², M.A. Diaz [id](#)^{137a,137b},
 F.G. Diaz Capriles [id](#)²⁴, M. Didenko [id](#)¹⁶³, E.B. Diehl [id](#)¹⁰⁶, L. Diehl [id](#)⁵⁴, S. Díez Cornell [id](#)⁴⁸,
 C. Díez Pardos [id](#)¹⁴¹, C. Dimitriadi [id](#)^{161,24,161}, A. Dimitrievska [id](#)^{17a}, J. Dingfelder [id](#)²⁴, I-M. Dinu [id](#)^{27b},
 S.J. Dittmeier [id](#)^{63b}, F. Dittus [id](#)³⁶, F. Djama [id](#)¹⁰², T. Djobava [id](#)^{149b}, J.I. Djuvslund [id](#)¹⁶,
 C. Doglioni [id](#)^{101,98}, A. Dohnalova [id](#)^{28a}, J. Dolejsi [id](#)¹³³, Z. Dolezal [id](#)¹³³, K.M. Dona [id](#)³⁹,
 M. Donadelli [id](#)^{83c}, B. Dong [id](#)¹⁰⁷, J. Donini [id](#)⁴⁰, A. D'Onofrio [id](#)^{77a,77b}, M. D'Onofrio [id](#)⁹²,
 J. Dopke [id](#)¹³⁴, A. Doria [id](#)^{72a}, N. Dos Santos Fernandes [id](#)^{130a}, P. Dougan [id](#)¹⁰¹, M.T. Dova [id](#)⁹⁰,
 A.T. Doyle [id](#)⁵⁹, M.A. Draguet [id](#)¹²⁶, E. Dreyer [id](#)¹⁶⁹, I. Drivas-koulouris [id](#)¹⁰, A.S. Drobac [id](#)¹⁵⁸,
 M. Drozdova [id](#)⁵⁶, D. Du [id](#)^{62a}, T.A. du Pree [id](#)¹¹⁴, F. Dubinin [id](#)³⁷, M. Dubovsky [id](#)^{28a}, E. Duchovni [id](#)¹⁶⁹,
 G. Duckeck [id](#)¹⁰⁹, O.A. Ducu [id](#)^{27b}, D. Duda [id](#)⁵², A. Dudarev [id](#)³⁶, E.R. Duden [id](#)²⁶, M. D'uffizi [id](#)¹⁰¹,
 L. Dufflot [id](#)⁶⁶, M. Dührssen [id](#)³⁶, C. Dülsen [id](#)¹⁷¹, A.E. Dumitriu [id](#)^{27b}, M. Dunford [id](#)^{63a}, S. Dungs [id](#)⁴⁹,
 K. Dunne [id](#)^{47a,47b}, A. Duperrin [id](#)¹⁰², H. Duran Yildiz [id](#)^{3a}, M. Düren [id](#)⁵⁸, A. Durglishvili [id](#)^{149b},
 B.L. Dwyer [id](#)¹¹⁵, G.I. Dyckes [id](#)^{17a}, M. Dyndal [id](#)^{86a}, S. Dysch [id](#)¹⁰¹, B.S. Dziedzic [id](#)⁸⁷,
 Z.O. Earnshaw [id](#)¹⁴⁶, G.H. Eberwein [id](#)¹²⁶, B. Eckerova [id](#)^{28a}, S. Eggebrecht [id](#)⁵⁵,
 E. Egidio Purcino De Souza [id](#)¹²⁷, L.F. Ehrke [id](#)⁵⁶, G. Eigen [id](#)¹⁶, K. Einsweiler [id](#)^{17a}, T. Ekelof [id](#)¹⁶¹,
 P.A. Ekman [id](#)⁹⁸, S. El Farkh [id](#)^{35b}, Y. El Ghazali [id](#)^{35b}, H. El Jarrari [id](#)^{35e,148}, A. El Moussaouy [id](#)¹⁰⁸,
 V. Ellajosyula [id](#)¹⁶¹, M. Ellert [id](#)¹⁶¹, F. Ellinghaus [id](#)¹⁷¹, A.A. Elliot [id](#)⁹⁴, N. Ellis [id](#)³⁶, J. Elmsheuser [id](#)²⁹,
 M. Elsing [id](#)³⁶, D. Emelianov [id](#)¹³⁴, Y. Enari [id](#)¹⁵³, I. Ene [id](#)^{17a}, S. Epari [id](#)¹³, J. Erdmann [id](#)⁴⁹,
 P.A. Erland [id](#)⁸⁷, M. Errenst [id](#)¹⁷¹, M. Escalier [id](#)⁶⁶, C. Escobar [id](#)¹⁶³, E. Etzion [id](#)¹⁵¹, G. Evans [id](#)^{130a},
 H. Evans [id](#)⁶⁸, L.S. Evans [id](#)⁹⁵, M.O. Evans [id](#)¹⁴⁶, A. Ezhilov [id](#)³⁷, S. Ezzarqtouni [id](#)^{35a}, F. Fabbri [id](#)⁵⁹,

L. Fabbri [ID^{23b,23a}](#), G. Facini [ID⁹⁶](#), V. Fadeyev [ID¹³⁶](#), R.M. Fakhruddinov [ID³⁷](#), S. Falciano [ID^{75a}](#),
 L.F. Falda Ulhoa Coelho [ID³⁶](#), P.J. Falke [ID²⁴](#), J. Faltova [ID¹³³](#), C. Fan [ID¹⁶²](#), Y. Fan [ID^{14a}](#), Y. Fang [ID^{14a,14e}](#),
 M. Fanti [ID^{71a,71b}](#), M. Faraj [ID^{69a,69b}](#), Z. Farazpay [ID⁹⁷](#), A. Farbin [ID⁸](#), A. Farilla [ID^{77a}](#), T. Farooque [ID¹⁰⁷](#),
 S.M. Farrington [ID⁵²](#), F. Fassi [ID^{35e}](#), D. Fassouliotis [ID⁹](#), M. Faucci Giannelli [ID^{76a,76b}](#), W.J. Fawcett [ID³²](#),
 L. Fayard [ID⁶⁶](#), P. Federic [ID¹³³](#), P. Federicova [ID¹³¹](#), O.L. Fedin [ID^{37,a}](#), G. Fedotov [ID³⁷](#), M. Feickert [ID¹⁷⁰](#),
 L. Feligioni [ID¹⁰²](#), D.E. Fellers [ID¹²³](#), C. Feng [ID^{62b}](#), M. Feng [ID^{14b}](#), Z. Feng [ID¹¹⁴](#), M.J. Fenton [ID¹⁶⁰](#),
 A.B. Fenyuk [ID³⁷](#), L. Ferencz [ID⁴⁸](#), R.A.M. Ferguson [ID⁹¹](#), S.I. Fernandez Luengo [ID^{137f}](#), M.J.V. Fernoux [ID¹⁰²](#),
 J. Ferrando [ID⁴⁸](#), A. Ferrari [ID¹⁶¹](#), P. Ferrari [ID^{114,113}](#), R. Ferrari [ID^{73a}](#), D. Ferrere [ID⁵⁶](#), C. Ferretti [ID¹⁰⁶](#),
 F. Fiedler [ID¹⁰⁰](#), P. Fiedler [ID¹³²](#), A. Filipčič [ID⁹³](#), E.K. Filmer [ID¹](#), F. Filthaut [ID¹¹³](#),
 M.C.N. Fiolhais [ID^{130a,130c,c}](#), L. Fiorini [ID¹⁶³](#), W.C. Fisher [ID¹⁰⁷](#), T. Fitschen [ID¹⁰¹](#), P.M. Fitzhugh [ID¹³⁵](#),
 I. Fleck [ID¹⁴¹](#), P. Fleischmann [ID¹⁰⁶](#), T. Flick [ID¹⁷¹](#), M. Flores [ID^{33d,ac}](#), L.R. Flores Castillo [ID^{64a}](#),
 L. Flores Sanz De Acedo [ID³⁶](#), F.M. Follega [ID^{78a,78b}](#), N. Fomin [ID¹⁶](#), J.H. Foo [ID¹⁵⁵](#), B.C. Forland [ID⁶⁸](#),
 A. Formica [ID¹³⁵](#), A.C. Forti [ID¹⁰¹](#), E. Fortin [ID³⁶](#), A.W. Fortman [ID⁶¹](#), M.G. Foti [ID^{17a}](#), L. Fountas [ID^{9j}](#),
 D. Fournier [ID⁶⁶](#), H. Fox [ID⁹¹](#), P. Francavilla [ID^{74a,74b}](#), S. Francescato [ID⁶¹](#), S. Franchellucci [ID⁵⁶](#),
 M. Franchini [ID^{23b,23a}](#), S. Franchino [ID^{63a}](#), D. Francis [ID³⁶](#), L. Franco [ID¹¹³](#), V. Franco Lima [ID³⁶](#),
 L. Franconi [ID⁴⁸](#), M. Franklin [ID⁶¹](#), G. Frattari [ID²⁶](#), A.C. Freegard [ID⁹⁴](#), W.S. Freund [ID^{83b}](#), Y.Y. Frid [ID¹⁵¹](#),
 J. Friend [ID⁵⁹](#), N. Fritzsche [ID⁵⁰](#), A. Froch [ID⁵⁴](#), D. Froidevaux [ID³⁶](#), J.A. Frost [ID¹²⁶](#), Y. Fu [ID^{62a}](#),
 M. Fujimoto [ID^{118,ad}](#), E. Fullana Torregrosa [ID^{163,*}](#), K.Y. Fung [ID^{64a}](#), E. Furtado De Simas Filho [ID^{83b}](#),
 M. Furukawa [ID¹⁵³](#), J. Fuster [ID¹⁶³](#), A. Gabrielli [ID^{23b,23a}](#), A. Gabrielli [ID¹⁵⁵](#), P. Gadow [ID³⁶](#),
 G. Gagliardi [ID^{57b,57a}](#), L.G. Gagnon [ID^{17a}](#), E.J. Gallas [ID¹²⁶](#), B.J. Gallop [ID¹³⁴](#), K.K. Gan [ID¹¹⁹](#),
 S. Ganguly [ID¹⁵³](#), J. Gao [ID^{62a}](#), Y. Gao [ID⁵²](#), F.M. Garay Walls [ID^{137a,137b}](#), B. Garcia [ID²⁹](#), C. García [ID¹⁶³](#),
 A. Garcia Alonso [ID¹¹⁴](#), A.G. Garcia Caffaro [ID¹⁷²](#), J.E. García Navarro [ID¹⁶³](#), M. Garcia-Sciveres [ID^{17a}](#),
 G.L. Gardner [ID¹²⁸](#), R.W. Gardner [ID³⁹](#), N. Garelli [ID¹⁵⁸](#), D. Garg [ID⁸⁰](#), R.B. Garg [ID^{143,n}](#), J.M. Gargan [ID⁵²](#),
 C.A. Garner [ID¹⁵⁵](#), C.M. Garvey [ID^{33a}](#), S.J. Gasiorowski [ID¹³⁸](#), P. Gaspar [ID^{83b}](#), G. Gaudio [ID^{73a}](#), V. Gautam [ID¹³](#),
 P. Gauzzi [ID^{75a,75b}](#), I.L. Gavrilenko [ID³⁷](#), A. Gavrilyuk [ID³⁷](#), C. Gay [ID¹⁶⁴](#), G. Gaycken [ID⁴⁸](#), E.N. Gazis [ID¹⁰](#),
 A.A. Geanta [ID^{27b}](#), C.M. Gee [ID¹³⁶](#), C. Gemme [ID^{57b}](#), M.H. Genest [ID⁶⁰](#), S. Gentile [ID^{75a,75b}](#),
 A.D. Gentry [ID¹¹²](#), S. George [ID⁹⁵](#), W.F. George [ID²⁰](#), T. Geralis [ID⁴⁶](#), P. Gessinger-Befurt [ID³⁶](#),
 M.E. Geyik [ID¹⁷¹](#), M. Ghani [ID¹⁶⁷](#), M. Ghneimat [ID¹⁴¹](#), K. Ghorbanian [ID⁹⁴](#), A. Ghosal [ID¹⁴¹](#),
 A. Ghosh [ID¹⁶⁰](#), A. Ghosh [ID⁷](#), B. Giacobbe [ID^{23b}](#), S. Giagu [ID^{75a,75b}](#), T. Giani [ID¹¹⁴](#), P. Giannetti [ID^{74a}](#),
 A. Giannini [ID^{62a}](#), S.M. Gibson [ID⁹⁵](#), M. Gignac [ID¹³⁶](#), D.T. Gil [ID^{86b}](#), A.K. Gilbert [ID^{86a}](#), B.J. Gilbert [ID⁴¹](#),
 D. Gillberg [ID³⁴](#), G. Gilles [ID¹¹⁴](#), N.E.K. Gillwald [ID⁴⁸](#), L. Ginabat [ID¹²⁷](#), D.M. Gingrich [ID^{2,ag}](#),
 M.P. Giordani [ID^{69a,69c}](#), P.F. Giraud [ID¹³⁵](#), G. Giugliarelli [ID^{69a,69c}](#), D. Giugni [ID^{71a}](#), F. Giuli [ID³⁶](#),
 I. Gkialas [ID^{9j}](#), L.K. Gladilin [ID³⁷](#), C. Glasman [ID⁹⁹](#), G.R. Gledhill [ID¹²³](#), G. Glemža [ID⁴⁸](#), M. Glisic [ID¹²³](#),
 I. Gnesi [ID^{43b,f}](#), Y. Go [ID^{29,ai}](#), M. Goblirsch-Kolb [ID³⁶](#), B. Gocke [ID⁴⁹](#), D. Godin [ID¹⁰⁸](#), B. Gokturk [ID^{21a}](#),
 S. Goldfarb [ID¹⁰⁵](#), T. Golling [ID⁵⁶](#), M.G.D. Gololo [ID^{33g}](#), D. Golubkov [ID³⁷](#), J.P. Gombas [ID¹⁰⁷](#),
 A. Gomes [ID^{130a,130b}](#), G. Gomes Da Silva [ID¹⁴¹](#), A.J. Gomez Delegido [ID¹⁶³](#), R. Gonçalo [ID^{130a,130c}](#),
 G. Gonella [ID¹²³](#), L. Gonella [ID²⁰](#), A. Gongadze [ID^{149c}](#), F. Gonnella [ID²⁰](#), J.L. Gonski [ID⁴¹](#),
 R.Y. González Andana [ID⁵²](#), S. González de la Hoz [ID¹⁶³](#), S. Gonzalez Fernandez [ID¹³](#),
 R. Gonzalez Lopez [ID⁹²](#), C. Gonzalez Renteria [ID^{17a}](#), M.V. Gonzalez Rodrigues [ID⁴⁸](#),
 R. Gonzalez Suarez [ID¹⁶¹](#), S. Gonzalez-Sevilla [ID⁵⁶](#), G.R. Gonzalvo Rodriguez [ID¹⁶³](#), L. Goossens [ID³⁶](#),
 B. Gorini [ID³⁶](#), E. Gorini [ID^{70a,70b}](#), A. Gorišek [ID⁹³](#), T.C. Gosart [ID¹²⁸](#), A.T. Goshaw [ID⁵¹](#), M.I. Gostkin [ID³⁸](#),
 S. Goswami [ID¹²¹](#), C.A. Gottardo [ID³⁶](#), S.A. Gotz [ID¹⁰⁹](#), M. Goughri [ID^{35b}](#), V. Goumarre [ID⁴⁸](#),
 A.G. Goussiou [ID¹³⁸](#), N. Govender [ID^{33c}](#), I. Grabowska-Bold [ID^{86a}](#), K. Graham [ID³⁴](#), E. Gramstad [ID¹²⁵](#),
 S. Grancagnolo [ID^{70a,70b}](#), M. Grandi [ID¹⁴⁶](#), C.M. Grant [ID^{1,135}](#), P.M. Gravila [ID^{27f}](#), F.G. Gravili [ID^{70a,70b}](#),
 H.M. Gray [ID^{17a}](#), M. Greco [ID^{70a,70b}](#), C. Grefe [ID²⁴](#), I.M. Gregor [ID⁴⁸](#), P. Grenier [ID¹⁴³](#), C. Grieco [ID¹³](#),
 A.A. Grillo [ID¹³⁶](#), K. Grimm [ID³¹](#), S. Grinstein [ID^{13,s}](#), J.-F. Grivaz [ID⁶⁶](#), E. Gross [ID¹⁶⁹](#),
 J. Grosse-Knetter [ID⁵⁵](#), C. Grud [ID¹⁰⁶](#), J.C. Grundy [ID¹²⁶](#), L. Guan [ID¹⁰⁶](#), W. Guan [ID²⁹](#), C. Gubbels [ID¹⁶⁴](#),

J.G.R. Guerrero Rojas ¹⁶³, G. Guerrieri ^{69a,69c}, F. Guescini ¹¹⁰, R. Gugel ¹⁰⁰, J.A.M. Guhit ¹⁰⁶, A. Guida ¹⁸, T. Guillemain ⁴, E. Guilloton ^{167,134}, S. Guindon ³⁶, F. Guo ^{14a,14e}, J. Guo ^{62c}, L. Guo ⁴⁸, Y. Guo ¹⁰⁶, R. Gupta ⁴⁸, S. Gurbuz ²⁴, S.S. Gurdasani ⁵⁴, G. Gustavino ³⁶, M. Guth ⁵⁶, P. Gutierrez ¹²⁰, L.F. Gutierrez Zagazeta ¹²⁸, C. Gutschow ⁹⁶, C. Gwenlan ¹²⁶, C.B. Gwilliam ⁹², E.S. Haaland ¹²⁵, A. Haas ¹¹⁷, M. Habedank ⁴⁸, C. Haber ^{17a}, H.K. Hadavand ⁸, A. Hadeef ¹⁰⁰, S. Hadzic ¹¹⁰, J.J. Hahn ¹⁴¹, E.H. Haines ⁹⁶, M. Haleem ¹⁶⁶, J. Haley ¹²¹, J.J. Hall ¹³⁹, G.D. Hallewell ¹⁰², L. Halser ¹⁹, K. Hamano ¹⁶⁵, M. Hamer ²⁴, G.N. Hamity ⁵², E.J. Hampshire ⁹⁵, J. Han ^{62b}, K. Han ^{62a}, L. Han ^{14c}, L. Han ^{62a}, S. Han ^{17a}, Y.F. Han ¹⁵⁵, K. Hanagaki ⁸⁴, M. Hance ¹³⁶, D.A. Hangal ^{41,ab}, H. Hanif ¹⁴², M.D. Hank ¹²⁸, R. Hankache ¹⁰¹, J.B. Hansen ⁴², J.D. Hansen ⁴², P.H. Hansen ⁴², K. Hara ¹⁵⁷, D. Harada ⁵⁶, T. Harenberg ¹⁷¹, S. Harkusha ³⁷, M.L. Harris ¹⁰³, Y.T. Harris ¹²⁶, J. Harrison ¹³, N.M. Harrison ¹¹⁹, P.F. Harrison ¹⁶⁷, N.M. Hartman ¹¹⁰, N.M. Hartmann ¹⁰⁹, Y. Hasegawa ¹⁴⁰, R. Hauser ¹⁰⁷, C.M. Hawkes ²⁰, R.J. Hawkings ³⁶, Y. Hayashi ¹⁵³, S. Hayashida ¹¹¹, D. Hayden ¹⁰⁷, C. Hayes ¹⁰⁶, R.L. Hayes ¹¹⁴, C.P. Hays ¹²⁶, J.M. Hays ⁹⁴, H.S. Hayward ⁹², F. He ^{62a}, M. He ^{14a,14e}, Y. He ¹⁵⁴, Y. He ⁴⁸, N.B. Heatley ⁹⁴, V. Hedberg ⁹⁸, A.L. Heggelund ¹²⁵, N.D. Hehir ^{94,*}, C. Heidegger ⁵⁴, K.K. Heidegger ⁵⁴, W.D. Heidorn ⁸¹, J. Heilman ³⁴, S. Heim ⁴⁸, T. Heim ^{17a}, J.G. Heinlein ¹²⁸, J.J. Heinrich ¹²³, L. Heinrich ^{110,ae}, J. Hejbal ¹³¹, L. Helary ⁴⁸, A. Held ¹⁷⁰, S. Hellesund ¹⁶, C.M. Helling ¹⁶⁴, S. Hellman ^{47a,47b}, R.C.W. Henderson ⁹¹, L. Henkelmann ³², A.M. Henriques Correia ³⁶, H. Herde ⁹⁸, Y. Hernández Jiménez ¹⁴⁵, L.M. Herrmann ²⁴, T. Herrmann ⁵⁰, G. Herten ⁵⁴, R. Hertenberger ¹⁰⁹, L. Hervas ³⁶, M.E. Hespings ¹⁰⁰, N.P. Hessey ^{156a}, H. Hibi ⁸⁵, E. Hill ¹⁵⁵, S.J. Hillier ²⁰, J.R. Hinds ¹⁰⁷, F. Hinterkeuser ²⁴, M. Hirose ¹²⁴, S. Hirose ¹⁵⁷, D. Hirschbuehl ¹⁷¹, T.G. Hitchings ¹⁰¹, B. Hiti ⁹³, J. Hobbs ¹⁴⁵, R. Hobincu ^{27e}, N. Hod ¹⁶⁹, M.C. Hodgkinson ¹³⁹, B.H. Hodgkinson ³², A. Hoecker ³⁶, J. Hofer ⁴⁸, T. Holm ²⁴, M. Holzbock ¹¹⁰, L.B.A.H. Hommels ³², B.P. Honan ¹⁰¹, J. Hong ^{62c}, T.M. Hong ¹²⁹, B.H. Hooberman ¹⁶², W.H. Hopkins ⁶, Y. Horii ¹¹¹, S. Hou ¹⁴⁸, A.S. Howard ⁹³, J. Howarth ⁵⁹, J. Hoya ⁶, M. Hrabovsky ¹²², A. Hrynevich ⁴⁸, T. Hryn'ova ⁴, P.J. Hsu ⁶⁵, S.-C. Hsu ¹³⁸, Q. Hu ^{62a}, Y.F. Hu ^{14a,14e}, S. Huang ^{64b}, X. Huang ^{14c}, Y. Huang ¹³⁹, Y. Huang ^{14a}, Z. Huang ¹⁰¹, Z. Hubacek ¹³², M. Huebner ²⁴, F. Huegging ²⁴, T.B. Huffman ¹²⁶, C.A. Hugli ⁴⁸, M. Huhtinen ³⁶, S.K. Huiberts ¹⁶, R. Hulskens ¹⁰⁴, N. Huseynov ¹², J. Huston ¹⁰⁷, J. Huth ⁶¹, R. Hyneman ¹⁴³, G. Iacobucci ⁵⁶, G. Iakovidis ²⁹, I. Ibragimov ¹⁴¹, L. Iconomidou-Fayard ⁶⁶, P. Iengo ^{72a,72b}, R. Iguchi ¹⁵³, T. Iizawa ¹²⁶, Y. Ikegami ⁸⁴, N. Ilic ¹⁵⁵, H. Imam ^{35a}, M. Ince Lezki ⁵⁶, T. Ingebretsen Carlson ^{47a,47b}, G. Introzzi ^{73a,73b}, M. Iodice ^{77a}, V. Ippolito ^{75a,75b}, R.K. Irwin ⁹², M. Ishino ¹⁵³, W. Islam ¹⁷⁰, C. Issever ^{18,48}, S. Istin ^{21a,ak}, H. Ito ¹⁶⁸, J.M. Iturbe Ponce ^{64a}, R. Iuppa ^{78a,78b}, A. Ivina ¹⁶⁹, J.M. Izen ⁴⁵, V. Izzo ^{72a}, P. Jacka ^{131,132}, P. Jackson ¹, R.M. Jacobs ⁴⁸, B.P. Jaeger ¹⁴², C.S. Jagfeld ¹⁰⁹, G. Jain ^{156a}, P. Jain ⁵⁴, G. Jäkel ¹⁷¹, K. Jakobs ⁵⁴, T. Jakoubek ¹⁶⁹, J. Jamieson ⁵⁹, K.W. Janas ^{86a}, M. Javurkova ¹⁰³, F. Jeanneau ¹³⁵, L. Jeanty ¹²³, J. Jejelava ^{149a,z}, P. Jenni ^{54,g}, C.E. Jessiman ³⁴, S. Jézéquel ⁴, C. Jia ^{62b}, J. Jia ¹⁴⁵, X. Jia ⁶¹, X. Jia ^{14a,14e}, Z. Jia ^{14c}, Y. Jiang ^{62a}, S. Jiggins ⁴⁸, J. Jimenez Pena ¹³, S. Jin ^{14c}, A. Jinaru ^{27b}, O. Jinnouchi ¹⁵⁴, P. Johansson ¹³⁹, K.A. Johns ⁷, J.W. Johnson ¹³⁶, D.M. Jones ³², E. Jones ⁴⁸, P. Jones ³², R.W.L. Jones ⁹¹, T.J. Jones ⁹², H.L. Joos ^{55,36}, R. Joshi ¹¹⁹, J. Jovicevic ¹⁵, X. Ju ^{17a}, J.J. Junggeburth ¹⁰³, T. Junkermann ^{63a}, A. Juste Rozas ^{13,s}, M.K. Juzek ⁸⁷, S. Kabana ^{137e}, A. Kaczmarska ⁸⁷, M. Kado ¹¹⁰, H. Kagan ¹¹⁹, M. Kagan ¹⁴³, A. Kahn ⁴¹, A. Kahn ¹²⁸, C. Kahra ¹⁰⁰, T. Kaji ¹⁵³, E. Kajomovitz ¹⁵⁰, N. Kakati ¹⁶⁹, I. Kalaitzidou ⁵⁴, C.W. Kalderon ²⁹, A. Kamenshchikov ¹⁵⁵, N.J. Kang ¹³⁶, D. Kar ^{33g}, K. Karava ¹²⁶, M.J. Kareem ^{156b}, E. Karentzos ⁵⁴, I. Karkanias ¹⁵², O. Karkout ¹¹⁴, S.N. Karpov ³⁸, Z.M. Karpova ³⁸, V. Kartvelishvili ⁹¹, A.N. Karyukhin ³⁷,

E. Kasimi ¹⁵², J. Katzy ⁴⁸, S. Kaur ³⁴, K. Kawade ¹⁴⁰, M.P. Kawale ¹²⁰, C. Kawamoto ⁸⁸,
 T. Kawamoto ¹³⁵, E.F. Kay ³⁶, F.I. Kaya ¹⁵⁸, S. Kazakos ¹⁰⁷, V.F. Kazanin ³⁷, Y. Ke ¹⁴⁵,
 J.M. Keaveney ^{33a}, R. Keeler ¹⁶⁵, G.V. Kehris ⁶¹, J.S. Keller ³⁴, A.S. Kelly ⁹⁶, J.J. Kempster ¹⁴⁶,
 K.E. Kennedy ⁴¹, P.D. Kennedy ¹⁰⁰, O. Kepka ¹³¹, B.P. Kerridge ¹⁶⁷, S. Kersten ¹⁷¹,
 B.P. Kerševan ⁹³, S. Keshri ⁶⁶, L. Keszeghova ^{28a}, S. Ketabchi Haghighat ¹⁵⁵, M. Khandoga ¹²⁷,
 A. Khanov ¹²¹, A.G. Kharlamov ³⁷, T. Kharlamova ³⁷, E.E. Khoda ¹³⁸, M. Kholodenko ³⁷,
 T.J. Khoo ¹⁸, G. Khoriali ¹⁶⁶, J. Khubua ^{149b}, Y.A.R. Khwaira ⁶⁶, A. Kilgallon ¹²³,
 D.W. Kim ^{47a,47b}, Y.K. Kim ³⁹, N. Kimura ⁹⁶, M.K. Kingston ⁵⁵, A. Kirchoff ⁵⁵, C. Kirfel ²⁴,
 F. Kirfel ²⁴, J. Kirk ¹³⁴, A.E. Kiryunin ¹¹⁰, C. Kitsaki ¹⁰, O. Kivernyk ²⁴, M. Klassen ^{63a},
 C. Klein ³⁴, L. Klein ¹⁶⁶, M.H. Klein ¹⁰⁶, M. Klein ⁹², S.B. Klein ⁵⁶, U. Klein ⁹²,
 P. Klimek ³⁶, A. Klimentov ²⁹, T. Klioutchnikova ³⁶, P. Kluit ¹¹⁴, S. Kluth ¹¹⁰, E. Kneringer ⁷⁹,
 T.M. Knight ¹⁵⁵, A. Knue ⁴⁹, R. Kobayashi ⁸⁸, D. Kobylanski ¹⁶⁹, S.F. Koch ¹²⁶,
 M. Kocian ¹⁴³, P. Kodyš ¹³³, D.M. Koeck ¹²³, P.T. Koenig ²⁴, T. Koffas ³⁴, M. Kolb ¹³⁵,
 I. Koletsou ⁴, T. Komarek ¹²², K. Köneke ⁵⁴, A.X.Y. Kong ¹, T. Kono ¹¹⁸, N. Konstantinidis ⁹⁶,
 B. Konya ⁹⁸, R. Kopeliansky ⁶⁸, S. Koperny ^{86a}, K. Korcyl ⁸⁷, K. Kordas ^{152,e}, G. Koren ¹⁵¹,
 A. Korn ⁹⁶, S. Korn ⁵⁵, I. Korolkov ¹³, N. Korotkova ³⁷, B. Kortman ¹¹⁴, O. Kortner ¹¹⁰,
 S. Kortner ¹¹⁰, W.H. Kostecka ¹¹⁵, V.V. Kostyukhin ¹⁴¹, A. Kotskechagia ¹³⁵, A. Kotwal ⁵¹,
 A. Koulouris ³⁶, A. Kourkoumeli-Charalampidi ^{73a,73b}, C. Kourkoumelis ⁹, E. Kourlitis ^{110,ae},
 O. Kovanda ¹⁴⁶, R. Kowalewski ¹⁶⁵, W. Kozanecki ¹³⁵, A.S. Kozhin ³⁷, V.A. Kramarenko ³⁷,
 G. Kramberger ⁹³, P. Kramer ¹⁰⁰, M.W. Krasny ¹²⁷, A. Krasnahorkay ³⁶, J.W. Kraus ¹⁷¹,
 J.A. Kremer ⁴⁸, T. Kresse ⁵⁰, J. Kretschmar ⁹², K. Kreul ¹⁸, P. Krieger ¹⁵⁵,
 S. Krishnamurthy ¹⁰³, M. Krivos ¹³³, K. Krizka ²⁰, K. Kroeninger ⁴⁹, H. Kroha ¹¹⁰, J. Kroll ¹³¹,
 J. Kroll ¹²⁸, K.S. Krowpman ¹⁰⁷, U. Kruchonak ³⁸, H. Krüger ²⁴, N. Krumnack ⁸¹, M.C. Kruse ⁵¹,
 J.A. Krzysiak ⁸⁷, O. Kuchinskaia ³⁷, S. Kuday ^{3a}, S. Kuehn ³⁶, R. Kuesters ⁵⁴, T. Kuhl ⁴⁸,
 V. Kukhtin ³⁸, Y. Kulchitsky ^{37,a}, S. Kuleshov ^{137d,137b}, M. Kumar ^{33g}, N. Kumari ⁴⁸,
 A. Kupco ¹³¹, T. Kupfer ⁴⁹, A. Kupich ³⁷, O. Kuprash ⁵⁴, H. Kurashige ⁸⁵, L.L. Kurchaninov ^{156a},
 O. Kurdysh ⁶⁶, Y.A. Kurochkin ³⁷, A. Kurova ³⁷, M. Kuze ¹⁵⁴, A.K. Kvam ¹⁰³, J. Kvitá ¹²²,
 T. Kwan ¹⁰⁴, N.G. Kyriacou ¹⁰⁶, L.A.O. Laatu ¹⁰², C. Lacasta ¹⁶³, F. Lacava ^{75a,75b},
 H. Lacker ¹⁸, D. Lacour ¹²⁷, N.N. Lad ⁹⁶, E. Ladygin ³⁸, B. Laforge ¹²⁷, T. Lagouri ^{137e},
 F.Z. Lahbabi ^{35a}, S. Lai ⁵⁵, I.K. Lakomic ^{86a}, N. Lalloue ⁶⁰, J.E. Lambert ¹⁶⁵, S. Lammers ⁶⁸,
 W. Lampl ⁷, C. Lampoudis ^{152,e}, A.N. Lancaster ¹¹⁵, E. Lançon ²⁹, U. Landgraf ⁵⁴,
 M.P.J. Landon ⁹⁴, V.S. Lang ⁵⁴, R.J. Langenberg ¹⁰³, O.K.B. Langrekken ¹²⁵, A.J. Lankford ¹⁶⁰,
 F. Lanni ³⁶, K. Lantzsch ²⁴, A. Lanza ^{73a}, A. Lapertosa ^{57b,57a}, J.F. Laporte ¹³⁵, T. Lari ^{71a},
 F. Lasagni Manghi ^{23b}, M. Lassnig ³⁶, V. Latonova ¹³¹, A. Laudrain ¹⁰⁰, A. Laurier ¹⁵⁰,
 S.D. Lawlor ¹³⁹, Z. Lawrence ¹⁰¹, M. Lazzaroni ^{71a,71b}, B. Le ¹⁰¹, E.M. Le Boulicaut ⁵¹,
 B. Leban ⁹³, A. Lebedev ⁸¹, M. LeBlanc ¹⁰¹, F. Ledroit-Guillon ⁶⁰, A.C.A. Lee ⁹⁶, S.C. Lee ¹⁴⁸,
 S. Lee ^{47a,47b}, T.F. Lee ⁹², L.L. Leeuw ^{33c}, H.P. Lefebvre ⁹⁵, M. Lefebvre ¹⁶⁵, C. Leggett ^{17a},
 G. Lehmann Miotto ³⁶, M. Leigh ⁵⁶, W.A. Leight ¹⁰³, W. Leinonen ¹¹³, A. Leisos ^{152,r},
 M.A.L. Leite ^{83c}, C.E. Leitgeb ⁴⁸, R. Leitner ¹³³, K.J.C. Leney ⁴⁴, T. Lenz ²⁴, S. Leone ^{74a},
 C. Leonidopoulos ⁵², A. Leopold ¹⁴⁴, C. Leroy ¹⁰⁸, R. Les ¹⁰⁷, C.G. Lester ³²,
 M. Levchenko ³⁷, J. Levêque ⁴, D. Levin ¹⁰⁶, L.J. Levinson ¹⁶⁹, M.P. Lewicki ⁸⁷, D.J. Lewis ⁴,
 A. Li ⁵, B. Li ^{62b}, C. Li ^{62a}, C-Q. Li ^{62c}, H. Li ^{62a}, H. Li ^{62b}, H. Li ^{14c}, H. Li ^{14b}, H. Li ^{62b},
 K. Li ¹³⁸, L. Li ^{62c}, M. Li ^{14a,14e}, Q.Y. Li ^{62a}, S. Li ^{14a,14e}, S. Li ^{62d,62c,d}, T. Li ⁵, X. Li ¹⁰⁴,
 Z. Li ¹²⁶, Z. Li ¹⁰⁴, Z. Li ⁹², Z. Li ^{14a,14e}, S. Liang ^{14a,14e}, Z. Liang ^{14a}, M. Liberatore ¹³⁵,
 B. Liberti ^{76a}, K. Lie ^{64c}, J. Lieber Marin ^{83b}, H. Lien ⁶⁸, K. Lin ¹⁰⁷, R.E. Lindley ⁷,
 J.H. Lindon ², E. Lipeles ¹²⁸, A. Lipniacka ¹⁶, A. Lister ¹⁶⁴, J.D. Little ⁴, B. Liu ^{14a},
 B.X. Liu ¹⁴², D. Liu ^{62d,62c}, J.B. Liu ^{62a}, J.K.K. Liu ³², K. Liu ^{62d,62c}, M. Liu ^{62a},

M.Y. Liu ^{62a}, P. Liu ^{14a}, Q. Liu ^{62d,138,62c}, X. Liu ^{62a}, Y. Liu ^{14d,14e}, Y.L. Liu ^{62b}, Y.W. Liu ^{62a},
J. Llorente Merino ¹⁴², S.L. Lloyd ⁹⁴, E.M. Lobodzinska ⁴⁸, P. Loch ⁷, S. Loffredo ^{76a,76b},
T. Lohse ¹⁸, K. Lohwasser ¹³⁹, E. Loiacono ⁴⁸, M. Lokajicek ^{131,*}, J.D. Lomas ²⁰,
J.D. Long ¹⁶², I. Longarini ¹⁶⁰, L. Longo ^{70a,70b}, R. Longo ¹⁶², I. Lopez Paz ⁶⁷,
A. Lopez Solis ⁴⁸, J. Lorenz ¹⁰⁹, N. Lorenzo Martinez ⁴, A.M. Lory ¹⁰⁹,
G. Löschke Centeno ¹⁴⁶, O. Loseva ³⁷, X. Lou ^{47a,47b}, X. Lou ^{14a,14e}, A. Lounis ⁶⁶, J. Love ⁶,
P.A. Love ⁹¹, G. Lu ^{14a,14e}, M. Lu ⁸⁰, S. Lu ¹²⁸, Y.J. Lu ⁶⁵, H.J. Lubatti ¹³⁸, C. Luci ^{75a,75b},
F.L. Lucio Alves ^{14c}, A. Lucotte ⁶⁰, F. Luehring ⁶⁸, I. Luise ¹⁴⁵, O. Lukianchuk ⁶⁶,
O. Lundberg ¹⁴⁴, B. Lund-Jensen ¹⁴⁴, N.A. Luongo ¹²³, M.S. Lutz ¹⁵¹, A.B. Lux ²⁵, D. Lynn ²⁹,
H. Lyons ⁹², R. Lysak ¹³¹, E. Lytken ⁹⁸, V. Lyubushkin ³⁸, T. Lyubushkina ³⁸, M.M. Lyukova ¹⁴⁵,
H. Ma ²⁹, K. Ma ^{62a}, L.L. Ma ^{62b}, Y. Ma ¹²¹, D.M. Mac Donell ¹⁶⁵, G. Maccarrone ⁵³,
J.C. MacDonald ¹⁰⁰, P.C. Machado De Abreu Farias ^{83b}, R. Madar ⁴⁰, W.F. Mader ⁵⁰,
T. Madula ⁹⁶, J. Maeda ⁸⁵, T. Maeno ²⁹, H. Maguire ¹³⁹, V. Maiboroda ¹³⁵,
A. Maio ^{130a,130b,130d}, K. Maj ^{86a}, O. Majersky ⁴⁸, S. Majewski ¹²³, N. Makovec ⁶⁶,
V. Maksimovic ¹⁵, B. Malaescu ¹²⁷, Pa. Malecki ⁸⁷, V.P. Maleev ³⁷, F. Malek ⁶⁰, M. Mali ⁹³,
D. Malito ⁹⁵, U. Mallik ⁸⁰, S. Maltezos ¹⁰, S. Malyukov ³⁸, J. Mamuzic ¹³, G. Mancini ⁵³,
G. Manco ^{73a,73b}, J.P. Mandalia ⁹⁴, I. Mandić ⁹³, L. Manhaes de Andrade Filho ^{83a},
I.M. Maniatis ¹⁶⁹, J. Manjarres Ramos ^{102,aa}, D.C. Mankad ¹⁶⁹, A. Mann ¹⁰⁹, B. Mansoulie ¹³⁵,
S. Manzoni ³⁶, A. Marantis ^{152,r}, G. Marchiori ⁵, M. Marcisovsky ¹³¹, C. Marcon ^{71a},
M. Marinescu ²⁰, M. Marjanovic ¹²⁰, E.J. Marshall ⁹¹, Z. Marshall ^{17a}, S. Marti-Garcia ¹⁶³,
T.A. Martin ¹⁶⁷, V.J. Martin ⁵², B. Martin dit Latour ¹⁶, L. Martinelli ^{75a,75b}, M. Martinez ^{13,s},
P. Martinez Agullo ¹⁶³, V.I. Martinez Outschoorn ¹⁰³, P. Martinez Suarez ¹³, S. Martin-Haugh ¹³⁴,
V.S. Martoiu ^{27b}, A.C. Martyniuk ⁹⁶, A. Marzin ³⁶, D. Mascione ^{78a,78b}, L. Masetti ¹⁰⁰,
T. Mashimo ¹⁵³, J. Masik ¹⁰¹, A.L. Maslennikov ³⁷, L. Massa ^{23b}, P. Massarotti ^{72a,72b},
P. Mastrandrea ^{74a,74b}, A. Mastroberardino ^{43b,43a}, T. Masubuchi ¹⁵³, T. Mathisen ¹⁶¹,
J. Matousek ¹³³, N. Matsuzawa ¹⁵³, J. Maurer ^{27b}, B. Maček ⁹³, D.A. Maximov ³⁷, R. Mazini ¹⁴⁸,
I. Maznas ¹⁵², M. Mazza ¹⁰⁷, S.M. Mazza ¹³⁶, E. Mazzeo ^{71a,71b}, C. Mc Ginn ²⁹,
J.P. Mc Gowan ¹⁰⁴, S.P. Mc Kee ¹⁰⁶, E.F. McDonald ¹⁰⁵, A.E. McDougall ¹¹⁴, J.A. Mcfayden ¹⁴⁶,
R.P. McGovern ¹²⁸, G. Mchedlidze ^{149b}, R.P. Mckenzie ^{33g}, T.C. Mclachlan ⁴⁸,
D.J. McLaughlin ⁹⁶, S.J. McMahon ¹³⁴, P.C. McNamara ¹⁰⁵, C.M. Mcpartland ⁹²,
R.A. McPherson ^{165,w}, S. Mehlhase ¹⁰⁹, A. Mehta ⁹², D. Melini ¹⁵⁰, B.R. Mellado Garcia ^{33g},
A.H. Melo ⁵⁵, F. Meloni ⁴⁸, A.M. Mendes Jacques Da Costa ¹⁰¹, H.Y. Meng ¹⁵⁵, L. Meng ⁹¹,
S. Menke ¹¹⁰, M. Mentink ³⁶, E. Meoni ^{43b,43a}, C. Merlassino ¹²⁶, L. Merola ^{72a,72b},
C. Meroni ^{71a,71b}, G. Merz ¹⁰⁶, O. Meshkov ³⁷, J. Metcalfe ⁶, A.S. Mete ⁶, C. Meyer ⁶⁸,
J-P. Meyer ¹³⁵, R.P. Middleton ¹³⁴, L. Mijović ⁵², G. Mikenberg ¹⁶⁹, M. Mikestikova ¹³¹,
M. Mikuž ⁹³, H. Mildner ¹⁰⁰, A. Milic ³⁶, C.D. Milke ⁴⁴, D.W. Miller ³⁹, L.S. Miller ³⁴,
A. Milov ¹⁶⁹, D.A. Milstead ^{47a,47b}, T. Min ^{14c}, A.A. Minaenko ³⁷, I.A. Minashvili ^{149b}, L. Mince ⁵⁹,
A.I. Mincer ¹¹⁷, B. Mindur ^{86a}, M. Mineev ³⁸, Y. Mino ⁸⁸, L.M. Mir ¹³, M. Miralles Lopez ¹⁶³,
M. Mironova ^{17a}, A. Mishima ¹⁵³, M.C. Missio ¹¹³, A. Mitra ¹⁶⁷, V.A. Mitsou ¹⁶³,
Y. Mitsumori ¹¹¹, O. Miu ¹⁵⁵, P.S. Miyagawa ⁹⁴, T. Mkrtchyan ^{63a}, M. Mlinarevic ⁹⁶,
T. Mlinarevic ⁹⁶, M. Mlynarikova ³⁶, S. Mobius ¹⁹, P. Moder ⁴⁸, P. Mogg ¹⁰⁹,
A.F. Mohammed ^{14a,14e}, S. Mohapatra ⁴¹, G. Mokgatitwane ^{33g}, L. Moleri ¹⁶⁹, B. Mondal ¹⁴¹,
S. Mondal ¹³², K. Mönig ⁴⁸, E. Monnier ¹⁰², L. Monsonis Romero ¹⁶³, J. Montejo Berlingen ¹³,
M. Montella ¹¹⁹, F. Montekali ^{77a,77b}, F. Monticelli ⁹⁰, S. Monzani ^{69a,69c}, N. Morange ⁶⁶,
A.L. Moreira De Carvalho ^{130a}, M. Moreno Llácer ¹⁶³, C. Moreno Martinez ⁵⁶, P. Morettini ^{57b},
S. Morgenstern ³⁶, M. Morii ⁶¹, M. Morinaga ¹⁵³, A.K. Morley ³⁶, F. Morodei ^{75a,75b},
L. Morvaj ³⁶, P. Moschovakos ³⁶, B. Moser ³⁶, M. Mosidze ^{149b}, T. Moskalets ⁵⁴,

P. Moskvitina ¹¹³, J. Moss ^{31,1}, E.J.W. Moyse ¹⁰³, O. Mtintsilana ^{33g}, S. Muanza ¹⁰²,
 J. Mueller ¹²⁹, D. Muenstermann ⁹¹, R. Müller ¹⁹, G.A. Mullier ¹⁶¹, A.J. Mullin³², J.J. Mullin¹²⁸,
 D.P. Mungo ¹⁵⁵, D. Munoz Perez ¹⁶³, F.J. Munoz Sanchez ¹⁰¹, M. Murin ¹⁰¹, W.J. Murray ^{167,134},
 A. Murrone ^{71a,71b}, J.M. Muse ¹²⁰, M. Muškinja ^{17a}, C. Mwewa ²⁹, A.G. Myagkov ^{37,a},
 A.J. Myers ⁸, A.A. Myers¹²⁹, G. Myers ⁶⁸, M. Myska ¹³², B.P. Nachman ^{17a}, O. Nackenhorst ⁴⁹,
 A. Nag ⁵⁰, K. Nagai ¹²⁶, K. Nagano ⁸⁴, J.L. Nagle ^{29,ai}, E. Nagy ¹⁰², A.M. Nairz ³⁶,
 Y. Nakahama ⁸⁴, K. Nakamura ⁸⁴, K. Nakkalil ⁵, H. Nanjo ¹²⁴, R. Narayan ⁴⁴,
 E.A. Narayanan ¹¹², I. Naryshkin ³⁷, M. Naseri ³⁴, S. Nasri ¹⁵⁹, C. Nass ²⁴, G. Navarro ^{22a},
 J. Navarro-Gonzalez ¹⁶³, R. Nayak ¹⁵¹, A. Nayaz ¹⁸, P.Y. Nechaeva ³⁷, F. Nechansky ⁴⁸,
 L. Nedic ¹²⁶, T.J. Neep ²⁰, A. Negri ^{73a,73b}, M. Negrini ^{23b}, C. Nellist ¹¹⁴, C. Nelson ¹⁰⁴,
 K. Nelson ¹⁰⁶, S. Nemecek ¹³¹, M. Nessi ^{36,h}, M.S. Neubauer ¹⁶², F. Neuhaus ¹⁰⁰,
 J. Neundorf ⁴⁸, R. Newhouse ¹⁶⁴, P.R. Newman ²⁰, C.W. Ng ¹²⁹, Y.W.Y. Ng ⁴⁸, B. Ngair ^{35e},
 H.D.N. Nguyen ¹⁰⁸, R.B. Nickerson ¹²⁶, R. Nicolaidou ¹³⁵, J. Nielsen ¹³⁶, M. Niemeyer ⁵⁵,
 J. Niermann ^{55,36}, N. Nikiforou ³⁶, V. Nikolaenko ^{37,a}, I. Nikolic-Audit ¹²⁷, K. Nikolopoulos ²⁰,
 P. Nilsson ²⁹, I. Ninca ⁴⁸, H.R. Nindhito ⁵⁶, G. Ninio ¹⁵¹, A. Nisati ^{75a}, N. Nishu ²,
 R. Nisius ¹¹⁰, J-E. Nitschke ⁵⁰, E.K. Nkadimeng ^{33g}, T. Nobe ¹⁵³, D.L. Noel ³²,
 T. Nommensen ¹⁴⁷, M.B. Norfolk ¹³⁹, R.R.B. Norisam ⁹⁶, B.J. Norman ³⁴, J. Novak ⁹³,
 T. Novak ⁴⁸, L. Novotny ¹³², R. Novotny ¹¹², L. Nozka ¹²², K. Ntekas ¹⁶⁰,
 N.M.J. Nunes De Moura Junior ^{83b}, E. Nurse⁹⁶, J. Ocariz ¹²⁷, A. Ochi ⁸⁵, I. Ochoa ^{130a},
 S. Oerdek ^{48,i}, J.T. Offermann ³⁹, A. Ogrodnik ¹³³, A. Oh ¹⁰¹, C.C. Ohm ¹⁴⁴, H. Oide ⁸⁴,
 R. Oishi ¹⁵³, M.L. Ojeda ⁴⁸, M.W. O'Keefe⁹², Y. Okumura ¹⁵³, L.F. Oleiro Seabra ^{130a},
 S.A. Olivares Pino ^{137d}, D. Oliveira Damazio ²⁹, D. Oliveira Goncalves ^{83a}, J.L. Oliver ¹⁶⁰,
 A. Olszewski ⁸⁷, Ö.O. Öncel ⁵⁴, A.P. O'Neill ¹⁹, A. Onofre ^{130a,130e}, P.U.E. Onyisi ¹¹,
 M.J. Oreglia ³⁹, G.E. Orellana ⁹⁰, D. Orestano ^{77a,77b}, N. Orlando ¹³, R.S. Orr ¹⁵⁵,
 V. O'Shea ⁵⁹, L.M. Osojnak ¹²⁸, R. Ospanov ^{62a}, G. Otero y Garzon ³⁰, H. Otono ⁸⁹,
 P.S. Ott ^{63a}, G.J. Ottino ^{17a}, M. Ouchrif ^{35d}, J. Ouellette ²⁹, F. Ould-Saada ¹²⁵, M. Owen ⁵⁹,
 R.E. Owen ¹³⁴, K.Y. Oyulmaz ^{21a}, V.E. Ozcan ^{21a}, N. Ozturk ⁸, S. Ozturk ⁸², H.A. Pacey ¹²⁶,
 A. Pacheco Pages ¹³, C. Padilla Aranda ¹³, G. Padovano ^{75a,75b}, S. Pagan Griso ^{17a},
 G. Palacino ⁶⁸, A. Palazzo ^{70a,70b}, S. Palestini ³⁶, J. Pan ¹⁷², T. Pan ^{64a}, D.K. Panchal ¹¹,
 C.E. Pandini ¹¹⁴, J.G. Panduro Vazquez ⁹⁵, H.D. Pandya ¹, H. Pang ^{14b}, P. Pani ⁴⁸,
 G. Panizzo ^{69a,69c}, L. Paolozzi ⁵⁶, C. Papadatos ¹⁰⁸, S. Parajuli ⁴⁴, A. Paramonov ⁶,
 C. Paraskevopoulos ¹⁰, D. Paredes Hernandez ^{64b}, T.H. Park ¹⁵⁵, M.A. Parker ³², F. Parodi ^{57b,57a},
 E.W. Parrish ¹¹⁵, V.A. Parrish ⁵², J.A. Parsons ⁴¹, U. Parzefall ⁵⁴, B. Pascual Dias ¹⁰⁸,
 L. Pascual Dominguez ¹⁵¹, E. Pasqualucci ^{75a}, S. Passaggio ^{57b}, F. Pastore ⁹⁵, P. Pasuwan ^{47a,47b},
 P. Patel ⁸⁷, U.M. Patel ⁵¹, J.R. Pater ¹⁰¹, T. Pauly ³⁶, J. Parkes ¹⁴³, M. Pedersen ¹²⁵,
 R. Pedro ^{130a}, S.V. Peleganchuk ³⁷, O. Penc ³⁶, E.A. Pender ⁵², H. Peng ^{62a}, K.E. Pensi ¹⁰⁹,
 M. Penzin ³⁷, B.S. Peralva ^{83d}, A.P. Pereira Peixoto ⁶⁰, L. Pereira Sanchez ^{47a,47b},
 D.V. Perepelitsa ^{29,ai}, E. Perez Codina ^{156a}, M. Perganti ¹⁰, L. Perini ^{71a,71b,*}, H. Pernegger ³⁶,
 O. Perrin ⁴⁰, K. Peters ⁴⁸, R.F.Y. Peters ¹⁰¹, B.A. Petersen ³⁶, T.C. Petersen ⁴², E. Petit ¹⁰²,
 V. Petousis ¹³², C. Petridou ^{152,e}, A. Petrukhin ¹⁴¹, M. Pettee ^{17a}, N.E. Pettersson ³⁶,
 A. Petukhov ³⁷, K. Petukhova ¹³³, R. Pezoa ^{137f}, L. Pezzotti ³⁶, G. Pezzullo ¹⁷², T.M. Pham ¹⁷⁰,
 T. Pham ¹⁰⁵, P.W. Phillips ¹³⁴, G. Piacquadio ¹⁴⁵, E. Pianori ^{17a}, F. Piazza ^{71a,71b}, R. Piegai ³⁰,
 D. Pietreanu ^{27b}, A.D. Pilkington ¹⁰¹, M. Pinamonti ^{69a,69c}, J.L. Pinfeld ²,
 B.C. Pinheiro Pereira ^{130a}, A.E. Pinto Pinoargote ^{100,135}, L. Pintucci ^{69a,69c}, K.M. Piper ¹⁴⁶,
 A. Pirttikoski ⁵⁶, D.A. Pizzi ³⁴, L. Pizzimento ^{64b}, A. Pizzini ¹¹⁴, M.-A. Pleier ²⁹, V. Plesanovs⁵⁴,
 V. Pleskot ¹³³, E. Plotnikova³⁸, G. Poddar ⁴, R. Poettgen ⁹⁸, L. Poggioli ¹²⁷, I. Pokharel ⁵⁵,
 S. Polacek ¹³³, G. Polesello ^{73a}, A. Poley ^{142,156a}, R. Polifka ¹³², A. Polini ^{23b}, C.S. Pollard ¹⁶⁷,

Z.B. Pollock [id119](#), V. Polychronakos [id29](#), E. Pompa Pacchi [id75a,75b](#), D. Ponomarenko [id113](#), L. Pontecorvo [id36](#), S. Popa [id27a](#), G.A. Popeneciu [id27d](#), A. Poreba [id36](#), D.M. Portillo Quintero [id156a](#), S. Pospisil [id132](#), M.A. Postill [id139](#), P. Postolache [id27c](#), K. Potamianos [id167](#), P.A. Potepa [id86a](#), I.N. Potrap [id38](#), C.J. Potter [id32](#), H. Potti [id1](#), T. Poulsen [id48](#), J. Poveda [id163](#), M.E. Pozo Astigarraga [id36](#), A. Prades Ibanez [id163](#), J. Pretel [id54](#), D. Price [id101](#), M. Primavera [id70a](#), M.A. Principe Martin [id99](#), R. Privara [id122](#), T. Procter [id59](#), M.L. Proffitt [id138](#), N. Proklova [id128](#), K. Prokofiev [id64c](#), G. Proto [id110](#), S. Protopopescu [id29](#), J. Proudfoot [id6](#), M. Przybycien [id86a](#), W.W. Przygoda [id86b](#), J.E. Puddefoot [id139](#), D. Pudzha [id37](#), D. Pyatiizbyantseva [id37](#), J. Qian [id106](#), D. Qichen [id101](#), Y. Qin [id101](#), T. Qiu [id52](#), A. Quadt [id55](#), M. Queitsch-Maitland [id101](#), G. Quetant [id56](#), R.P. Quinn [id164](#), G. Rabanal Bolanos [id61](#), D. Rafanoharana [id54](#), F. Ragusa [id71a,71b](#), J.L. Rainbolt [id39](#), J.A. Raine [id56](#), S. Rajagopalan [id29](#), E. Ramakoti [id37](#), K. Ran [id48,14e](#), N.P. Rapheeha [id33g](#), H. Rasheed [id27b](#), V. Raskina [id127](#), D.F. Rassloff [id63a](#), S. Rave [id100](#), B. Ravina [id55](#), I. Ravinovich [id169](#), M. Raymond [id36](#), A.L. Read [id125](#), N.P. Readioff [id139](#), D.M. Rebutzi [id73a,73b](#), G. Redlinger [id29](#), A.S. Reed [id110](#), K. Reeves [id26](#), J.A. Reidelsturz [id171](#), D. Reikher [id151](#), A. Rej [id141](#), C. Rembser [id36](#), A. Renardi [id48](#), M. Renda [id27b](#), M.B. Rendel [id110](#), F. Renner [id48](#), A.G. Rennie [id160](#), A.L. Rescia [id48](#), S. Resconi [id71a](#), M. Ressegotti [id57b,57a](#), S. Rettie [id36](#), J.G. Reyes Rivera [id107](#), E. Reynolds [id17a](#), O.L. Rezanova [id37](#), P. Reznicek [id133](#), N. Ribaric [id91](#), E. Ricci [id78a,78b](#), R. Richter [id110](#), S. Richter [id47a,47b](#), E. Richter-Was [id86b](#), M. Ridel [id127](#), S. Ridouani [id35d](#), P. Rieck [id117](#), P. Riedler [id36](#), E.M. Riefel [id47a,47b](#), M. Rijssenbeek [id145](#), A. Rimoldi [id73a,73b](#), M. Rimoldi [id48](#), L. Rinaldi [id23b,23a](#), T.T. Rinn [id29](#), M.P. Rinnagel [id109](#), G. Ripellino [id161](#), I. Riu [id13](#), P. Rivadeneira [id48](#), J.C. Rivera Vergara [id165](#), F. Rizatdinova [id121](#), E. Rizvi [id94](#), B.A. Roberts [id167](#), B.R. Roberts [id17a](#), S.H. Robertson [id104,w](#), D. Robinson [id32](#), C.M. Robles Gajardo [id137f](#), M. Robles Manzano [id100](#), A. Robson [id59](#), A. Rocchi [id76a,76b](#), C. Roda [id74a,74b](#), S. Rodriguez Bosca [id63a](#), Y. Rodriguez Garcia [id22a](#), A. Rodriguez Rodriguez [id54](#), A.M. Rodríguez Vera [id156b](#), S. Roe [id36](#), J.T. Roemer [id160](#), A.R. Roepe-Gier [id136](#), J. Roggel [id171](#), O. Røhne [id125](#), R.A. Rojas [id103](#), C.P.A. Roland [id68](#), J. Roloff [id29](#), A. Romaniouk [id37](#), E. Romano [id73a,73b](#), M. Romano [id23b](#), A.C. Romero Hernandez [id162](#), N. Rompotis [id92](#), L. Roos [id127](#), S. Rosati [id75a](#), B.J. Rosser [id39](#), E. Rossi [id126](#), E. Rossi [id72a,72b](#), L.P. Rossi [id57b](#), L. Rossini [id54](#), R. Rosten [id119](#), M. Rotaru [id27b](#), B. Rottler [id54](#), C. Rougier [id102,aa](#), D. Rousseau [id66](#), D. Rousso [id32](#), A. Roy [id162](#), S. Roy-Garand [id155](#), A. Rozanov [id102](#), Y. Rozen [id150](#), X. Ruan [id33g](#), A. Rubio Jimenez [id163](#), A.J. Ruby [id92](#), V.H. Ruelas Rivera [id18](#), T.A. Ruggeri [id1](#), A. Ruggiero [id126](#), A. Ruiz-Martinez [id163](#), A. Rummler [id36](#), Z. Rurikova [id54](#), N.A. Rusakovich [id38](#), H.L. Russell [id165](#), G. Russo [id75a,75b](#), J.P. Rutherford [id7](#), S. Rutherford Colmenares [id32](#), K. Rybacki [id91](#), M. Rybar [id133](#), E.B. Rye [id125](#), A. Ryzhov [id44](#), J.A. Sabater Iglesias [id56](#), P. Sabatini [id163](#), L. Sabetta [id75a,75b](#), H.F-W. Sadrozinski [id136](#), F. Safai Tehrani [id75a](#), B. Safarzadeh Samani [id134](#), M. Safdari [id143](#), S. Saha [id165](#), M. Sahinsoy [id110](#), M. Saimpert [id135](#), M. Saito [id153](#), T. Saito [id153](#), D. Salamani [id36](#), A. Salnikov [id143](#), J. Salt [id163](#), A. Salvador Salas [id13](#), D. Salvatore [id43b,43a](#), F. Salvatore [id146](#), A. Salzburger [id36](#), D. Sammel [id54](#), D. Sampsonidis [id152,e](#), D. Sampsonidou [id123](#), J. Sánchez [id163](#), A. Sanchez Pineda [id4](#), V. Sanchez Sebastian [id163](#), H. Sandaker [id125](#), C.O. Sander [id48](#), J.A. Sandesara [id103](#), M. Sandhoff [id171](#), C. Sandoval [id22b](#), D.P.C. Sankey [id134](#), T. Sano [id88](#), A. Sansoni [id53](#), L. Santi [id75a,75b](#), C. Santoni [id40](#), H. Santos [id130a,130b](#), S.N. Santpur [id17a](#), A. Santra [id169](#), K.A. Saoucha [id116b](#), J.G. Saraiva [id130a,130d](#), J. Sardain [id7](#), O. Sasaki [id84](#), K. Sato [id157](#), C. Sauer [id63b](#), F. Sauerburger [id54](#), E. Sauvan [id4](#), P. Savard [id155,ag](#), R. Sawada [id153](#), C. Sawyer [id134](#), L. Sawyer [id97](#), I. Sayago Galvan [id163](#), C. Sbarra [id23b](#), A. Sbrizzi [id23b,23a](#), T. Scanlon [id96](#), J. Schaarschmidt [id138](#), P. Schacht [id110](#), U. Schäfer [id100](#), A.C. Schaffer [id66,44](#), D. Schaile [id109](#), R.D. Schamberger [id145](#), C. Scharf [id18](#), M.M. Schefer [id19](#), V.A. Schegelsky [id37](#), D. Scheirich [id133](#), F. Schenck [id18](#), M. Schernau [id160](#), C. Scheulen [id55](#), C. Schiavi [id57b,57a](#), E.J. Schioppa [id70a,70b](#), M. Schioppa [id43b,43a](#), B. Schlag [id143,n](#), K.E. Schleicher [id54](#), S. Schlenker [id36](#), J. Schmeing [id171](#), M.A. Schmidt [id171](#),

K. Schmieden ¹⁰⁰, C. Schmitt ¹⁰⁰, S. Schmitt ⁴⁸, L. Schoeffel ¹³⁵, A. Schoening ^{63b},
 P.G. Scholer ⁵⁴, E. Schopf ¹²⁶, M. Schott ¹⁰⁰, J. Schovancova ³⁶, S. Schramm ⁵⁶,
 F. Schroeder ¹⁷¹, T. Schroer ⁵⁶, H-C. Schultz-Coulon ^{63a}, M. Schumacher ⁵⁴, B.A. Schumm ¹³⁶,
 Ph. Schune ¹³⁵, A.J. Schuy ¹³⁸, H.R. Schwartz ¹³⁶, A. Schwartzman ¹⁴³, T.A. Schwarz ¹⁰⁶,
 Ph. Schwemling ¹³⁵, R. Schwienhorst ¹⁰⁷, A. Sciandra ¹³⁶, G. Sciolla ²⁶, F. Scuri ^{74a},
 C.D. Sebastiani ⁹², K. Sedlaczek ¹¹⁵, P. Seema ¹⁸, S.C. Seidel ¹¹², A. Seiden ¹³⁶,
 B.D. Seidlitz ⁴¹, C. Seitz ⁴⁸, J.M. Seixas ^{83b}, G. Sekhniaidze ^{72a}, S.J. Sekula ⁴⁴, L. Selem ⁶⁰,
 N. Semprini-Cesari ^{23b,23a}, D. Sengupta ⁵⁶, V. Senthilkumar ¹⁶³, L. Serin ⁶⁶, L. Serkin ^{69a,69b},
 M. Sessa ^{76a,76b}, H. Severini ¹²⁰, F. Sforza ^{57b,57a}, A. Sfyrly ⁵⁶, E. Shabalina ⁵⁵, R. Shaheen ¹⁴⁴,
 J.D. Shahinian ¹²⁸, D. Shaked Renous ¹⁶⁹, L.Y. Shan ^{14a}, M. Shapiro ^{17a}, A. Sharma ³⁶,
 A.S. Sharma ¹⁶⁴, P. Sharma ⁸⁰, S. Sharma ⁴⁸, P.B. Shatalov ³⁷, K. Shaw ¹⁴⁶, S.M. Shaw ¹⁰¹,
 A. Shcherbakova ³⁷, Q. Shen ^{62c,5}, P. Sherwood ⁹⁶, L. Shi ⁹⁶, X. Shi ^{14a}, C.O. Shimmin ¹⁷²,
 J.D. Shinner ⁹⁵, I.P.J. Shipsey ¹²⁶, S. Shirabe ^{56,h}, M. Shiyakova ^{38,u}, J. Shlomi ¹⁶⁹,
 M.J. Shochet ³⁹, J. Shojaii ¹⁰⁵, D.R. Shope ¹²⁵, B. Shrestha ¹²⁰, S. Shrestha ^{119,aj},
 E.M. Shrif ^{33g}, M.J. Shroff ¹⁶⁵, P. Sicho ¹³¹, A.M. Sickles ¹⁶², E. Sideras Haddad ^{33g},
 A. Sidoti ^{23b}, F. Siegert ⁵⁰, Dj. Sijacki ¹⁵, R. Sikora ^{86a}, F. Sili ⁹⁰, J.M. Silva ²⁰,
 M.V. Silva Oliveira ²⁹, S.B. Silverstein ^{47a}, S. Simion ⁶⁶, R. Simoniello ³⁶, E.L. Simpson ⁵⁹,
 H. Simpson ¹⁴⁶, L.R. Simpson ¹⁰⁶, N.D. Simpson ⁹⁸, S. Simsek ⁸², S. Sindhu ⁵⁵, P. Sinervo ¹⁵⁵,
 S. Singh ¹⁵⁵, S. Sinha ⁴⁸, S. Sinha ¹⁰¹, M. Sioli ^{23b,23a}, I. Siral ³⁶, E. Sitnikova ⁴⁸,
 S.Yu. Sivoklov ^{37,*}, J. Sjölin ^{47a,47b}, A. Skaf ⁵⁵, E. Skorda ²⁰, P. Skubic ¹²⁰, M. Slawinska ⁸⁷,
 V. Smakhtin ¹⁶⁹, B.H. Smart ¹³⁴, J. Smiesko ³⁶, S.Yu. Smirnov ³⁷, Y. Smirnov ³⁷,
 L.N. Smirnova ^{37,a}, O. Smirnova ⁹⁸, A.C. Smith ⁴¹, E.A. Smith ³⁹, H.A. Smith ¹²⁶,
 J.L. Smith ⁹², R. Smith ¹⁴³, M. Smizanska ⁹¹, K. Smolek ¹³², A.A. Snesarev ³⁷, S.R. Snider ¹⁵⁵,
 H.L. Snoek ¹¹⁴, S. Snyder ²⁹, R. Sobie ^{165,w}, A. Soffer ¹⁵¹, C.A. Solans Sanchez ³⁶,
 E.Yu. Soldatov ³⁷, U. Soldevila ¹⁶³, A.A. Solodkov ³⁷, S. Solomon ²⁶, A. Soloshenko ³⁸,
 K. Solovieva ⁵⁴, O.V. Solovyanov ⁴⁰, V. Solovyev ³⁷, P. Sommer ³⁶, A. Sonay ¹³,
 W.Y. Song ^{156b}, J.M. Sonneveld ¹¹⁴, A. Sopczak ¹³², A.L. Sopio ⁹⁶, F. Sopkova ^{28b},
 V. Sothilingam ^{63a}, S. Sottocornola ⁶⁸, R. Soualah ^{116b}, Z. Soumami ^{35e}, D. South ⁴⁸,
 N. Soybelman ¹⁶⁹, S. Spagnolo ^{70a,70b}, M. Spalla ¹¹⁰, D. Sperlich ⁵⁴, G. Spigo ³⁶, S. Spinali ⁹¹,
 D.P. Spiteri ⁵⁹, M. Spousta ¹³³, E.J. Staats ³⁴, A. Stabile ^{71a,71b}, R. Stamen ^{63a}, A. Stampekis ²⁰,
 M. Standke ²⁴, E. Stanecka ⁸⁷, M.V. Stange ⁵⁰, B. Stanislaus ^{17a}, M.M. Stanitzki ⁴⁸, B. Stapf ⁴⁸,
 E.A. Starchenko ³⁷, G.H. Stark ¹³⁶, J. Stark ^{102,aa}, D.M. Starko ^{156b}, P. Staroba ¹³¹,
 P. Starovoitov ^{63a}, S. Stärz ¹⁰⁴, R. Staszewski ⁸⁷, G. Stavropoulos ⁴⁶, J. Steentoft ¹⁶¹,
 P. Steinberg ²⁹, B. Stelzer ^{142,156a}, H.J. Stelzer ¹²⁹, O. Stelzer-Chilton ^{156a}, H. Stenzel ⁵⁸,
 T.J. Stevenson ¹⁴⁶, G.A. Stewart ³⁶, J.R. Stewart ¹²¹, M.C. Stockton ³⁶, G. Stoicea ^{27b},
 M. Stolarski ^{130a}, S. Stonjek ¹¹⁰, A. Straessner ⁵⁰, J. Strandberg ¹⁴⁴, S. Strandberg ^{47a,47b},
 M. Stratmann ¹⁷¹, M. Strauss ¹²⁰, T. Strebler ¹⁰², P. Strizenc ^{28b}, R. Ströhmer ¹⁶⁶,
 D.M. Strom ¹²³, L.R. Strom ⁴⁸, R. Stroynowski ⁴⁴, A. Strubig ^{47a,47b}, S.A. Stucci ²⁹,
 B. Stugu ¹⁶, J. Stupak ¹²⁰, N.A. Styles ⁴⁸, D. Su ¹⁴³, S. Su ^{62a}, W. Su ^{62d}, X. Su ^{62a,66},
 K. Sugizaki ¹⁵³, V.V. Sulin ³⁷, M.J. Sullivan ⁹², D.M.S. Sultan ^{78a,78b}, L. Sultanaliev ³⁷,
 S. Sultansoy ^{3b}, T. Sumida ⁸⁸, S. Sun ¹⁰⁶, S. Sun ¹⁷⁰, O. Sunneborn Gudnadottir ¹⁶¹, N. Sur ¹⁰²,
 M.R. Sutton ¹⁴⁶, H. Suzuki ¹⁵⁷, M. Svatos ¹³¹, M. Swiatlowski ^{156a}, T. Swirski ¹⁶⁶,
 I. Sykora ^{28a}, M. Sykora ¹³³, T. Sykora ¹³³, D. Ta ¹⁰⁰, K. Tackmann ^{48,t}, A. Taffard ¹⁶⁰,
 R. Tafirout ^{156a}, J.S. Tafoya Vargas ⁶⁶, E.P. Takeva ⁵², Y. Takubo ⁸⁴, M. Talby ¹⁰²,
 A.A. Talyshev ³⁷, K.C. Tam ^{64b}, N.M. Tamir ¹⁵¹, A. Tanaka ¹⁵³, J. Tanaka ¹⁵³, R. Tanaka ⁶⁶,
 M. Tanasini ^{57b,57a}, Z. Tao ¹⁶⁴, S. Tapia Araya ^{137f}, S. Tapprogge ¹⁰⁰,
 A. Tarek Abouelfadl Mohamed ¹⁰⁷, S. Tarem ¹⁵⁰, K. Tariq ^{14a}, G. Tarna ^{102,27b}, G.F. Tartarelli ^{71a},

P. Tas ¹³³, M. Tasevsky ¹³¹, E. Tassi ^{43b,43a}, A.C. Tate ¹⁶², G. Tateno ¹⁵³, Y. Tayalati ^{35e,v},
 G.N. Taylor ¹⁰⁵, W. Taylor ^{156b}, H. Teagle ⁹², A.S. Tee ¹⁷⁰, R. Teixeira De Lima ¹⁴³,
 P. Teixeira-Dias ⁹⁵, J.J. Teoh ¹⁵⁵, K. Terashi ¹⁵³, J. Terron ⁹⁹, S. Terzo ¹³, M. Testa ⁵³,
 R.J. Teuscher ^{155,w}, A. Thaler ⁷⁹, O. Theiner ⁵⁶, N. Themistokleous ⁵², T. Theveneaux-Pelzer ¹⁰²,
 O. Thielmann ¹⁷¹, D.W. Thomas ⁹⁵, J.P. Thomas ²⁰, E.A. Thompson ^{17a}, P.D. Thompson ²⁰,
 E. Thomson ¹²⁸, Y. Tian ⁵⁵, V. Tikhomirov ^{37,a}, Yu.A. Tikhonov ³⁷, S. Timoshenko ³⁷,
 D. Timoshyn ¹³³, E.X.L. Ting ¹, P. Tipton ¹⁷², S.H. Tlou ^{33g}, A. Tnourji ⁴⁰, K. Todome ¹⁵⁴,
 S. Todorova-Nova ¹³³, S. Todt ⁵⁰, M. Togawa ⁸⁴, J. Tojo ⁸⁹, S. Tokár ^{28a}, K. Tokushuku ⁸⁴,
 O. Toldaiev ⁶⁸, R. Tombs ³², M. Tomoto ^{84,111}, L. Tompkins ^{143,n}, K.W. Topolnicki ^{86b},
 E. Torrence ¹²³, H. Torres ^{102,aa}, E. Torró Pastor ¹⁶³, M. Toscani ³⁰, C. Tosciri ³⁹, M. Tost ¹¹,
 D.R. Tovey ¹³⁹, A. Traeet ¹⁶, I.S. Trandafir ^{27b}, T. Trefzger ¹⁶⁶, A. Tricoli ²⁹, I.M. Trigger ^{156a},
 S. Trincaz-Duvoid ¹²⁷, D.A. Trischuk ²⁶, B. Trocmé ⁶⁰, C. Troncon ^{71a}, L. Truong ^{33c},
 M. Trzebinski ⁸⁷, A. Trzupsek ⁸⁷, F. Tsai ¹⁴⁵, M. Tsai ¹⁰⁶, A. Tsiamis ^{152,e}, P.V. Tsiareshka ³⁷,
 S. Tsigaridas ^{156a}, A. Tsirigotis ^{152,r}, V. Tsiskaridze ¹⁵⁵, E.G. Tskhadadze ^{149a},
 M. Tsopoulou ^{152,e}, Y. Tsujikawa ⁸⁸, I.I. Tsukerman ³⁷, V. Tsulaia ^{17a}, S. Tsuno ⁸⁴, O. Tsur ¹⁵⁰,
 K. Tsuru ¹¹⁸, D. Tsybychev ¹⁴⁵, Y. Tu ^{64b}, A. Tudorache ^{27b}, V. Tudorache ^{27b}, A.N. Tuna ³⁶,
 S. Turchikhin ^{57b,57a}, I. Turk Cakir ^{3a}, R. Turra ^{71a}, T. Turtuvshin ^{38,x}, P.M. Tuts ⁴¹,
 S. Tzamarias ^{152,e}, P. Tzani ¹⁰, E. Tzovara ¹⁰⁰, F. Ukegawa ¹⁵⁷, P.A. Ulloa Poblete ^{137c,137b},
 E.N. Umaka ²⁹, G. Unal ³⁶, M. Unal ¹¹, A. Undrus ²⁹, G. Unel ¹⁶⁰, J. Urban ^{28b},
 P. Urquijo ¹⁰⁵, G. Usai ⁸, R. Ushioda ¹⁵⁴, M. Usman ¹⁰⁸, Z. Uysal ^{21b}, L. Vacavant ¹⁰²,
 V. Vacek ¹³², B. Vachon ¹⁰⁴, K.O.H. Vadla ¹²⁵, T. Vafeiadis ³⁶, A. Vaitkus ⁹⁶, C. Valderanis ¹⁰⁹,
 E. Valdes Santurio ^{47a,47b}, M. Valente ^{156a}, S. Valentinetti ^{23b,23a}, A. Valero ¹⁶³,
 E. Valiente Moreno ¹⁶³, A. Vallier ^{102,aa}, J.A. Valls Ferrer ¹⁶³, D.R. Van Arneman ¹¹⁴,
 T.R. Van Daalen ¹³⁸, A. Van Der Graaf ⁴⁹, P. Van Gemmeren ⁶, M. Van Rijnbach ^{125,36},
 S. Van Stroud ⁹⁶, I. Van Vulpen ¹¹⁴, M. Vanadia ^{76a,76b}, W. Vandelli ³⁶, M. Vandenbroucke ¹³⁵,
 E.R. Vandewall ¹²¹, D. Vannicola ¹⁵¹, L. Vannoli ^{57b,57a}, R. Vari ^{75a}, E.W. Varnes ⁷,
 C. Varni ^{17b}, T. Varol ¹⁴⁸, D. Varouchas ⁶⁶, L. Varriale ¹⁶³, K.E. Varvell ¹⁴⁷, M.E. Vasile ^{27b},
 L. Vaslin ⁴⁰, G.A. Vasquez ¹⁶⁵, A. Vasyukov ³⁸, F. Vazeille ⁴⁰, T. Vazquez Schroeder ³⁶,
 J. Veatch ³¹, V. Vecchio ¹⁰¹, M.J. Veen ¹⁰³, I. Veliscek ¹²⁶, L.M. Veloce ¹⁵⁵, F. Veloso ^{130a,130c},
 S. Veneziano ^{75a}, A. Ventura ^{70a,70b}, S. Ventura Gonzalez ¹³⁵, A. Verbytskyi ¹¹⁰,
 M. Verducci ^{74a,74b}, C. Vergis ²⁴, M. Verissimo De Araujo ^{83b}, W. Verkerke ¹¹⁴,
 J.C. Vermeulen ¹¹⁴, C. Vernieri ¹⁴³, M. Vessella ¹⁰³, M.C. Vetterli ^{142,ag}, A. Vgenopoulos ^{152,e},
 N. Viaux Maira ^{137f}, T. Vickey ¹³⁹, O.E. Vickey Boeriu ¹³⁹, G.H.A. Viehhauser ¹²⁶, L. Vignani ^{63b},
 M. Villa ^{23b,23a}, M. Villaplana Perez ¹⁶³, E.M. Villhauer ⁵², E. Vilucchi ⁵³, M.G. Vinciter ³⁴,
 G.S. Virdee ²⁰, A. Vishwakarma ⁵², A. Visibile ¹¹⁴, C. Vittori ³⁶, I. Vivarelli ¹⁴⁶,
 E. Voevodina ¹¹⁰, F. Vogel ¹⁰⁹, P. Vokac ¹³², Yu. Volkotrub ^{86a}, J. Von Ahnen ⁴⁸,
 E. Von Toerne ²⁴, B. Vormwald ³⁶, V. Vorobel ¹³³, K. Vorobev ³⁷, M. Vos ¹⁶³, K. Voss ¹⁴¹,
 J.H. Vossebeld ⁹², M. Vozak ¹¹⁴, L. Vozdecky ⁹⁴, N. Vranjes ¹⁵, M. Vranjes Milosavljevic ¹⁵,
 M. Vreeswijk ¹¹⁴, R. Vuillermet ³⁶, O. Vujanovic ¹⁰⁰, I. Vukotic ³⁹, S. Wada ¹⁵⁷, C. Wagner ¹⁰³,
 J.M. Wagner ^{17a}, W. Wagner ¹⁷¹, S. Wahdan ¹⁷¹, H. Wahlberg ⁹⁰, M. Wakida ¹¹¹, J. Walder ¹³⁴,
 R. Walker ¹⁰⁹, W. Walkowiak ¹⁴¹, A. Wall ¹²⁸, T. Wamorkar ⁶, A.Z. Wang ¹⁷⁰, C. Wang ¹⁰⁰,
 C. Wang ^{62c}, H. Wang ^{17a}, J. Wang ^{64a}, R.-J. Wang ¹⁰⁰, R. Wang ⁶¹, R. Wang ⁶,
 S.M. Wang ¹⁴⁸, S. Wang ^{62b}, T. Wang ^{62a}, W.T. Wang ⁸⁰, W. Wang ^{14a}, X. Wang ^{14c},
 X. Wang ¹⁶², X. Wang ^{62c}, Y. Wang ^{62d}, Y. Wang ^{14c}, Z. Wang ¹⁰⁶, Z. Wang ^{62d,51,62c},
 Z. Wang ¹⁰⁶, A. Warburton ¹⁰⁴, R.J. Ward ²⁰, N. Warrack ⁵⁹, A.T. Watson ²⁰, H. Watson ⁵⁹,
 M.F. Watson ²⁰, E. Watton ^{59,134}, G. Watts ¹³⁸, B.M. Waugh ⁹⁶, C. Weber ²⁹, H.A. Weber ¹⁸,
 M.S. Weber ¹⁹, S.M. Weber ^{63a}, C. Wei ^{62a}, Y. Wei ¹²⁶, A.R. Weidberg ¹²⁶, E.J. Weik ¹¹⁷,

J. Weingarten ⁴⁹, M. Weirich ¹⁰⁰, C. Weiser ⁵⁴, C.J. Wells ⁴⁸, T. Wenaus ²⁹, B. Wendland ⁴⁹, T. Wengler ³⁶, N.S. Wenke ¹¹⁰, N. Wermes ²⁴, M. Wessels ^{63a}, A.M. Wharton ⁹¹, A.S. White ⁶¹, A. White ⁸, M.J. White ¹, D. Whiteson ¹⁶⁰, L. Wickremasinghe ¹²⁴, W. Wiedenmann ¹⁷⁰, C. Wiel ⁵⁰, M. Wielers ¹³⁴, C. Wiglesworth ⁴², D.J. Wilbern ¹²⁰, H.G. Wilkens ³⁶, D.M. Williams ⁴¹, H.H. Williams ¹²⁸, S. Williams ³², S. Willocq ¹⁰³, B.J. Wilson ¹⁰¹, P.J. Windischhofer ³⁹, F.I. Winkel ³⁰, F. Winklmeier ¹²³, B.T. Winter ⁵⁴, J.K. Winter ¹⁰¹, M. Wittgen ¹⁴³, M. Wobisch ⁹⁷, Z. Wolfs ¹¹⁴, J. Wollrath ¹⁶⁰, M.W. Wolter ⁸⁷, H. Wolters ^{130a,130c}, A.F. Wongel ⁴⁸, S.D. Worm ⁴⁸, B.K. Wosiek ⁸⁷, K.W. Woźniak ⁸⁷, S. Wozniwski ⁵⁵, K. Wraight ⁵⁹, C. Wu ²⁰, J. Wu ^{14a,14e}, M. Wu ^{64a}, M. Wu ¹¹³, S.L. Wu ¹⁷⁰, X. Wu ⁵⁶, Y. Wu ^{62a}, Z. Wu ¹³⁵, J. Wuerzinger ^{110,ae}, T.R. Wyatt ¹⁰¹, B.M. Wynne ⁵², S. Xella ⁴², L. Xia ^{14c}, M. Xia ^{14b}, J. Xiang ^{64c}, M. Xie ^{62a}, X. Xie ^{62a}, S. Xin ^{14a,14e}, A. Xiong ¹²³, J. Xiong ^{17a}, D. Xu ^{14a}, H. Xu ^{62a}, L. Xu ^{62a}, R. Xu ¹²⁸, T. Xu ¹⁰⁶, Y. Xu ^{14b}, Z. Xu ⁵², Z. Xu ^{14a}, B. Yabsley ¹⁴⁷, S. Yacoob ^{33a}, Y. Yamaguchi ¹⁵⁴, E. Yamashita ¹⁵³, H. Yamauchi ¹⁵⁷, T. Yamazaki ^{17a}, Y. Yamazaki ⁸⁵, J. Yan ^{62c}, S. Yan ¹²⁶, Z. Yan ²⁵, H.J. Yang ^{62c,62d}, H.T. Yang ^{62a}, S. Yang ^{62a}, T. Yang ^{64c}, X. Yang ^{62a}, X. Yang ^{14a}, Y. Yang ⁴⁴, Y. Yang ^{62a}, Z. Yang ^{62a}, W.-M. Yao ^{17a}, Y.C. Yap ⁴⁸, H. Ye ^{14c}, H. Ye ⁵⁵, J. Ye ^{14a}, S. Ye ²⁹, X. Ye ^{62a}, Y. Yeh ⁹⁶, I. Yeletsikh ³⁸, B.K. Yeo ^{17b}, M.R. Yexley ⁹⁶, P. Yin ⁴¹, K. Yorita ¹⁶⁸, S. Younas ^{27b}, C.J.S. Young ³⁶, C. Young ¹⁴³, C. Yu ^{14a,14e}, Y. Yu ^{62a}, J. Yuan ^{14a,14e}, M. Yuan ¹⁰⁶, R. Yuan ^{62b}, L. Yue ⁹⁶, M. Zaazoua ^{62a}, B. Zabinski ⁸⁷, E. Zaid ⁵², T. Zakareishvili ^{149b}, N. Zakharchuk ³⁴, S. Zambito ⁵⁶, J.A. Zamora Saa ^{137d,137b}, J. Zang ¹⁵³, D. Zanzi ⁵⁴, O. Zaplatilek ¹³², C. Zeitnitz ¹⁷¹, H. Zeng ^{14a}, J.C. Zeng ¹⁶², D.T. Zenger Jr ²⁶, O. Zenin ³⁷, T. Ženiš ^{28a}, S. Zenz ⁹⁴, S. Zerradi ^{35a}, D. Zerwas ⁶⁶, M. Zhai ^{14a,14e}, B. Zhang ^{14c}, D.F. Zhang ¹³⁹, J. Zhang ^{62b}, J. Zhang ⁶, K. Zhang ^{14a,14e}, L. Zhang ^{14c}, P. Zhang ^{14a,14e}, R. Zhang ¹⁷⁰, S. Zhang ¹⁰⁶, T. Zhang ¹⁵³, X. Zhang ^{62c}, X. Zhang ^{62b}, Y. Zhang ^{62c,5}, Y. Zhang ⁹⁶, Z. Zhang ^{17a}, Z. Zhang ⁶⁶, H. Zhao ¹³⁸, P. Zhao ⁵¹, T. Zhao ^{62b}, Y. Zhao ¹³⁶, Z. Zhao ^{62a}, A. Zhemchugov ³⁸, J. Zheng ^{14c}, K. Zheng ¹⁶², X. Zheng ^{62a}, Z. Zheng ¹⁴³, D. Zhong ¹⁶², B. Zhou ¹⁰⁶, H. Zhou ⁷, N. Zhou ^{62c}, Y. Zhou ⁷, C.G. Zhu ^{62b}, J. Zhu ¹⁰⁶, Y. Zhu ^{62c}, Y. Zhu ^{62a}, X. Zhuang ^{14a}, K. Zhukov ³⁷, V. Zhulanov ³⁷, N.I. Zimine ³⁸, J. Zinsser ^{63b}, M. Ziolkowski ¹⁴¹, L. Živković ¹⁵, A. Zoccoli ^{23b,23a}, K. Zoch ⁶¹, T.G. Zorbas ¹³⁹, O. Zormpa ⁴⁶, W. Zou ⁴¹, L. Zwalinski ³⁶.

¹Department of Physics, University of Adelaide, Adelaide; Australia.

²Department of Physics, University of Alberta, Edmonton AB; Canada.

³(^a)Department of Physics, Ankara University, Ankara; (^b)Division of Physics, TOBB University of Economics and Technology, Ankara; Türkiye.

⁴LAPP, Université Savoie Mont Blanc, CNRS/IN2P3, Annecy; France.

⁵APC, Université Paris Cité, CNRS/IN2P3, Paris; France.

⁶High Energy Physics Division, Argonne National Laboratory, Argonne IL; United States of America.

⁷Department of Physics, University of Arizona, Tucson AZ; United States of America.

⁸Department of Physics, University of Texas at Arlington, Arlington TX; United States of America.

⁹Physics Department, National and Kapodistrian University of Athens, Athens; Greece.

¹⁰Physics Department, National Technical University of Athens, Zografou; Greece.

¹¹Department of Physics, University of Texas at Austin, Austin TX; United States of America.

¹²Institute of Physics, Azerbaijan Academy of Sciences, Baku; Azerbaijan.

¹³Institut de Física d'Altes Energies (IFAE), Barcelona Institute of Science and Technology, Barcelona; Spain.

¹⁴(^a)Institute of High Energy Physics, Chinese Academy of Sciences, Beijing; (^b)Physics Department,

Tsinghua University, Beijing;^(c)Department of Physics, Nanjing University, Nanjing;^(d)School of Science, Shenzhen Campus of Sun Yat-sen University;^(e)University of Chinese Academy of Science (UCAS), Beijing; China.

¹⁵Institute of Physics, University of Belgrade, Belgrade; Serbia.

¹⁶Department for Physics and Technology, University of Bergen, Bergen; Norway.

¹⁷(^a)Physics Division, Lawrence Berkeley National Laboratory, Berkeley CA;^(b)University of California, Berkeley CA; United States of America.

¹⁸Institut für Physik, Humboldt Universität zu Berlin, Berlin; Germany.

¹⁹Albert Einstein Center for Fundamental Physics and Laboratory for High Energy Physics, University of Bern, Bern; Switzerland.

²⁰School of Physics and Astronomy, University of Birmingham, Birmingham; United Kingdom.

²¹(^a)Department of Physics, Bogazici University, Istanbul;^(b)Department of Physics Engineering, Gaziantep University, Gaziantep;^(c)Department of Physics, Istanbul University, Istanbul; Türkiye.

²²(^a)Facultad de Ciencias y Centro de Investigaciones, Universidad Antonio Nariño,

Bogotá;^(b)Departamento de Física, Universidad Nacional de Colombia, Bogotá; Colombia.

²³(^a)Dipartimento di Fisica e Astronomia A. Righi, Università di Bologna, Bologna;^(b)INFN Sezione di Bologna; Italy.

²⁴Physikalisches Institut, Universität Bonn, Bonn; Germany.

²⁵Department of Physics, Boston University, Boston MA; United States of America.

²⁶Department of Physics, Brandeis University, Waltham MA; United States of America.

²⁷(^a)Transilvania University of Brasov, Brasov;^(b)Horia Hulubei National Institute of Physics and Nuclear Engineering, Bucharest;^(c)Department of Physics, Alexandru Ioan Cuza University of Iasi, Iasi;^(d)National Institute for Research and Development of Isotopic and Molecular Technologies, Physics Department, Cluj-Napoca;^(e)National University of Science and Technology Politehnica, Bucharest;^(f)West University in Timisoara, Timisoara;^(g)Faculty of Physics, University of Bucharest, Bucharest; Romania.

²⁸(^a)Faculty of Mathematics, Physics and Informatics, Comenius University, Bratislava;^(b)Department of Subnuclear Physics, Institute of Experimental Physics of the Slovak Academy of Sciences, Kosice; Slovak Republic.

²⁹Physics Department, Brookhaven National Laboratory, Upton NY; United States of America.

³⁰Universidad de Buenos Aires, Facultad de Ciencias Exactas y Naturales, Departamento de Física, y CONICET, Instituto de Física de Buenos Aires (IFIBA), Buenos Aires; Argentina.

³¹California State University, CA; United States of America.

³²Cavendish Laboratory, University of Cambridge, Cambridge; United Kingdom.

³³(^a)Department of Physics, University of Cape Town, Cape Town;^(b)iThemba Labs, Western

Cape;^(c)Department of Mechanical Engineering Science, University of Johannesburg,

Johannesburg;^(d)National Institute of Physics, University of the Philippines Diliman

(Philippines);^(e)University of South Africa, Department of Physics, Pretoria;^(f)University of Zululand, KwaDlangezwa;^(g)School of Physics, University of the Witwatersrand, Johannesburg; South Africa.

³⁴Department of Physics, Carleton University, Ottawa ON; Canada.

³⁵(^a)Faculté des Sciences Ain Chock, Réseau Universitaire de Physique des Hautes Energies - Université Hassan II, Casablanca;^(b)Faculté des Sciences, Université Ibn-Tofail, Kénitra;^(c)Faculté des Sciences Semlalia, Université Cadi Ayyad, LPHEA-Marrakech;^(d)LPMR, Faculté des Sciences, Université Mohamed Premier, Oujda;^(e)Faculté des sciences, Université Mohammed V, Rabat;^(f)Institute of Applied Physics, Mohammed VI Polytechnic University, Ben Guerir; Morocco.

³⁶CERN, Geneva; Switzerland.

³⁷Affiliated with an institute covered by a cooperation agreement with CERN.

³⁸Affiliated with an international laboratory covered by a cooperation agreement with CERN.

- ³⁹Enrico Fermi Institute, University of Chicago, Chicago IL; United States of America.
- ⁴⁰LPC, Université Clermont Auvergne, CNRS/IN2P3, Clermont-Ferrand; France.
- ⁴¹Nevis Laboratory, Columbia University, Irvington NY; United States of America.
- ⁴²Niels Bohr Institute, University of Copenhagen, Copenhagen; Denmark.
- ⁴³(^a)Dipartimento di Fisica, Università della Calabria, Rende; (^b)INFN Gruppo Collegato di Cosenza, Laboratori Nazionali di Frascati; Italy.
- ⁴⁴Physics Department, Southern Methodist University, Dallas TX; United States of America.
- ⁴⁵Physics Department, University of Texas at Dallas, Richardson TX; United States of America.
- ⁴⁶National Centre for Scientific Research "Demokritos", Agia Paraskevi; Greece.
- ⁴⁷(^a)Department of Physics, Stockholm University; (^b)Oskar Klein Centre, Stockholm; Sweden.
- ⁴⁸Deutsches Elektronen-Synchrotron DESY, Hamburg and Zeuthen; Germany.
- ⁴⁹Fakultät Physik , Technische Universität Dortmund, Dortmund; Germany.
- ⁵⁰Institut für Kern- und Teilchenphysik, Technische Universität Dresden, Dresden; Germany.
- ⁵¹Department of Physics, Duke University, Durham NC; United States of America.
- ⁵²SUPA - School of Physics and Astronomy, University of Edinburgh, Edinburgh; United Kingdom.
- ⁵³INFN e Laboratori Nazionali di Frascati, Frascati; Italy.
- ⁵⁴Physikalisches Institut, Albert-Ludwigs-Universität Freiburg, Freiburg; Germany.
- ⁵⁵II. Physikalisches Institut, Georg-August-Universität Göttingen, Göttingen; Germany.
- ⁵⁶Département de Physique Nucléaire et Corpusculaire, Université de Genève, Genève; Switzerland.
- ⁵⁷(^a)Dipartimento di Fisica, Università di Genova, Genova; (^b)INFN Sezione di Genova; Italy.
- ⁵⁸II. Physikalisches Institut, Justus-Liebig-Universität Giessen, Giessen; Germany.
- ⁵⁹SUPA - School of Physics and Astronomy, University of Glasgow, Glasgow; United Kingdom.
- ⁶⁰LPSC, Université Grenoble Alpes, CNRS/IN2P3, Grenoble INP, Grenoble; France.
- ⁶¹Laboratory for Particle Physics and Cosmology, Harvard University, Cambridge MA; United States of America.
- ⁶²(^a)Department of Modern Physics and State Key Laboratory of Particle Detection and Electronics, University of Science and Technology of China, Hefei; (^b)Institute of Frontier and Interdisciplinary Science and Key Laboratory of Particle Physics and Particle Irradiation (MOE), Shandong University, Qingdao; (^c)School of Physics and Astronomy, Shanghai Jiao Tong University, Key Laboratory for Particle Astrophysics and Cosmology (MOE), SKLPPC, Shanghai; (^d)Tsung-Dao Lee Institute, Shanghai; China.
- ⁶³(^a)Kirchhoff-Institut für Physik, Ruprecht-Karls-Universität Heidelberg, Heidelberg; (^b)Physikalisches Institut, Ruprecht-Karls-Universität Heidelberg, Heidelberg; Germany.
- ⁶⁴(^a)Department of Physics, Chinese University of Hong Kong, Shatin, N.T., Hong Kong; (^b)Department of Physics, University of Hong Kong, Hong Kong; (^c)Department of Physics and Institute for Advanced Study, Hong Kong University of Science and Technology, Clear Water Bay, Kowloon, Hong Kong; China.
- ⁶⁵Department of Physics, National Tsing Hua University, Hsinchu; Taiwan.
- ⁶⁶IJCLab, Université Paris-Saclay, CNRS/IN2P3, 91405, Orsay; France.
- ⁶⁷Centro Nacional de Microelectrónica (IMB-CNM-CSIC), Barcelona; Spain.
- ⁶⁸Department of Physics, Indiana University, Bloomington IN; United States of America.
- ⁶⁹(^a)INFN Gruppo Collegato di Udine, Sezione di Trieste, Udine; (^b)ICTP, Trieste; (^c)Dipartimento Politecnico di Ingegneria e Architettura, Università di Udine, Udine; Italy.
- ⁷⁰(^a)INFN Sezione di Lecce; (^b)Dipartimento di Matematica e Fisica, Università del Salento, Lecce; Italy.
- ⁷¹(^a)INFN Sezione di Milano; (^b)Dipartimento di Fisica, Università di Milano, Milano; Italy.
- ⁷²(^a)INFN Sezione di Napoli; (^b)Dipartimento di Fisica, Università di Napoli, Napoli; Italy.
- ⁷³(^a)INFN Sezione di Pavia; (^b)Dipartimento di Fisica, Università di Pavia, Pavia; Italy.
- ⁷⁴(^a)INFN Sezione di Pisa; (^b)Dipartimento di Fisica E. Fermi, Università di Pisa, Pisa; Italy.
- ⁷⁵(^a)INFN Sezione di Roma; (^b)Dipartimento di Fisica, Sapienza Università di Roma, Roma; Italy.

- ^{76(a)}INFN Sezione di Roma Tor Vergata;^(b)Dipartimento di Fisica, Università di Roma Tor Vergata, Roma; Italy.
- ^{77(a)}INFN Sezione di Roma Tre;^(b)Dipartimento di Matematica e Fisica, Università Roma Tre, Roma; Italy.
- ^{78(a)}INFN-TIFPA;^(b)Università degli Studi di Trento, Trento; Italy.
- ⁷⁹Universität Innsbruck, Department of Astro and Particle Physics, Innsbruck; Austria.
- ⁸⁰University of Iowa, Iowa City IA; United States of America.
- ⁸¹Department of Physics and Astronomy, Iowa State University, Ames IA; United States of America.
- ⁸²Istinye University, Sariyer, Istanbul; Türkiye.
- ^{83(a)}Departamento de Engenharia Elétrica, Universidade Federal de Juiz de Fora (UFJF), Juiz de Fora;^(b)Universidade Federal do Rio De Janeiro COPPE/EE/IF, Rio de Janeiro;^(c)Instituto de Física, Universidade de São Paulo, São Paulo;^(d)Rio de Janeiro State University, Rio de Janeiro; Brazil.
- ⁸⁴KEK, High Energy Accelerator Research Organization, Tsukuba; Japan.
- ⁸⁵Graduate School of Science, Kobe University, Kobe; Japan.
- ^{86(a)}AGH University of Krakow, Faculty of Physics and Applied Computer Science, Krakow;^(b)Marian Smoluchowski Institute of Physics, Jagiellonian University, Krakow; Poland.
- ⁸⁷Institute of Nuclear Physics Polish Academy of Sciences, Krakow; Poland.
- ⁸⁸Faculty of Science, Kyoto University, Kyoto; Japan.
- ⁸⁹Research Center for Advanced Particle Physics and Department of Physics, Kyushu University, Fukuoka ; Japan.
- ⁹⁰Instituto de Física La Plata, Universidad Nacional de La Plata and CONICET, La Plata; Argentina.
- ⁹¹Physics Department, Lancaster University, Lancaster; United Kingdom.
- ⁹²Oliver Lodge Laboratory, University of Liverpool, Liverpool; United Kingdom.
- ⁹³Department of Experimental Particle Physics, Jožef Stefan Institute and Department of Physics, University of Ljubljana, Ljubljana; Slovenia.
- ⁹⁴School of Physics and Astronomy, Queen Mary University of London, London; United Kingdom.
- ⁹⁵Department of Physics, Royal Holloway University of London, Egham; United Kingdom.
- ⁹⁶Department of Physics and Astronomy, University College London, London; United Kingdom.
- ⁹⁷Louisiana Tech University, Ruston LA; United States of America.
- ⁹⁸Fysiska institutionen, Lunds universitet, Lund; Sweden.
- ⁹⁹Departamento de Física Teórica C-15 and CIAFF, Universidad Autónoma de Madrid, Madrid; Spain.
- ¹⁰⁰Institut für Physik, Universität Mainz, Mainz; Germany.
- ¹⁰¹School of Physics and Astronomy, University of Manchester, Manchester; United Kingdom.
- ¹⁰²CPPM, Aix-Marseille Université, CNRS/IN2P3, Marseille; France.
- ¹⁰³Department of Physics, University of Massachusetts, Amherst MA; United States of America.
- ¹⁰⁴Department of Physics, McGill University, Montreal QC; Canada.
- ¹⁰⁵School of Physics, University of Melbourne, Victoria; Australia.
- ¹⁰⁶Department of Physics, University of Michigan, Ann Arbor MI; United States of America.
- ¹⁰⁷Department of Physics and Astronomy, Michigan State University, East Lansing MI; United States of America.
- ¹⁰⁸Group of Particle Physics, University of Montreal, Montreal QC; Canada.
- ¹⁰⁹Fakultät für Physik, Ludwig-Maximilians-Universität München, München; Germany.
- ¹¹⁰Max-Planck-Institut für Physik (Werner-Heisenberg-Institut), München; Germany.
- ¹¹¹Graduate School of Science and Kobayashi-Maskawa Institute, Nagoya University, Nagoya; Japan.
- ¹¹²Department of Physics and Astronomy, University of New Mexico, Albuquerque NM; United States of America.
- ¹¹³Institute for Mathematics, Astrophysics and Particle Physics, Radboud University/Nikhef, Nijmegen;

Netherlands.

¹¹⁴Nikhef National Institute for Subatomic Physics and University of Amsterdam, Amsterdam; Netherlands.

¹¹⁵Department of Physics, Northern Illinois University, DeKalb IL; United States of America.

¹¹⁶(^a)New York University Abu Dhabi, Abu Dhabi;(^b)University of Sharjah, Sharjah; United Arab Emirates.

¹¹⁷Department of Physics, New York University, New York NY; United States of America.

¹¹⁸Ochanomizu University, Otsuka, Bunkyo-ku, Tokyo; Japan.

¹¹⁹Ohio State University, Columbus OH; United States of America.

¹²⁰Homer L. Dodge Department of Physics and Astronomy, University of Oklahoma, Norman OK; United States of America.

¹²¹Department of Physics, Oklahoma State University, Stillwater OK; United States of America.

¹²²Palacký University, Joint Laboratory of Optics, Olomouc; Czech Republic.

¹²³Institute for Fundamental Science, University of Oregon, Eugene, OR; United States of America.

¹²⁴Graduate School of Science, Osaka University, Osaka; Japan.

¹²⁵Department of Physics, University of Oslo, Oslo; Norway.

¹²⁶Department of Physics, Oxford University, Oxford; United Kingdom.

¹²⁷LPNHE, Sorbonne Université, Université Paris Cité, CNRS/IN2P3, Paris; France.

¹²⁸Department of Physics, University of Pennsylvania, Philadelphia PA; United States of America.

¹²⁹Department of Physics and Astronomy, University of Pittsburgh, Pittsburgh PA; United States of America.

¹³⁰(^a)Laboratório de Instrumentação e Física Experimental de Partículas - LIP, Lisboa;(^b)Departamento de Física, Faculdade de Ciências, Universidade de Lisboa, Lisboa;(^c)Departamento de Física, Universidade de Coimbra, Coimbra;(^d)Centro de Física Nuclear da Universidade de Lisboa, Lisboa;(^e)Departamento de Física, Universidade do Minho, Braga;(^f)Departamento de Física Teórica y del Cosmos, Universidad de Granada, Granada (Spain);(^g)Departamento de Física, Instituto Superior Técnico, Universidade de Lisboa, Lisboa; Portugal.

¹³¹Institute of Physics of the Czech Academy of Sciences, Prague; Czech Republic.

¹³²Czech Technical University in Prague, Prague; Czech Republic.

¹³³Charles University, Faculty of Mathematics and Physics, Prague; Czech Republic.

¹³⁴Particle Physics Department, Rutherford Appleton Laboratory, Didcot; United Kingdom.

¹³⁵IRFU, CEA, Université Paris-Saclay, Gif-sur-Yvette; France.

¹³⁶Santa Cruz Institute for Particle Physics, University of California Santa Cruz, Santa Cruz CA; United States of America.

¹³⁷(^a)Departamento de Física, Pontificia Universidad Católica de Chile, Santiago;(^b)Millennium Institute for Subatomic physics at high energy frontier (SAPHIR), Santiago;(^c)Instituto de Investigación Multidisciplinario en Ciencia y Tecnología, y Departamento de Física, Universidad de La Serena;(^d)Universidad Andres Bello, Department of Physics, Santiago;(^e)Instituto de Alta Investigación, Universidad de Tarapacá, Arica;(^f)Departamento de Física, Universidad Técnica Federico Santa María, Valparaíso; Chile.

¹³⁸Department of Physics, University of Washington, Seattle WA; United States of America.

¹³⁹Department of Physics and Astronomy, University of Sheffield, Sheffield; United Kingdom.

¹⁴⁰Department of Physics, Shinshu University, Nagano; Japan.

¹⁴¹Department Physik, Universität Siegen, Siegen; Germany.

¹⁴²Department of Physics, Simon Fraser University, Burnaby BC; Canada.

¹⁴³SLAC National Accelerator Laboratory, Stanford CA; United States of America.

¹⁴⁴Department of Physics, Royal Institute of Technology, Stockholm; Sweden.

- ¹⁴⁵Departments of Physics and Astronomy, Stony Brook University, Stony Brook NY; United States of America.
- ¹⁴⁶Department of Physics and Astronomy, University of Sussex, Brighton; United Kingdom.
- ¹⁴⁷School of Physics, University of Sydney, Sydney; Australia.
- ¹⁴⁸Institute of Physics, Academia Sinica, Taipei; Taiwan.
- ¹⁴⁹^(a)E. Andronikashvili Institute of Physics, Iv. Javakhishvili Tbilisi State University, Tbilisi;^(b)High Energy Physics Institute, Tbilisi State University, Tbilisi;^(c)University of Georgia, Tbilisi; Georgia.
- ¹⁵⁰Department of Physics, Technion, Israel Institute of Technology, Haifa; Israel.
- ¹⁵¹Raymond and Beverly Sackler School of Physics and Astronomy, Tel Aviv University, Tel Aviv; Israel.
- ¹⁵²Department of Physics, Aristotle University of Thessaloniki, Thessaloniki; Greece.
- ¹⁵³International Center for Elementary Particle Physics and Department of Physics, University of Tokyo, Tokyo; Japan.
- ¹⁵⁴Department of Physics, Tokyo Institute of Technology, Tokyo; Japan.
- ¹⁵⁵Department of Physics, University of Toronto, Toronto ON; Canada.
- ¹⁵⁶^(a)TRIUMF, Vancouver BC;^(b)Department of Physics and Astronomy, York University, Toronto ON; Canada.
- ¹⁵⁷Division of Physics and Tomonaga Center for the History of the Universe, Faculty of Pure and Applied Sciences, University of Tsukuba, Tsukuba; Japan.
- ¹⁵⁸Department of Physics and Astronomy, Tufts University, Medford MA; United States of America.
- ¹⁵⁹United Arab Emirates University, Al Ain; United Arab Emirates.
- ¹⁶⁰Department of Physics and Astronomy, University of California Irvine, Irvine CA; United States of America.
- ¹⁶¹Department of Physics and Astronomy, University of Uppsala, Uppsala; Sweden.
- ¹⁶²Department of Physics, University of Illinois, Urbana IL; United States of America.
- ¹⁶³Instituto de Física Corpuscular (IFIC), Centro Mixto Universidad de Valencia - CSIC, Valencia; Spain.
- ¹⁶⁴Department of Physics, University of British Columbia, Vancouver BC; Canada.
- ¹⁶⁵Department of Physics and Astronomy, University of Victoria, Victoria BC; Canada.
- ¹⁶⁶Fakultät für Physik und Astronomie, Julius-Maximilians-Universität Würzburg, Würzburg; Germany.
- ¹⁶⁷Department of Physics, University of Warwick, Coventry; United Kingdom.
- ¹⁶⁸Waseda University, Tokyo; Japan.
- ¹⁶⁹Department of Particle Physics and Astrophysics, Weizmann Institute of Science, Rehovot; Israel.
- ¹⁷⁰Department of Physics, University of Wisconsin, Madison WI; United States of America.
- ¹⁷¹Fakultät für Mathematik und Naturwissenschaften, Fachgruppe Physik, Bergische Universität Wuppertal, Wuppertal; Germany.
- ¹⁷²Department of Physics, Yale University, New Haven CT; United States of America.
- ^a Also Affiliated with an institute covered by a cooperation agreement with CERN.
- ^b Also at An-Najah National University, Nablus; Palestine.
- ^c Also at Borough of Manhattan Community College, City University of New York, New York NY; United States of America.
- ^d Also at Center for High Energy Physics, Peking University; China.
- ^e Also at Center for Interdisciplinary Research and Innovation (CIRI-AUTH), Thessaloniki; Greece.
- ^f Also at Centro Studi e Ricerche Enrico Fermi; Italy.
- ^g Also at CERN, Geneva; Switzerland.
- ^h Also at Département de Physique Nucléaire et Corpusculaire, Université de Genève, Genève; Switzerland.
- ⁱ Also at Departament de Física de la Universitat Autònoma de Barcelona, Barcelona; Spain.
- ^j Also at Department of Financial and Management Engineering, University of the Aegean, Chios; Greece.

- k* Also at Department of Physics, Ben Gurion University of the Negev, Beer Sheva; Israel.
- l* Also at Department of Physics, California State University, Sacramento; United States of America.
- m* Also at Department of Physics, King's College London, London; United Kingdom.
- n* Also at Department of Physics, Stanford University, Stanford CA; United States of America.
- o* Also at Department of Physics, University of Fribourg, Fribourg; Switzerland.
- p* Also at Department of Physics, University of Thessaly; Greece.
- q* Also at Department of Physics, Westmont College, Santa Barbara; United States of America.
- r* Also at Hellenic Open University, Patras; Greece.
- s* Also at Institutio Catalana de Recerca i Estudis Avancats, ICREA, Barcelona; Spain.
- t* Also at Institut für Experimentalphysik, Universität Hamburg, Hamburg; Germany.
- u* Also at Institute for Nuclear Research and Nuclear Energy (INRNE) of the Bulgarian Academy of Sciences, Sofia; Bulgaria.
- v* Also at Institute of Applied Physics, Mohammed VI Polytechnic University, Ben Guerir; Morocco.
- w* Also at Institute of Particle Physics (IPP); Canada.
- x* Also at Institute of Physics and Technology, Mongolian Academy of Sciences, Ulaanbaatar; Mongolia.
- y* Also at Institute of Physics, Azerbaijan Academy of Sciences, Baku; Azerbaijan.
- z* Also at Institute of Theoretical Physics, Ilia State University, Tbilisi; Georgia.
- aa* Also at L2IT, Université de Toulouse, CNRS/IN2P3, UPS, Toulouse; France.
- ab* Also at Lawrence Livermore National Laboratory, Livermore; United States of America.
- ac* Also at National Institute of Physics, University of the Philippines Diliman (Philippines); Philippines.
- ad* Also at Ochanomizu University, Otsuka, Bunkyo-ku, Tokyo; Japan.
- ae* Also at Technical University of Munich, Munich; Germany.
- af* Also at The Collaborative Innovation Center of Quantum Matter (CICQM), Beijing; China.
- ag* Also at TRIUMF, Vancouver BC; Canada.
- ah* Also at Università di Napoli Parthenope, Napoli; Italy.
- ai* Also at University of Colorado Boulder, Department of Physics, Colorado; United States of America.
- aj* Also at Washington College, Chestertown, MD; United States of America.
- ak* Also at Yeditepe University, Physics Department, Istanbul; Türkiye.
- * Deceased